Design of self-repairable superhydrophobic and switchable surfaces using colloidal particles

D I S S E R T A T I O N

zur Erlangung des akademischen Grades

Doctor rerum naturalium

(Dr. rer. nat.)

vorgelegt

der Fakultät Mathematik und Naturwissenschaften

der Technischen Universität Dresden

von

Nikolay Puretskiy

geboren am 06. Juli 1987 in Tula, Russland

Die Dissertation wurde in der Zeit von Oktober 2009 bis Oktober 2013
im Leibniz-Institut für Polymerforschung Dresden e. V. angefertigt

Gutachter: Prof. Manfred Stamm

Prof. Vladimir V. Tsukruk

Eingereicht am 15. November 2013

Tag der Verteidigung: 25. Februar 2014

To my family

Table of contents

Preface

1 Introduction

1.1 Motivation

The design of functional materials with complex properties is very important for different applications, such as coatings, microelectronics, biotechnologies and medicine. It is also crucial that such kinds of materials have a long service lifetime. Unfortunately, cracks or other types of damages may occur during everyday use and some parts of the material should be changed for the regeneration of the initial properties. One of the approaches to avoid the replacement is utilization of self-healing materials.

Self-healing or self-repairable materials are materials that have the intrinsic ability to partially or completely repair damage occurring during their service lifetime. There are a lot of examples of self-healing effect in biology because regeneration is one of the unique abilities of living organisms. This process allows biological species to recover and maintain their integrity after disturbance or damage. Self-healing can take place either at the level of single molecules or at the macroscopic level, and some examples of this process are the merging of broken bones and the closure and healing of injuries of blood vessels. However, man-made materials generally do not possess such self-healing ability. Different strategies and approaches to design self-healing materials, which are important in engineering, have been investigated, in particular, metals, ceramics and polymers [1].

Most of the works were focused on regeneration of integrity of materials. On the other hand, surface properties of materials, which also play highly important role, remained out of scope of self-healing approach. One of the very interesting and technically attractive surface properties is superhydrophobicity. Superhydrophobic surfaces with apparent advancing and receding contact angles above 150° and contact angle hysteresis (the difference between them) less than 10° play an important role in technical applications, ranging from self-cleaning window glasses, paints and textiles (due to self-cleaning effect) to low-friction surfaces for fluid flow and energy conservation [2], and allow longer life-time of materials.

Lotus leaves have been the inspiration for the development of several artificial self-cleaning biomimetic materials. On Lotus leaves, water droplets roll in addition to sliding over the leaf surface and in this way collect dirt and other particles from the surface. The superhydrophobicity and self-cleaning of the Lotus leaves was found to be a result of the hierarchical surface structure built by randomly oriented small hydrophobic wax tubules on the top of a convex cell papillae.

Superhydrophobic and self-cleaning plant surfaces are always correlated with the presence of three-dimensionally structured waxes, but both properties are optimized in surfaces with hierarchical surface structures with multiple-length-scale roughness. Water on such a surface forms a spherical droplet and both the contact area and adhesion to the surface are dramatically reduced [3].

Another prominent property, which also remained out of focus of self-healing technology, is ability of some materials to switch different surface characteristic such as hydrophilicity, hydrophobicity, charge etc. Generally, switchable or stimuli-responsive surfaces are the surfaces that demonstrate a considerable switching of properties in response to small variations of environmental conditions [4]. Introduction of functional groups specifically sensitive to changes in pH, light, temperature or electric field is one of the approaches for the design of stimuli-responsive surfaces [4]. Another approach involves chemical immobilization of two sorts of incompatible polymer chains onto one substrate [5]. Exposure to a solvent selective for one of the polymers results in the switching of chemical composition in the topmost polymer layer [6]. Stimuli-responsive surfaces are, therefore, designed using mainly self-assembled monolayers by surface immobilization of polymers (polymer brushes) [7] or using metal oxides [8]. Up to date, stimuli-responsive surfaces sensitive to solvents [9], pH [10], salt concentration [10], electric [11] and magnetic [12] fields, light [13], as well as temperature [14], have been applied to control wettability, adhesion, charge and interactions with proteins and cells [4, 15, 16]. In most cases switching properties are provided by thin layer of switchable materials (polymer, silane) that is extremely sensitive to mechanical treatment.

1.2 Goals

The main aim of this work is a design and of self-repairable material with superhydrophobic and switchable properties using colloidal particles. Up to date nanoparticles may obtained at low cost and can be used for repair micro-damages in polymer materials, for preparation of superhydrophobic films and for design of material with switching properties.

Use of **nanoparticles to repair** cracks in polymeric materials is an emerging but nonetheless promising approach for the design of self-healing materials [17-19]. In this technique the ability of nanoparticles to fill cracks is used. Nanoparticles have a tendency to be driven towards the damaged region at relatively short time scales, if the polymer chains are flexible. Once the particle migration has occurred, the system can then be fixated by cooling or hardening after a chemical reaction of cross-linking, so that the coating forms a solid nanocomposite layer that effectively repairs the flaws in the damaged surface. During the self-healing process nanoparticles or colloidal particles will form initial structures on the interfaces and initial interfacial properties will therefore be restored. Also, colloidal particles are able to form different structures on the interfaces, that could dramatically change the wetting properties and, in fact, even superhydrophobic surfaces could be obtained.

The use of **colloidal particles** is one of the methods for the preparation of **superhydrophobic surfaces** [20-24] and has a number of certain advantages. First, particles with different size and surface chemistry can be synthesized. Second, particles may be dispersed in liquids and deposited on large areas at low cost. One way to design a superhydrophobic surface using colloidal particles is to assemble them into agglomerates [21, 22]. Another approach is to use raspberry-like particles – colloidal particles coated by smaller ones [23, 24]. In both cases, surfaces with hierarchical topography are formed.

Finally, **colloidal particles** on interfaces can be used for the design of **switchable coatings and textiles**. Several examples of such kind of systems are already listed in section 1.2.

New functional materials with all described properties (superhydrophobicity, self-healing and switching ability) or pairwise superhydrophobicity and self-healing properties or both switching and self-

healing characteristic can be obtained by the combination of the approaches based on utilization of nanoparticles on the surfaces. Colloidal particles with simple spherical or with complex geometry can be used to reach necessary interfacial properties. Incorporation of the particles into matrix with low melting point, i.e. paraffin wax, gives a mechanical stability of the composite and an ability to manipulate of the particles on the surface by heat utilization (Figure 1).
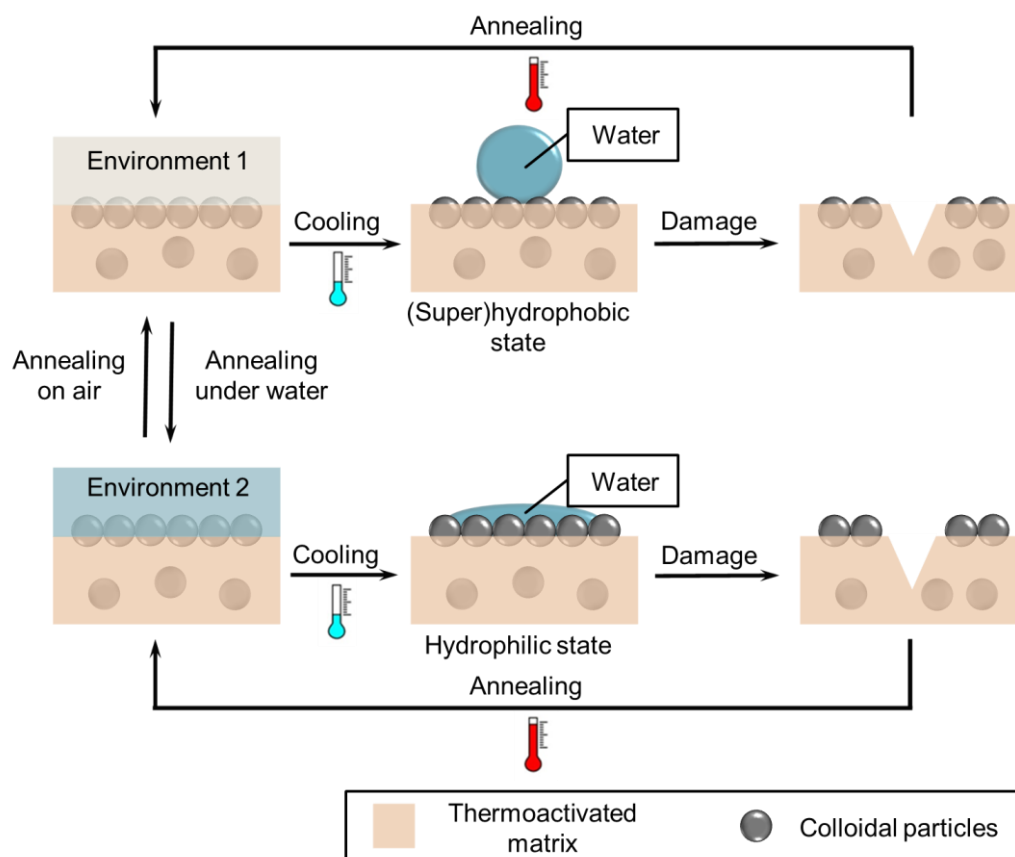
Figure 1. Scheme of the approach base on particle-thermoactivated matrix: particles immersion into matrix depends on the initial annealing environment and surfaces with (super)hydrophobic or hydrophilic properties can be obtained. After damage initial surface properties can be easily restored by annealing under specific conditions.

1.3 Outline

This thesis consists of 4 main chapters. In **Chapter 1** the general introduction, motivation and goals are given.

Theoretical background and experimental methods related to presented work are described in **Chapter 2**. This is included general aspects, definitions and some recent examples of self-healing materials, superhydrophobic surface and composites with switching properties. Also here experimental methods for characterization of obtained films and materials are described.

Chapter 3 consolidates experimental details, results and discussions for preparation and properties of either complex colloidal particles or composites, basically particle-solid oil (paraffin wax, perfluorodecane) mixtures. Chapter 3 is subdivided into 3 parts. In the section 3.1 preparation and interfacial properties of complex colloidal particles are discussed. In the section 3.2 composites with switchable properties are described. Section 3.3 is about preparation and characteristics of superhydrophobic films. Each section is introduced, discussed and summarized separately.

At the end of this thesis, **Chapter 4**, the conclusions of this work, potential applications as well as possible outlook for future research in this area are presented.

2 Theoretical background and methods

2.1 State of the art

2.1.1 Introduction

Biological materials or species are evolutionary optimized functional systems. One of their most outstanding properties is the self-healing and regeneration of a function upon external mechanical forces when a considerable part of the specie could be damaged or completely lost. In nature, self-healing takes place either at the single molecule level or at the microscopic level. Examples of this process are the repair of DNA-molecules, the merging of broken bones, the closure and healing of injuries in blood vessels. However, man-made materials generally do not possess this healing ability (Figure 2). The general approaches for the preparation of self-healing materials and some important examples, especially in the field of polymer science, will be described in section 2.1.2. The self-healing effect plays an important role in the recovery of either mechanical properties of the materials or in the prevention of the damage in the surface layer, therefore, providing the material's resistance and prolonging the service lifetime.

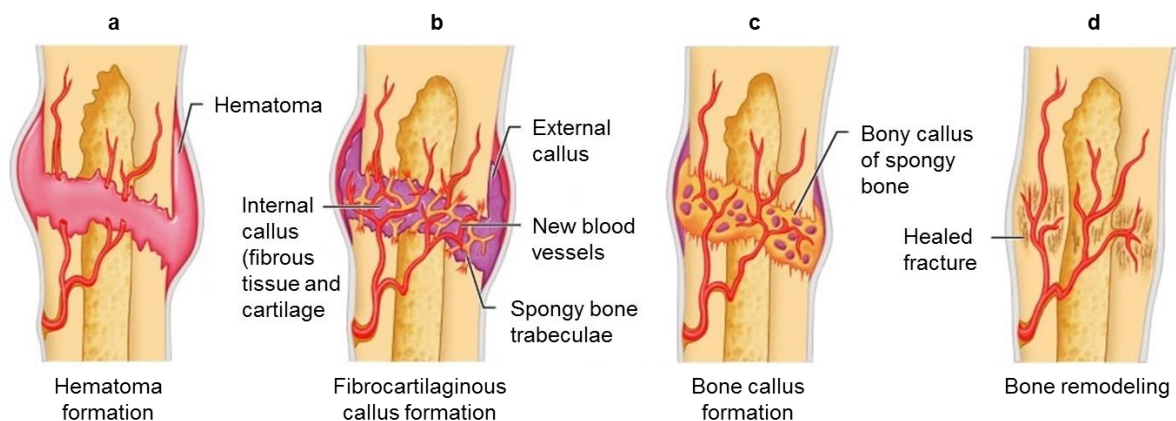**Figure 2.** Scheme of repairing fracture bone in different stage of healing: fracture hematoma (a); fibrocartilaginous callus (soft callus) formation (b); bony callus (hard callus) formation (c); bone remodeling (d)[*].

---

[*] Image adopted from http://apbrwww5.apsu.edu/thompsonj/Anatomy%20&%20Physiology/2010/2010%20Exam%20Reviews/Exam%202%20Review/CH%206%20Process%20of%20Fracture%20Repair.htm (15.10.2013)

Control of surface properties is very important for the design of superhydrophobic coatings, which, in fact, also allow extension the lifetime of the materials. Such kinds of interfaces with both advancing and receding water contact angles above 150°, low contact angle hysteresis (difference between advancing and receding contact angles) and low roll-off angle (less than 10°) play an important role in different technical applications, ranging from self-cleaning window glasses, paints and textiles to low-friction surfaces for fluid flow and energy conservation [2]. Superhydrophobicity gives the opportunity to reduce surface contamination, as well as to prevent corrosion by reducing the amount of contact with water. Some theoretical background of this phenomenon, applications of superhydrophobic surfaces and their preparation methods are described more detailed in section 2.1.3.

Nevertheless, a lot of materials with superhydrophobic properties do not possess mechanical resistance and, after the top layer gets damaged, lose their superhydrophobicity. Approaches for the preparation of materials with durable or easy-reparable, as well as self-healing superhydrophobic properties are shown in section 2.1.4.

Figure 3. Water droplet on lotus leaf – demonstration of superhydrophobic effect [†].

Surfaces with adaptive properties, which are also known as stimuli-responsive or switchable surfaces, could also be used for the improvement of the

---

[†] Image adopted from http://printsofjapan.wordpress.com/2009/09/13/the-lotus-%E8%93%AE/ (15.10.2013)

material characteristics. Generally switching behavior is widely used in biological systems, for instance plants, in order to change conformation as well as properties under external stimuli (Figure 4). Those biological systems lead for the design different types of stimuli responsive artificial materials. Examples of "smart" materials used for the preparation of surfaces with switchable wetting properties are pointed out in section 2.1.5.
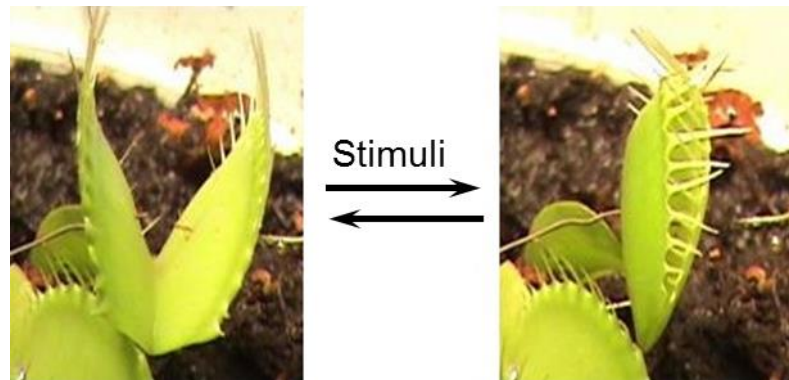
Figure 4. Open – close behavior of Dionaea muscipula under external stimuli [25].

2.1.2 Self-repairable materials

Self-healing materials can be prepared by using different strategies and approaches, which depend on the material class. A lot of examples of the self-healing effect are demonstrated in certain metals, ceramics and polymers. Though these materials possess different intrinsic properties, according to [1], the same self-healing concept is used for all of them and can be illustrated by a scheme presented at Figure 5.
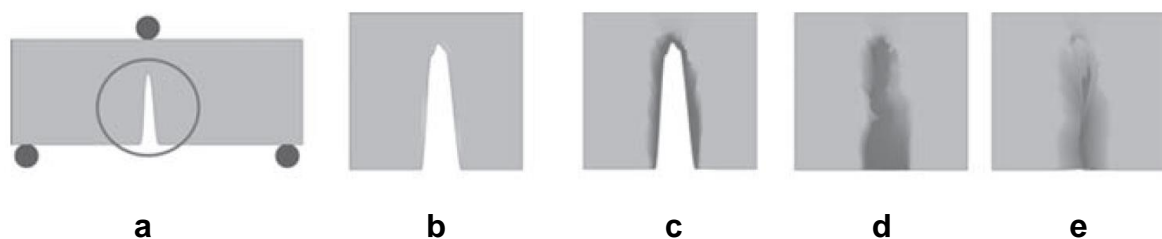
Figure 5. General concept of self-healing materials: a) crack induction by mechanical force; b) crack view; c) induction of the "mobile phase"; d) crack closure by the "mobile phase"; e) immobilization after healing.

Under the influence of a mechanical force (Figure 5, a and b) a crack can form. Self-healing can start both on microscopic and macroscopic levels by a subsequent generation of the "mobile phase" (Figure 5, c). The "Mobile phase" is triggered either by the occurrence of damage in an ideal case, or by an external stimuli like temperature and light. Damage can be removed due to a directed mass transport toward the damage site and a subsequent local melding reaction (Figure 5, d). The crack planes reconnect by physical interactions or by chemical rebinding. These processes can occur jointly. After healing, the previous mobile phase is immobilized again, resulting in an ideal case of fully restored properties (Figure 5, e). The principle described above can be used for different material classes. However, the healing temperature can be varied depending on the materials and according to their intrinsic properties. For instance, for concrete an ambient temperature is sufficient. Low temperature (< 120 °C) is required for polymers and their composites, and high – for metals (< 600 °C) and ceramics (> 600 °C). The size of the damage, which is able to be healed, can vary substantially, according to the size and the number of species being transported.

Generally, self-healing materials can be divided into two different classes, depending on the required trigger and the nature of the self-healing process: **non-autonomic** (require an external stimuli like heat, light or a laser beam) and **autonomic** (the damage itself is the stimulus for healing) [1], Figure 6.
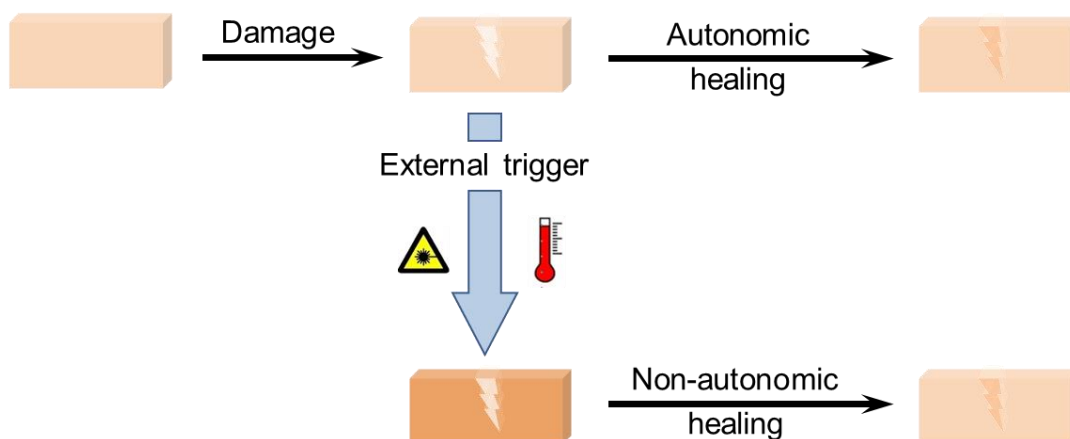

Figure 6. Illustration of autonomic / non-autonomic self-healing classification: autonomic healing case – the damage itself is the stimulus for healing; non-autonomic case – require an external stimuli like heat or irradiation with light / laser beam.

For distinguishing the materials into subclasses other properties of the self-healing process can be also used. The terms **"extrinsic"** and **"intrinsic"** are among the most used for the determination of these subclasses [26-28]; Figure 7. In case of extrinsic self-healing materials, the healing process is based on external healing components (i.e. micro- or nanocapsules) intentionally embedded into the matrix materials (Figure 7a). These capsules can provide the mobile phase after damage (Figure 7b). Alternatively, intrinsic self-healing requires no separate healing agent. Although this concept is preferable, according to the material class and the mechanism of healing, it cannot always be used. The examples of intrinsic healing are the formation of primary or secondary chemical bonds, physical interactions such as wetting or adhesion between the interfaces of the crack.
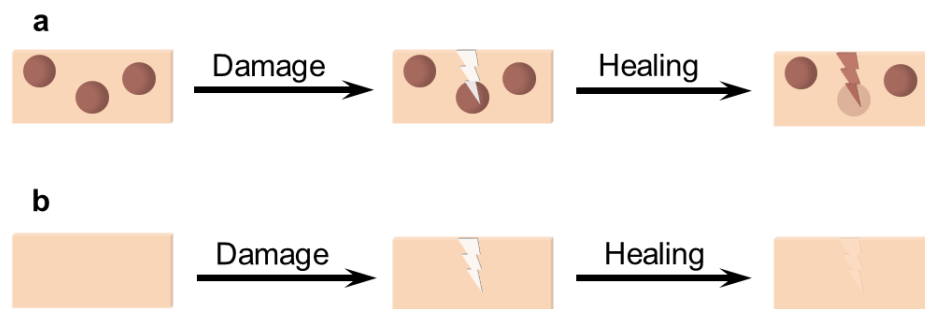
Figure 7. "Extrinsic" (a) and "intrinsic" (b) self-healing concepts. In case of "extrinsic" healing repairing based on external components intentionally embedded into the matrix (a); by "intrinsic" healing material itself possesses repairability without any separate healing agent (b).

Due to an intensive research within the last 15 years, several different concepts for self-healing materials in different classes (i.e. polymers, polymer composites, metals and ceramics) are developed. In this part some of the recent developments in the design of self-healing polymers and their composites are discussed.

Polymers and their composites are widely used nowadays in the coatings industry (e.g. lacks and covers for transport vehicles), civil engineering an electronics. Nevertheless, as many other materials, polymers can also be destructed during the service lifetime by different factors such as mechanical load, influence of thermal and chemical factors as well as UV-irradiation [29]. As a

result of the influence of external stress, a formation of microcracks can occur, which could be very critical for a polymer coating. For the visible or detectable damages in polymer materials different repairing techniques can be applied.

General classification of the methods of repairing and self-healing of polymers based on autonomic / non-autonomic and extrinsic / intrinsic concepts presented on Figure 8.
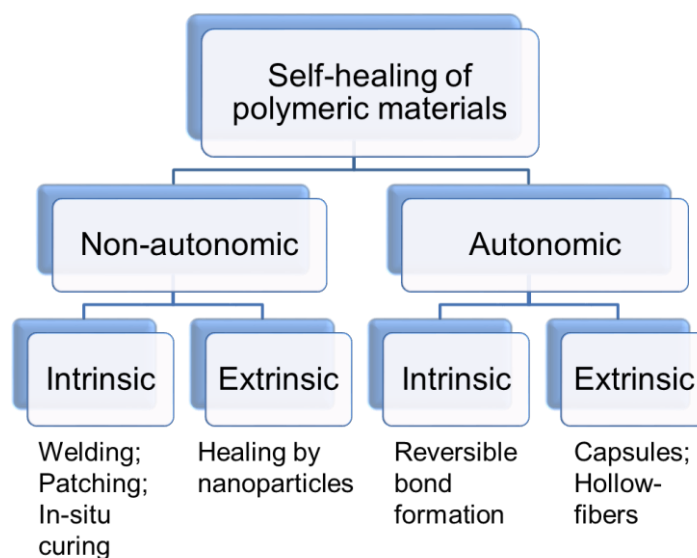
Figure 8. General classification of self-healing approaches for polymeric materials.

Further description of self-healing polymer and its composites is done according this classification, although some of transformations such as repairing by reversible bond formation may occur without external stimuli like heat (autonomic intrinsic healing) or under heating (non-autonomic intrinsic healing).

Non-autonomic healing

Non-autonomic approaches of the self-healing were the first widely investigated group of self-healing methods. **Intrinsic non-autonomic repairing approaches**, also named as traditional methods of healing of the polymer composites, includes welding, patching and in-situ curing of a new resin. Welding enables the rejoining of fractured surfaces or fusing of new materials to the damaged region of the polymer composite [30]. During welding the chain entangles [31] between two contacting polymers by passing through two polymer surfaces with a series of transactions, which include surface rearrangement, surface

approach, wetting and diffusion [32, 33] and initial physical properties of the damage area are recovered [32, 34]. After the formation of an entanglement of the polymer chains the process can be considered as complete. The main factors influencing this process are temperature [35, 36], surface roughness [37, 38], possibility of chemical bonding between the surfaces [39] and the presence of solvents [40, 41]. The main application of welding is presented in the field of repairing of thermoplastic materials [42, 43].

Patching based repairing involves the covering or replacing of the damaged material with a new one, which can be attached mechanically or by adhesive bonding to provide stiffness for the damaged site. The repairing by patching can be achieved by direct attachment of superficial patches [44] or by removal of the damaged material followed by an attachment of superficial patches with or without an additional replacement material [45, 46].

In-situ curing of a new resin is similar to patching because a new material is used for preserving the mechanical stiffness. Direct addition of the uncured resin to the damaged region of a composite is used in some patching techniques [47-49]. Due to a diffusion of the uncured resin into damaged component, adhesive forces allow to hold the patch in place [50].

Traditional methods for the repairing of thermoplastics include, firstly, bonding through fusion according to different welding types (e.g. resistance heating or ultrasonic welding) and, secondly, adhesive bonding and mechanical fastening (e.g. riveting) [30].

Nonetheless, all of the traditional repairing methods described above are not effective for healing of invisible microcracks and, additionally, they require reliable detection techniques and qualified work. As a mean of healing of invisible microcracks in polymeric composites the self-healing concept was proposed [37] and is now widely used for either thermoplastic or thermoset materials.

Self-healing of thermoplastic polymers is a well-known process and can be achieved by different mechanisms, which include molecular interdiffusion, photo-induced healing, recombination of the chain ends, healing by reversible bond formation under heating (this approach can also be performed at ambient temperature and it is described in section devoted especially autonomic self-healing), living polymer approach and self-healing by nanoparticles [30].

Healing of thermoplastic polymers by molecular interdiffusion was strongly investigated in the last two decades of the 20th century. It was found, that after two pieces of the same polymer are brought into contact at a temperature above its glass transition, the interface gradually disappears and the crack further heals by molecular interdiffusion across the interface. Influence of different ambient parameters such as temperature, pressure, healing time [51] and the presence of solvent [40] as well as properties of the polymers themselves (e.g. molecular weight) [51], were investigated in terms of the healing process.

Photo-induced healing can be achieved by an addition of photochemical groups (e.g. cinnamoyl groups) to the polymer. The healing process in this case is successful if a proper light wavelength (mostly UV-light is used for healing) is selected and the efficiency of the healing can be improved by additional heating [52]. Photo-induced healing is limited by the illuminated surface area and cannot be used for the healing of internal damage.

Structural (strength) and molecular (chain scission) damages can be healed by a technique, which involves a recombination of chain ends. This healing procedure can be applied for a certain type of thermoplastics (e.g. polycarbonate and polybutalene terephthalate) that are capable of recombinating chain ends via a specific reaction mechanism [53, 54].

Living polymer approach was proposed for providing protection against damages related to ionizing radiation [55]. In this method living polymers with a number of macroradicals (polymer chains containing radicals) are used as matrix resins. The chain ends of the living polymers possess an ability to resume the polymerization if an additional monomer is added to the system. Radicals can be generated by an exposure to ionization or UV-irradiation (damage factors) and directly recombine with each other.

Using nanoparticles to repair cracks in a polymeric matrix is an emerging and interesting approach for the design of self-healing materials. It can be considered as an example of **extrinsic non-autonomic healing approach**. It does not involve breaking and rejoining of polymer chains, however, rather it uses a dispersed particulate phase to fill cracks and flaws as they occur. First attempts were made by a computer simulation of the self-healing process [17, 19]. The modeling results indicate that nanoparticles have a tendency to be driven towards the damaged area by a polymer induced depletion attraction and the

system nanoparticles-polymer can potentially heal multiple times, as long as the nanoparticles remain available within the material. After the particle migration has occurred, the system can be cooled down and / or solidified, that effectively repairs the flaws in the damaged surface. Gupta et al [18] experimentally confirmed some aspects of the computer simulation and demonstrated the migration and clustering of the embedded nanoparticles around the cracks in a multilayer composite structure. It was also shown that smaller particles are more effective than larger ones for the migration to the damaged region at relatively short time scales due to an easier diffusion, though the computer simulation predicted an opposite behavior [19].

Nanoparticle filler

Propagating crack tip

Particles driven
to pre-craze region

Crack with nanoparticles
migrating to edge

Nanoparticles segregated in
pre-crazes beside the crack

Crack with nanoparticles
preferentially located
in damaged areas

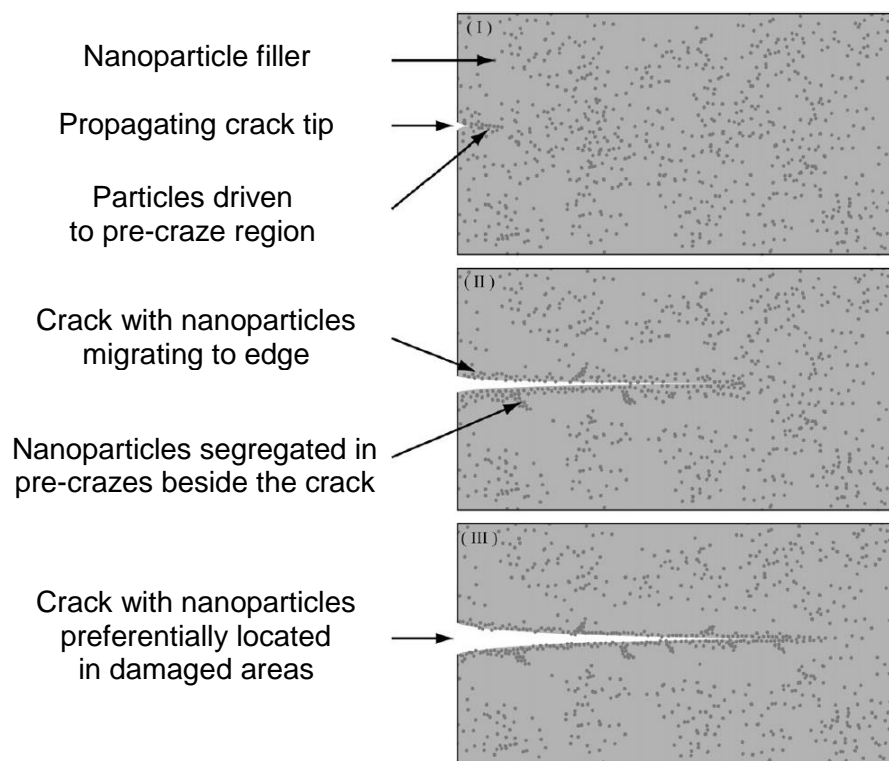**Figure 9.** Schematic diagram of nanoparticle movement during crack growth in thermoplastics [56].

The phenomenon of self-healing by nanoparticles has been explained by Lee et al [56]. The polymer chains close to the nanoparticles can be stretched and extended, driven by the tendency to minimize nanoparticles-polymer interactions via segregation of the nanoparticles in the crack and pre-crack regions (Figure 9).

Other example of extrinsic non-autonomic healing is utilizing of thermoplastic additives for the design of thermoset self-healing materials which was firstly reported by Zako et al [57]. In this approach incorporated thermoplastic particles melt upon applied heat and fill the damage sites of the thermoset polymer matrix (e.g. thermoplastic epoxy particles in a glass fiber-reinforced epoxy composite). Further investigations were made by Hayes et al [58, 59]. Instead of inclusion of the thermoplastic, these authors proposed to use a "solid solution" of the thermoplastic and thermoset polymers. In this case polymers should be compatible to each other and chemically not react at ambient temperature, glass temperatures of thermoplastic and thermoset have to be similar and the molecular weight of thermoplastic additives has to be in balance to provide good mechanical properties and a rapid healing ability. Towards this approach, an epoxy containing polybisphenol-A-co-epichlorohydrin composite was reported [58] as model system.

Autonomic healing

Autonomic healing approaches are suitable both for some groups of thermoplastic and thermosets. Generally methods for the preparation of thermoset materials with a self-healing ability differ from the approaches used for the preparation of thermoplastics due to the rigidity and thermal stability of thermosets and because thermosets a possess crosslinked molecular structure. The most common approaches for the autonomic self-healing of such kind of materials involve incorporation of a self-healing agent within a brittle vessel prior to the addition of these vessels into the polymer matrix (**extrinsic autonomic self-healing**). The vessels fracture upon loading of the polymer, releasing the low viscosity self-healing agents to the damaged area for further curing and filling of the microcracks. The following approaches are used for the preparation of self-healing thermoset materials: hollow fiber approach, microencapsulation, using of thermally reversible crosslinked polymers, inclusion of thermoplastic additives, chain rearrangement and metal-ion-mediated healing [30]. Self-healing with shape memory polymers or swollen materials and self-healing via passivation can also be added to the list [30].

In the hollow-fiber approach healing takes place when the healing agent is released from the hollow fibers in order to fill internal flaws and perform an in situ cure. This concept has been initially applied to cementitious materials to alter the

cement matrix permeability, repair cracks and prevent corrosion and was then further extended for polymer materials [60-62], for example, an epoxy composite incorporated with small hollow glass fibers [63, 64]. Although the idea of the hollow approach is very interesting, this concept may not be suitable for healing on a smooth surface due to large diameters of the fibers. Furthermore, Li et al [65] have shown that the introduction of large hollow fibers in a brittle matrix with the achievement of a certain level of healing negatively affects to the mechanical properties of the system due to a high stress concentration.

The most studied approach in recent years is microencapsulation. Basically, this approach involves incorporation of a microencapsulated healing agent and dispersed catalyst within a polymer matrix (Figure 10).
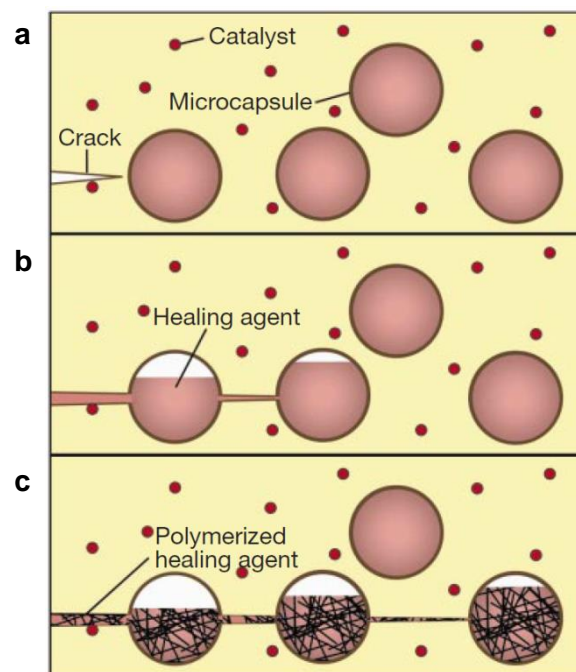
Figure 10. The autonomic healing concept. A microencapsulated healing agent is embedded in a structural composite matrix containing a catalyst capable of polymerizing the healing agent. a) Cracks form in the matrix wherever damage occurs; b) the crack ruptures the microcapsules, releasing of the healing agent into the crack plane through capillary action occurs; c) the healing agent contacts the catalyst, triggering polymerization that bonds the crack faces closed [66].

This technique is mostly applicable for systems based on the ring-opening metathesis polymerization with bis(tricyclohexylphosphine) benzylidine ruthenium(IV) dichloride (Grubbs' catalyst) and dicyclopentadiene [66-78] or 5-ethylidene-2-norbornene [73] or their blends [74]. Protection of either the healing

agent or the catalyst and manufacturing of the effective self-healing microcapsules are required for this type of systems. A suitable self-healing system should be easily encapsulated, remain stable and reactive over the whole service lifetime and respond quickly to repair damage once triggered. The resulting microcapsules need to possess sufficient strength to remain intact during processing of the polymer matrix, rupture in the event of the crack, be capable of releasing the healing agent or catalyst into the crack and have minimal adverse influence on the properties of the neat polymer resin or reinforced composite [30]. Microencapsulation based on a polycondensation reaction is reported for di-n-butyltin dilaurate as catalyst and a mixture of hydroxyl end-functionalised polydimethylsiloxane and polydiethoxysiloxane [79] and epoxy (healing agent)-amine (catalyst) [80-82] systems. The main advantages of the technique proposed by Cho et al [79] over ring-opening metathesis polymerization mentioned above are: the healing chemistry remains stable in humid ambient conditions; availability of the healing chemical, its low cost and simplicity of the process; an easy application of the healing agent into the polymer matrix.

Finally, as it was mentioned by White et al [66], the microencapsulation approach is also potentially applicable to other brittle materials such as ceramics and glasses.

Some polymer classes possess an ability for autonomic regeneration without external components (**autonomic intrinsic self-healing**). In the approach, called self-healing via reversible bond formation, the chain mobility in the thermoplastics is used to heal damages at ambient temperature by an inclusion of reversible bonds (e.g. hydrogen or ionic bonds) in the polymer matrix. This method can be used for the design of repairable organo-siloxane polymers [83] or ionomers [30] (Eisenberg et al [84] classified ionomers as polymers comprising of less than 15 mol% ionic groups along the polymer backbone). However, sometimes an external energy (heat or UV-light) is needed for healing [83]. In that case this process should be classified as non-autonomic.

There are also some examples, when using thermally reversible cross-linked polymers there is no necessity of incorporation of the healing agent or catalyst in the polymer matrix, although heat is required for the initiation of the repairing process. As it was mentioned in several publications [85, 86], this class can be considered as autonomic self-healing materials provided that the heat source

is integrated into the system. Chen et al [85, 86] has demonstrated the self-healing behavior of a cross-linked composite by using a thermally reversible Diels-Alder reaction and a mixture of furan-based and maleimido-based monomers. Epoxy-based precursors for the preparation of furan and maleimide monomers are reported by Liu et al [87, 88]. Using 2,2,6,6-tetramethylpiperidine-1-oxy-containing alkoxyamine derivatives as junctions between the polymer segments is an alternative to the Diels-Alder reaction and another way for the preparation of thermally reversible cross-linked polymers [89-92]. When the heat is applied, the junction groups disconnect and then reconnect with both similar and not similar sites. However, the healing process only takes place in anisole at 100 °C.

Healing of thermosets has also been shown on the example of rearrangement of polymer chains at ambient or elevated temperatures. Yamaguchi et al [93] presented a self-healing thermoset based on molecular interdiffusion of dangling chains, whose number could be varied by the crosslinking ratio. In this case polyurethane network was made by using a tri-functional polyisocyanate, polyester-diol and dibutyl-tin-dilaurate catalyst.

Self-healing via metal-ion – mediated reactions was developed for the repair of lightly crosslinked hydrophilic polymer gels [94, 95]. In this technique metal-ions incorporated into a hydrogel (e.g. gel based on acryloyl-6-amino caproic acid [94]) help to rearrange the crosslinked network. However, properties of the repaired material differ from initial one.

Approaches based on the employment of shape memory alloys [96-98], passivating additives and water absorbent matrices for the design of self-healing thermosets are different from the ones described above, because in these methods structural defects are not repaired. Although, other properties such as smoothness and permeability can be recovered [30].

2.1.3 Superhydrophobic interfaces

The first appearance superhydrophobicity was found on the lotus leaves, hence, several effects related with superhydrophobic behavior are called lotus effects. On the lotus leaves water droplets roll off and remove contaminations. This self-cleaning effect is connected with a combination of intrinsic hydrophobicity and surface roughness [3]. Superhydrophobicity is mostly

characterized by means of contact angles (especially advancing and receding contact angles) and contact angle hysteresis.

Young [99] was the first to propose a model of wetting for an ideal smooth and chemically homogeneous flat surface by operating with the term "contact angle" (an angle measured through the liquid at the triple point where liquid/vapor interface meets a solid surface):

Equation (1)
$$\cos\theta_{flat} = \frac{\gamma_{sv} - \gamma_{sl}}{\gamma_{lv}},$$

where γ_{sv}, γ_{sl} and γ_{lv} are the interfacial tensions of the solid-vapor, solid-liquid and the liquid-vapor interface, respectively, and θ_{flat} – the contact angle. Nevertheless, the wetting phenomena of non-ideal surfaces is more complex due to roughness and chemical heterogeneity of these surfaces.

Wenzel [100] and Cassie et al [101] were the first who investigated the problem of wetting on rough surfaces. Two general cases were explored either the water fills the grooves of a rough surface, or the water drop remains on top of the asperities (Figure 11).
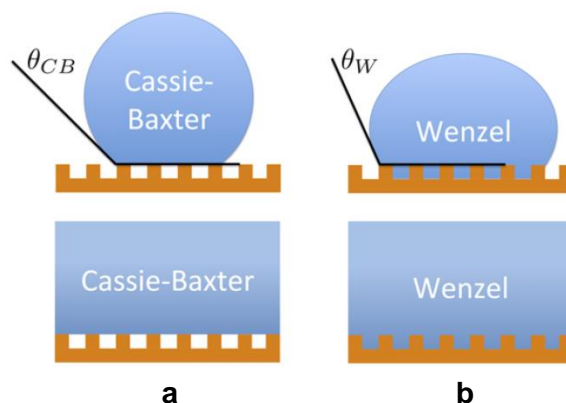
Figure 11. Illustration of Cassie-Baxter (a) and Wenzel (b) states. θ_{CB} and θ_W refer to the contact angles on rough substrate for Cassie-Baxter and Wenzel states respectively [102].

Two equations (2) and (3) for Wenzel and Cassie-Baxter cases, respectively, were derived:

Equation (2)
$$\cos\theta = r_s \cos\theta_{flat}$$

Equation (3)
$$\cos\theta = f \cos\theta_{flat} + f - 1$$

Combining equations (2) and (3), the general equation can be obtained:

Equation (4) $$\cos\theta = r_s f \cos\theta_{flat} + f - 1,$$

where r_s is the roughness factor, i.e. ratio between actual area and projected one, f – fraction of the solid material under the droplet (this parameter varies from 0 – drop does not touch the interface; to 1 – spreading); θ_{flat} – intrinsic liquid contact angle of a flat surface made of the same material, and θ – measured apparent contact angle on a non-ideal rough interface. This is also can be illustrated as dependence of $\cos\theta$ from $\cos\theta_{flat}$ and four different cases of wetting may occur (Figure 12) [103, 104].
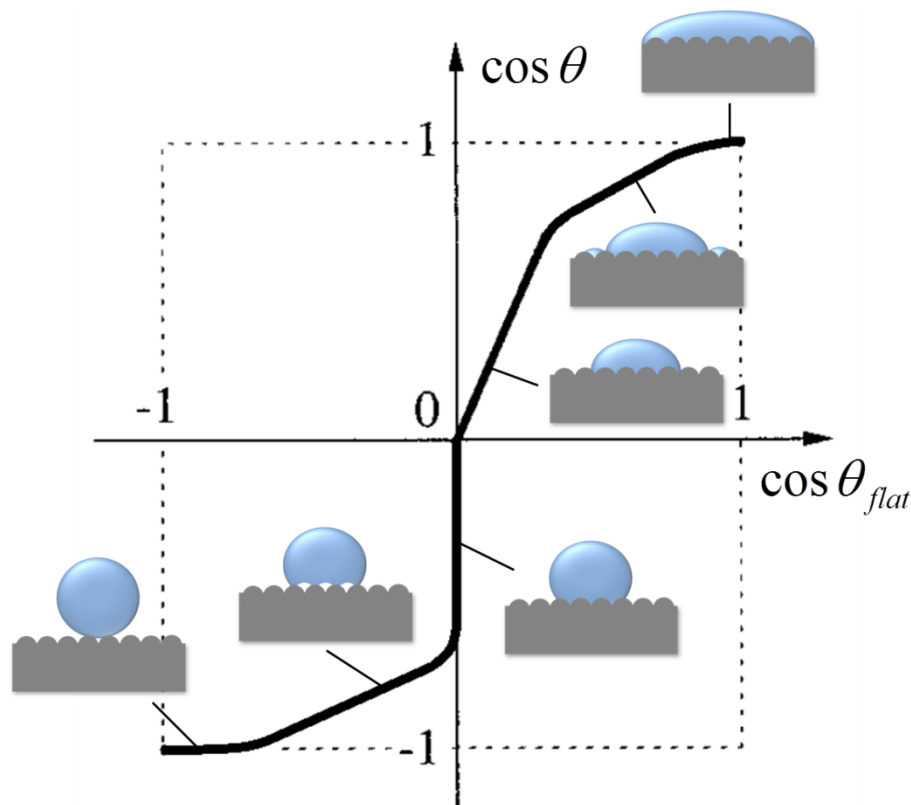
Figure 12. Schematic illustration theoretically predicted dependence $\cos\theta$ vs $\cos\theta_{flat}$.

According to theoretical predictions, roughness makes hydrophobic and hydrophilic surfaces more hydrophobic and hydrophilic, respectively. Nevertheless, experimental results have demonstrated some differences from the theoretical predictions described above. Thereby, attempts to improve the general Cassie-Baxter/Wenzel concept, as well as propositions for alternative

models were made. For instance, recently Extrand [105, 106] suggested that the contact line instead of contact area determines the wetting properties.

Along with further observations of superhydrophobic surfaces, the concept of contact angle hysteresis was developed for the characterization of wetting properties of a solid-liquid interface. Hysteresis occurs due to inhomogeneity (roughness as well as heterogeneity) of the surface. In case of an ideal (clean, planar and smooth) surface a contact angle θ_{flat} can be observed for a liquid droplet, which refers to the contact angle in Young's equation. In most situations the static contact angle does not turn out to be unique due to interfacial defects that are either chemical (stains, blotches) or physical (irregularities) [107]. During the inflation of the droplet its volume as well as the contact angle will both increase, but the contact angle area of the droplet on the surface will not change until it begins to advance. Eventually, the contact angle reaches a threshold value θ_{adv} – advancing contact angle – beyond which the contact line finally does move. Similarly to this, the threshold contact angle obtained during deflation, when the volume of the droplet as well as the contact angle will decrease, but the contact area will not change until the droplet begins to recede, corresponds to the receding angle [108-110] ‡. The difference between advancing and receding contact angles is called contact angle hysteresis [111, 112]. As a metastable droplet recedes on a solid surface, the contact angle can be at any value between the receding and advancing contact angles, while the contact angle hysteresis values may vary from less than 5° [113] to up to 40° [114]. Gupta et al [115] mentioned, that it is not possible to achieve contact angle hysteresis less than 1°, even by controlling the surface on a molecular scale, due to a certain roughness and heterogeneity. According to this point, it is not only the static contact angle but also the contact angle hysteresis that can characterize a surface, demonstrating its wettability [107]. Keeping that in mind a surface with advancing and receding contact angles above 150°, low contact angle hysteresis (< 5°) and low roll-off angle (below 10°) is considered as superhydrophobic [116].

As it was already mentioned, roughness play very important role for the design of superhydrophobic surfaces. Some theoretical predictions based on Wenzel (2) and Cassie-Baxter (3) equations shows that the values of contact

---

‡ Some additional explanations about advancing and receding contact angles are described in section 2.2.3.

angles (advancing and receding) are strongly depended on surface roughness [117]. So, quite hydrophobic flat surface with contact angle around 120° can become superhydrophobic after surface structuring. Although specific roughness ration should be keep in order to obtain superhydrophobicity (Figure 13).

Superhydrophobic surfaces are promising for a wide range of applications in non-wetting [118-122], self-cleaning [123-129], anti-fogging [130], anti-icing [131-137], buoyancy [138-140], corrosion-resistant [141-145], anti-biofouling [146], oil-water separation [147-152], low adhesion [2, 124, 153] and drag-reducing fields [154-156].
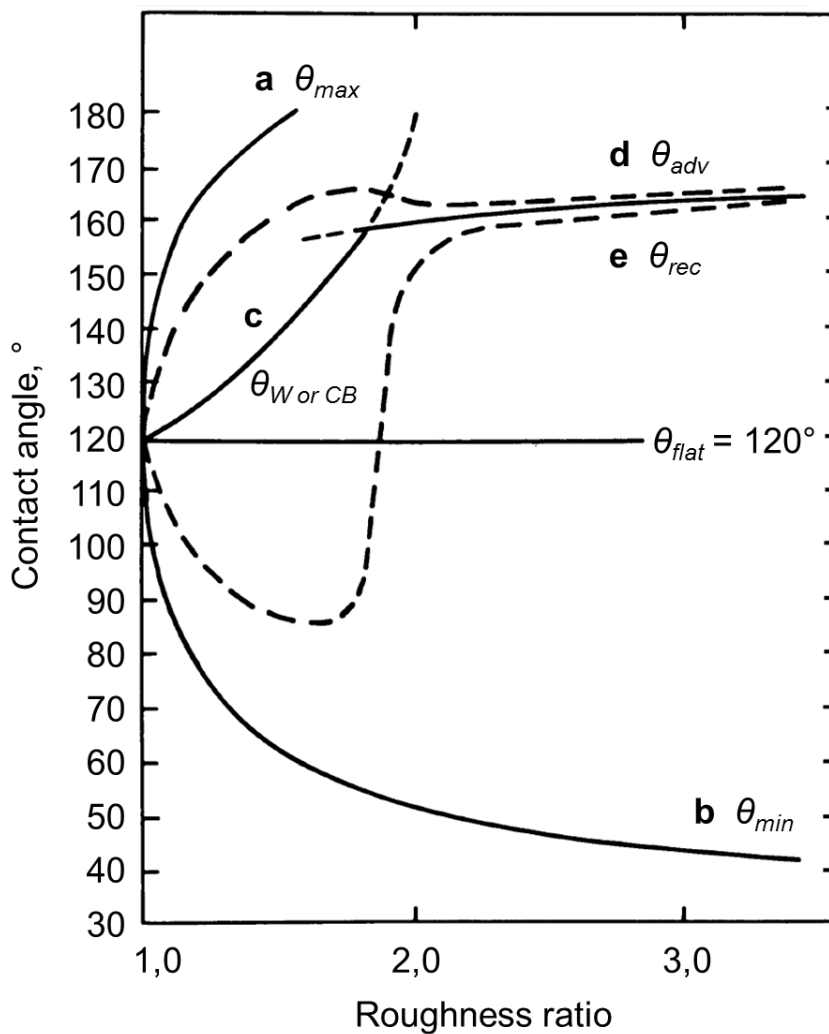
Figure 13. Effect of roughness on contact angle applying for flat surface with θ_{flat} = 120° calculations based on Wenzel and Cassie-Baxter approaches [117]: Maximum (θ_{max}, a) and minimum contact (θ_{min}, b) angles; most probable contact angle ($\theta_{W\ or\ CB}$, c) – lower part of curve calculated from Wenzel equation, upper – from Cassie-Baxter equation; possible curves for advancing (θ_{adv}, d) and receding (θ_{rec}, e) contact angles.

Fabrication of superhydrophobic surfaces

There are different approaches used for the preparation of surfaces with hierarchical roughness, which also possess intrinsic hydrophobicity (i.e. hydrophobic polymers such as polydimethylsiloxane or polytetrafluoroethylene). Both of these strategies lead to getting superhydrophobic surfaces. Phase separation [157], electrochemical [158] / chemical vapor deposition [159], template [160, 161] and plasma [162] methods, crystallization control [163], wet chemical reactions [164], sol-gel processing [165-168], lithography [127], electrospinning [169] and solution immersion [170] are commonly used for obtaining structured surfaces, which also possess the superhydrophobicity feature. However, several methods listed above are limited by up-scaling difficulties, a necessity for special equipment for the preparation or even impossibility of outdoor use.

Thus, the use of colloidal particles for the preparation of superhydrophobic surfaces [20-24] has several advantages. Firstly, particles with different size and surface chemistry can be synthesized. Furthermore, particles may be dispersed in liquids and deposited outdoors on large areas at low cost. Hierarchical topography of the surfaces incorporated with particles could be either achieved by assembling the particles into agglomerates [21, 22] or by using particles with special shapes (i.e. raspberry-like particles – colloidal particles coated with smaller ones) [23, 24].

2.1.4 Preparation of self-reparable superhydrophobic materials

Generally, superhydrophobic surfaces do not possess a resistance to damages, and after the topmost layer is damaged, superhydrophobicity can be lost. This problem can be solved by combining self-healing methods for repairing of the polymer matrix and the top layer with methods for the preparation of superhydrophobic surfaces. Although, technical difficulties and expenses do not allow to get such products with both properties easily. There are several approaches reported in recent years for the design of materials with repairable or durable properties [171, 172], Figure 14.
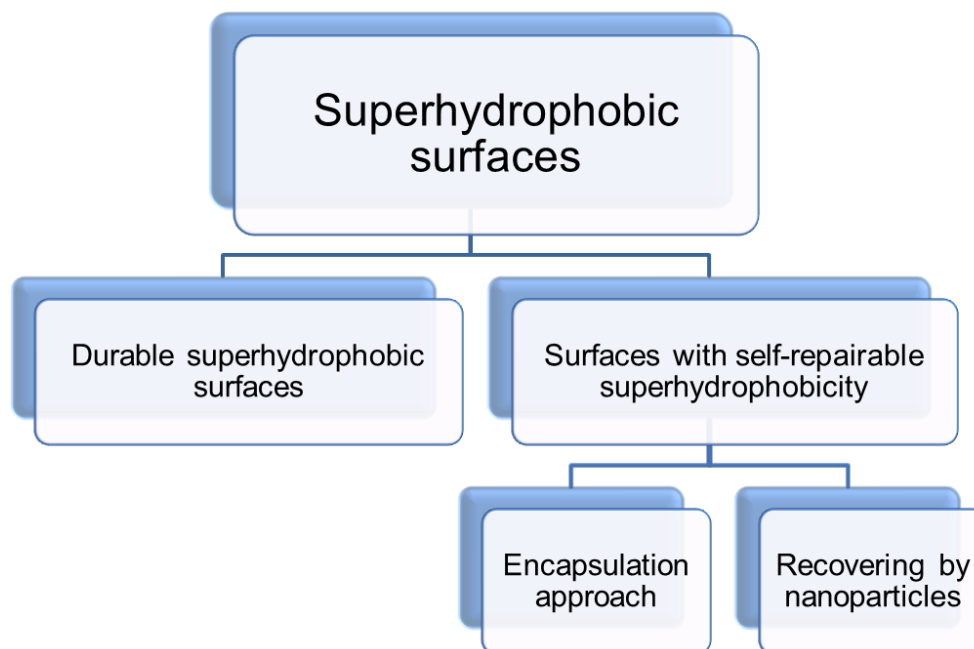
Figure 14. Schematic concepts for preparation superhydrophobic surfaces with long service lifetime.

The first concept for **increasing the service lifetime of superhydrophobic surfaces** is based on using durable materials [173]. For example, Su et al [174] reported about the fabrication of durable superhydrophobic coatings by using polyurethane with polydimethylsiloxane (PDMS) side chains. For the fabrication of polymer replica porous aluminium was used as a template. PDMS side chains provide superhydrophobic properties due to their very low surface tension.

Another technique for recovering superhydrophobicity is based on using easily repairable superhydrophobic materials and involves deposition of a new top layer. Such materials can be prepared by deposition of metal alkylcarboxylates, stearates [175, 176] and palmiates [177, 178] or by deposition of silver and perfluorodecanethriol [179] that forms a rough fractal surface on initially hydrophobic surfaces (Figure 15). The damaged surface (e.g. by scratching) can be easily recovered by spraying a new material on the damaged area.
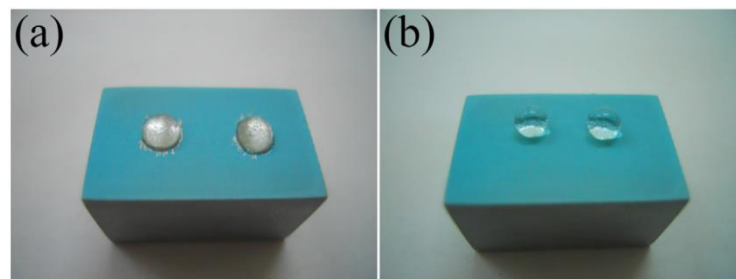
Figure 15. Illustration of the approach based on easily recoverable superhydrophobicity. Photographs of water droplets (a) on the surface partially damaged by scratching and (b) on the surface regenerated by freshly sprayed copper stearate suspension [176].

Generally, two approaches are used for the preparation of self-healing superhydrophobic materials. The first one is based on **encapsulation of a hydrophobic component in the pores of rough nanoporous materials**. Consequently, it recovers superhydrophobicity by quick migration to the surface after damage. Li et al [180] suggested an encapsulation of a highly reactive 1H,1H,2H,2H-perfluorooctyltriethoxysilane (POTS) in coatings with hierarchical structures prepared by layer-by-layer assembling of poly(allylamine hydrochloride) (PAH) and sulfonated poly(ether ether ketone) (SPEEK) with poly(acrylic acid) (PAA). The working principle of the obtained material is presented in Figure 16.
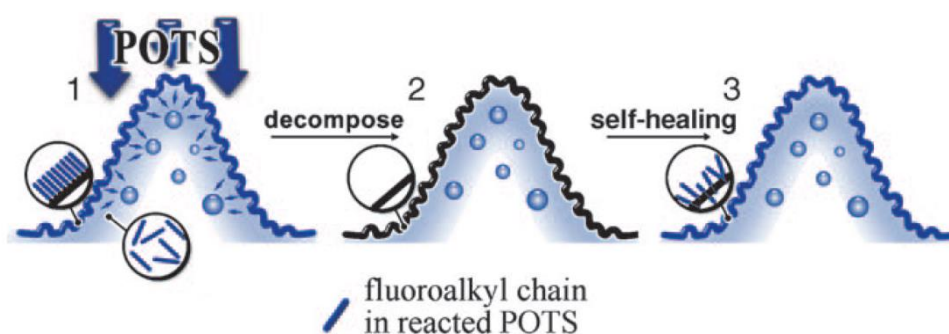
Figure 16. The working principle of self-healing superhydrophobic coatings. (1) A porous polymer coating with hierarchical structures at micro- and nanoscales can preserve an abundance of healing agent – fluoroalkylsilane; (2) the top fluoroalkylsilane layer is decomposed and the coating loses its superhydrophobicity; (3) the preserved healing agent can migrate to the coating surface and reveal superhydrophobicity [180].

The surface was damaged by a treatment with oxygen plasma and superhydrophobicity was completely lost. However, initial properties were

spontaneously recovered within time due to a migration of POTS to the interface. The same concept was used by Wang et al [181] for the preparation of a self-healing fabric. The authors used fluorinated-decyl polyhedral oligomeric silsesquioxane (FD-POSS) and fluorinated alkyl silane (FAS) as healing agents. The prepared coating possessed both superhydrophobic and superoleophobic properties, which could be restored after different types of damage (e.g. by acids, UV-light and abrasion). Nanoporous aluminium filled with perlfuorooctyl acid also possessed self-healing superhydrophobicity [182]. After a treatment of samples with oxygen plasma or abrasion migration of the acid occurred and initial properties were restored. The same working principle was used for preparation of the coating based on silica particles filled octadecylamine [183].

The second group of methods for the **preparation of self-healing superhydrophobic surfaces** is based on **using colloidal particles**. Colloidal particles possess an ability to spontaneously self-organize at interfaces and this property can be used for the design of superhydrophobic films. Recently, it was demonstrated that colloidal particles can dramatically affect the surface properties of liquids, i.e. highly hydrophobic particles segregate at the air-liquid droplets interface and form so-called liquid marbles (liquid droplets surrounded by hydrophobic particles) [184]. In another set of experiments it was demonstrated that, while floating on the water surface due to surface tensions, hydrophobic metallic particles [185] or porous Janus microparticles [186] formed a freely floating superhydrophobic self-cleaning layer. Deposition of load on such particle film does not result in increased interparticle distances in the areas where the film is extended, nor in the formation of wrinkles where the film is contracted. Particles reorganized into new close-packed layers with appropriate geometry. They recover superhydrophobicity when the surface layer was damaged.

2.1.5 Surfaces with switchable wettability

Typically different responsive polymers or self-assembled monolayers as well as metal oxides are introduced for the preparation of switchable surfaces [187]. Different surface properties, such as wettability [188, 189], adhesion [190, 191], roughness [192, 193] and biocompatibility [194, 195], can be changed on a special prepared surface by applying an external stimuli like photoillumination [196], heat [197] or potential [198-200].

Metal oxides

Particularly, to prepare materials with switchable wettability, chemical composition and / or surface topography should be changed under an external stimuli. This can be done by applying different functional groups present in polymers on the rough surface or by preparing a rough surface based on metal oxides. In this case, under illumination intrinsic properties of the surface can be changed [13, 196, 201]. Titanium dioxide was broadly studied among the photo-sensitive inorganic semiconductors. After illuminating surface of titanium dioxide with UV-light, the photo-generated cavity will react with the lattice oxygen to form surface oxygen vacancies that can combine with water molecules to form hydroxyl groups. The hydroxyl groups can dramatically increase the surface energy and hydrophilicity due to a possible formation of hydrogen bonding, which was reported by several researchers [8, 202, 203] for the switching behavior of anatase polycrystalline films from 72° to 0° for water contact angles under irradiation by UV- and visible light. In other words, structural titanium dioxide surfaces possess a switching behavior between superhydrophobicity and superhydrophilicity [204]. Some other semiconductor oxides, specifically zinc oxide [205, 206], tungsten(VI) oxide [207], vanadium(V) oxide [208] and tin(IV) oxide, also have switchable wetting properties due to a similar mechanism.

Self-assembled monolayers (SAMs) and brushes

Photo-organic materials due to a reversible conformation change can also be used for the preparation of surfaces with switchable wettability. Azobenzene and some its derivatives are broadly used for these purposes [209, 210] due to possible trans- and cis-transformations occurring under illumination by UV-(trans- -> cis-) and visible-(cis->trans-) light. It was also shown that the trans-conformation has a small dipole moment and a low surface energy, where the cis-conformation possesses a large dipole moment and a little higher free energy [211]. Other functional groups such as spiropyrans [212], dipyridyletethylenes [213], stilbenes [214] and pymrimidines [215] can also be used for the initiation of transformations, which lead to the switching of wettability.

Interaction with the surroundings and the material is affinity with the environment can be regulated with temperature. Thus, temperature can play an important role in the regulation of the surface free energy and wettability [189]. This fact is used for the preparation of surfaces with switchable wettability by using

thermoresponsive polymers such as poly(N-isopropylacryl-amide) (PNIPAAm), which possesses lower critical solution temperature (LCST) [216-219]. Below the LCST, the intermolecular H-bonding between PNIPAAm chains and water molecules is predominant. The polymer is swelled in this state and, therefore, surfaces covered with PNIPAAm possess hydrophilic properties. On the other hand, above the LCST, intermolecular H-bonding among the PNIPAAm chains results in collapsed chain conformation and therefore hydrophobic character of the surface [220, 221]. In case of PNIPAAm, the switching behavior can be achieved just by applying temperature below and above the LCST and the wetting properties of interface can thus be tuned (Figure 17). Some other thermoresponsive polymers also possess the same temperature related wetting properties [189].
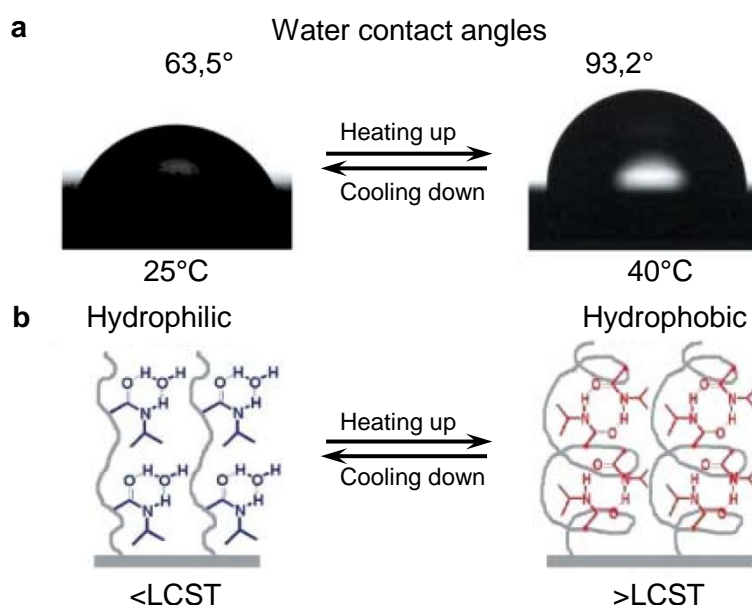
Figure 17. Thermally responsive wettability for a flat PNIPAAm-modified surface: (a) change of water drop profile when temperature was elevated from 25°C (left) to 40°C (right) with water contact angles of 63,5° and 93,2° respectively; (b) diagram of reversible formation of intermolecular hydrogen bonding between PNIPAAm chains and water molecules (left) and intermolecular hydrogen bonding between carbonyl and amino-groups in PNIPAAm chains (right) below and above the LCST, respectively [221].

Two classes of polyelectrolytes, namely, weak polyacids and weak polybases are used for tuning of the wetting properties by pH. At high pH values in the case of polyacids (low pH values in the case of polybases) electrostatic repulsion forces between the molecular chains dominate [222]. One of the

examples of such kind of transformation was show by Wang et al [223]. They used poly(styrene-methyl methacrylate-co-acrylic acid) crystal films in their experiments in the presence of sodium dodecylbenzenesulfonate. At pH 6, due to the formation of hydrogen bonds between carboxyl and sulfonate groups, long hydrophobic alkyl chains could be formed and exposed outside, leading to superhydrophobic properties of the surface. By base treatment the deprotonation of carboxylic groups and salt formation with sulfonic groups occurs, resulting in the switching of the surface properties to a hydrophilic state. Additionally, switchable wettability can be achieved by deprotonation and protonation of aminogroups in polydimethylaminomethacrylate grafted on anodized alumina [220]. Some other polycations [224, 225] and ionic liquids [226, 227] also possess a switching ability due to counterion exchange.

Moreover, switching of the surface wettability can be devised using heterogeneous or mixed polymer brushes [6] and some segmented copolymers [228-230] by treating them with different solvents. Due to a different solubility of the components and blocks, polymer chains can get different conformation and, thus, affect the surface free energy and wettability.

Wettability can also be tuned by using an optically active macromolecular compound that consists of chiral recognition, mediating and switching units [231]. Qing et al [231] reported that wettability of a textured silicon substrate covered with a copolymer, which contained optically active groups, can be switched between superhydrophobicity and hydrophilicity states under treatment with a D-luxose solution. This ability of the surfaces can be further used in chiral separation, smart microfluidic devices and bio-devices [232].

Systems with tunable electrical potential properties are responsible for fast changes in the chemistry, in some cases morphology and, therefore, wettability of the surface [233, 234]. Electrical potential responsive materials can be switched between reduction and oxidation states and change their wetting properties under regulation of the external electrical potential [235-237]. Wettability can be changed by alternating the external electrical field due to a decrease in the solid-liquid interfacial tension, related with the charge density across the solid-liquid interface [238-242]. In this case, no redox reaction occurs.

2.2 Experimental techniques and methodology

2.2.1 Introduction

There are several analytical methods used for the investigation of colloidal particles and composite surfaces incorporated with them. For example, particles size can be easily checked by scanning electron microscopy (SEM). SEM can also be used for the investigation morphology of the surfaces incorporated with particles. More information about topography and roughness can be acquired by using scanning force microscopy. Additional information about the surface roughness of the material can be obtained by optical imaging instruments such as MicroGlider.

Morphology and chemical composition of the surface strongly affect to the surface wettability. Wetting properties as well as superhydrophobic properties play a very important role in the design of materials with switchable wettability. Investigations of the surface wettability were performed by using water drop shape analysis.

Thus, a combination of different analytical techniques gives an opportunity to get more detailed information about the wetting properties of obtained surfaces and to characterize the particles used for the preparation of the surface.

In subsection 2.2.2 characterization methods used for the investigation of surface morphology are described. The wetting behavior measurement technique used in this work is elucidated in subsection 2.2.3. Null-ellipsometry, as a quick reference technique for the investigation of the polymer layer thickness on a planar surface, and other analytical techniques are described in section 2.2.4.

2.2.2 Characterization of surface morphology

In this work for characterization of surface morphology was performed by using SEM for routine measurements. SEM was also used for the control of particles sizes during their preparation due to convenient and fast measurement set-up.

To obtain more information about the surface morphology scanning force microscopy and optical measurement instruments such as MicroGlider were additionally used.

2.2.2.1 Scanning electron microscopy (SEM)

Scanning electron microscopy (SEM) can be used for the characterization of surface morphology due to an excellent visualization of the specimens and a high resolution down to the nanometer scale.

Modern scanning electron microscopes consist of two main components – the electron column and control console (PC). The electron column may be subdivided into an electron gun and two or more electron lenses, whitch influence the paths of the electrons traveling down an evacuated tube. The base of the column is usually taken up with vacuum pumps that generate a vacuum of about 10^{-4} Pa [243].

The basic principle of SEM is shown in Figure 18, but details of the electron-optical design may vary among different manufacturers.
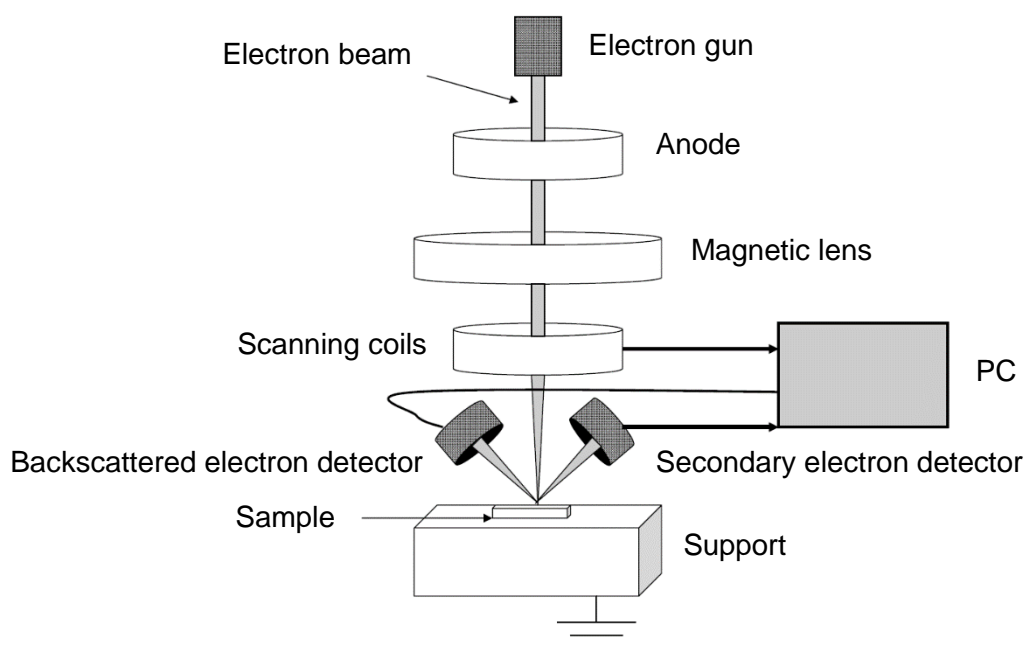
Figure 18. Basic principle of SEM [244].

The scanned image is formed point by point. The deflection system causes the beam to move to a series of discrete locations along a line and then along another line below the first, and so on, until a rectangular 'raster' is generated on the specimen. Simultaneously, the same scan generator creates a similar raster on the viewing screen. Two pairs of electromagnetic deflection coils (scan coils) are used to sweep the beam across the specimen. The first pair of coils deflects

the beam off the optical axis of the microscope and the second pair bends the beam back onto the axis at the pivot point of the scan (Figure 19). The magnification M of the image is the ratio of the length of the raster on the viewing screen to the corresponding length of the raster on the specimen (L). For instance, a 100-µm-wide raster on the specimen displayed on a 10-cm-wide viewing screen generates an image with 1000x magnification. During the increasing of the image magnification, the scan coils are excited less strongly, so that the beam can deflect across a smaller distance on the specimen. Note that the raster size on the specimen also depends on the working distance (the distance between a specimen and the bottom of the final lens). The magnification is automatically compensated for each working distance to assure that the indicated magnification is correct [243].
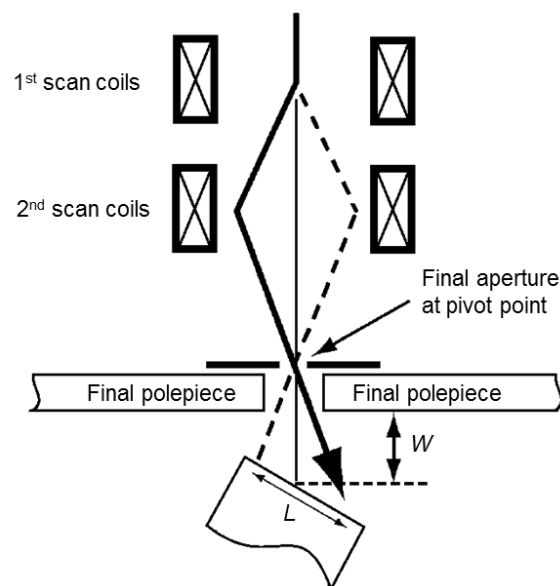
Figure 19. Deflection system inside the final lens. Working distance W is the distance between the specimen and the bottom of the final lens polepiece.

Image formation in the SEM is dependent on the acquisition of signals produced from the electron beam and the specimen interactions. These interactions can be divided into two major categories: elastic interactions and inelastic interactions. Elastic scattering results from a deflection of the incident electron by the specimen atomic nucleus or by outer shell electrons of similar energy. This kind of interaction is characterized by negligible energy loss during the collision and by a wide-angle directional change of the scattered electron.

Incident electrons that are elastically scattered through an angle of more than 90° are called backscattered electrons (BSE), and yield a useful signal for imaging the sample. Inelastic scattering occurs through a variety of interactions between the incident electrons and the electrons and atoms of the sample, and results in the primary beam electron transferring substantial energy to that atom. The amount of energy loss depends on whether the specimen electrons are excited separately or collectively and on the binding energy of the electron to the atom. As a result, the excitation of the specimen electrons during the ionization of specimen atoms leads to the generation of secondary electrons (SE), which are conventionally defined as possessing energies of less than 50 eV and can be used to image or analyze the sample. In addition to those signals that are utilized to form an image, a number of other signals are produced when an electron beam strikes the sample, including the emission of characteristic X-rays, Auger electrons, and cathodoluminescence. Figure 20 shows the regions from which different signals are detected [245].
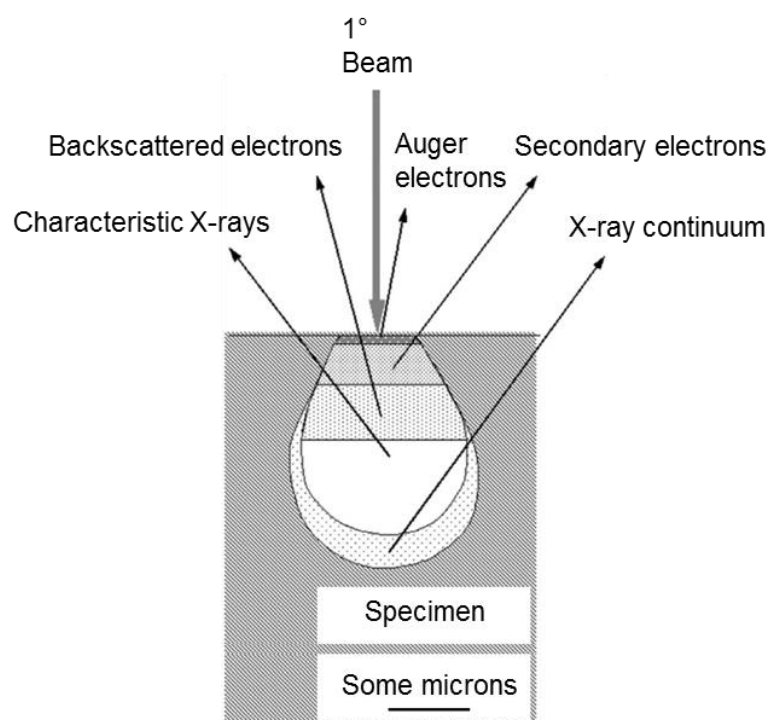

Figure 20. Illustration of several signals generated by the electron beam–specimen interaction in the scanning electron microscope and the regions from which the signals can be detected [245].

Widely differing energy characteristics of BSE and SE present a considerable challenge for the design of a detector that can use both of the signals. Alternatively, these differences permit the design of detectors that are selective for exclusively one of the signals and thus selective for specific specimen properties.

It was several years ago reported about a GEMINI principle of electron detection which is unique, because it uses a boosted detection lens, which projects the information from the only crossover – the focus – to the In-lens detector (Figure 21) [246]. The beam booster accelerates the electrons backwards while the optical principle of the GEMINI lens separates the different electron energies and brings them to different trajectories with different focal points. Due to this effect angle filtered information on different detectors at the beam axis is obtained. The real surface SE information is acquired on the In-lens detector, while the subsurface high angle and high resolution BSE information is projected to the PSF detector. Due to the fact that the GEMINI lens separates electrons with different energies (BSE, SE) because of its imaging principle, an energy filtered detection on different detectors can be obtained (Phase Space Filtered Detection – PSFD). This principle is used in the design of several Carl Zeiss microscopes and a typical scanning time for a picture is less than a second.

In this work scanning electron microscopy analysis was performed by using a NEON 40 workstation (Carl Zeiss AG, Germany), operating at 1 – 5 kV with SE2, In-lens and BSE detectors. To prevent the charging of the sample that can cause some image artefacts, the investigated samples preferably should be conductive. Non-conductive samples investigated in this work (different types of particles and particle-wax composites) were coated with metals such as platinum or gold by using a Leica EM SCD500 sputter coater connected with a Leica EM QSG100 thickness monitor in order to sputter an about 3 nm thick layer of metal from argon plasma. Cryo-transfer system Leica EM VCT100 was used for the preparation and transfer of some samples, which were investigated by cryo-SEM technique.
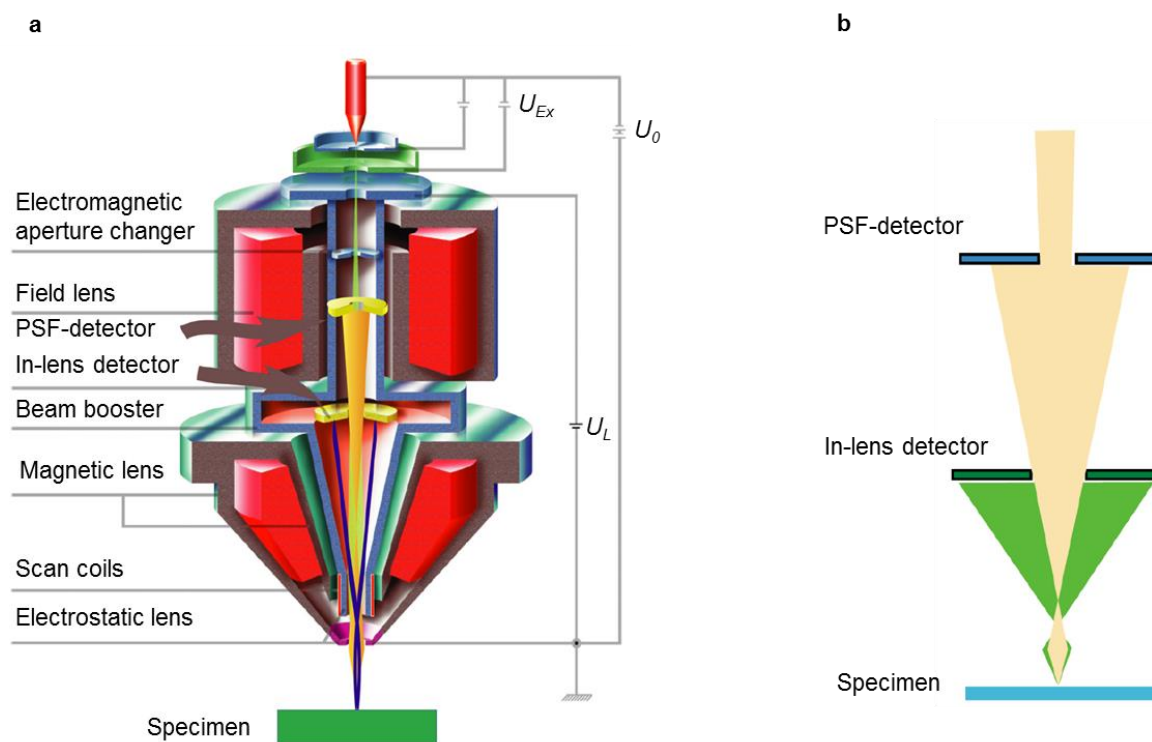
Figure 21. The GEMINI column: (a) general scheme of the GEMINI column; (b) scheme of In-lens and PSF detector.

2.2.2.2 Scanning force microscopy (SFM)

Generally, scanning force microscopy (SFM) or atomic force microscopy (AFM) is a form of scanning probe microscopy where a sharp probe is scanned across a surface and the probe/sample interaction is monitored (Figure 22) [247].
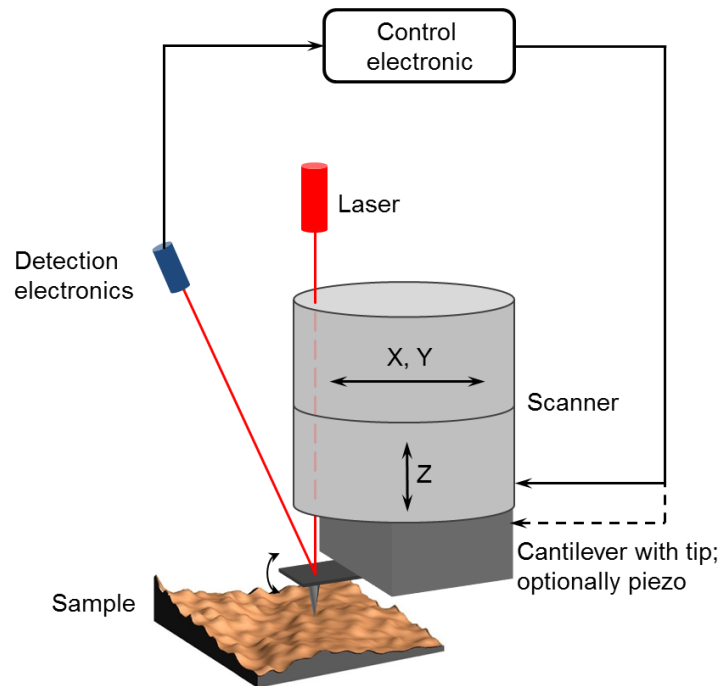
Figure 22. Schematic representation of AFM measurements.

Depending on the investigated material and the manner of scanning, AFM can be distinguished by different types of operation modes, such as contact, tapping and non-contact modes.

Contact mode AFM operates by scanning a tip attached to the end of a cantilever across the sample surface while monitoring the change in cantilever deflection with a split photodiode detector [247]. The tip contacts the surface through the adsorbed fluid layer on the sample surface. A feedback loop maintains a constant deflection between the cantilever and the sample by vertically moving the scanner at each (x,y) data point to maintain a "setpoint" deflection. By maintaining a constant cantilever deflection, the force between the tip and the sample remains constant. The force is calculated from Hooke's law:

Equation (5) $$F = -kx,$$

where F – force; k – spring constant and x – cantilever deflection. Sping constants usually range from 0,01 to 1,0 N/m, resulting in forces ranging from nN

to µN in an ambient atmosphere. The distance the scanner moves vertically at each (x, y) data point is stored by the computer to form the topographic image of the sample surface. Operation can take place in ambient and liquid environments. One of the examples of probes used for AFM contact mode is silicon nitride probes. For contact mode AFM imaging, it is necessary to have a cantilever which is soft enough to be deflected by very small forces (i.e. small force constant) and has a high enough resonant frequency to not be susceptible to vibrational instabilities. This is accomplished by making the cantilever short to provide a high resonant frequency and thin to provide a small force constant. For the silicon nitride tips, there are 4 cantilevers with different geometries attached to each substrate, resulting in 4 different spring constants (0,58; 0,32; 0,12; 0,06 N/m) with nominal tip radius of curvature 20 – 60 nm. Contact mode AFM possesses high scan speeds and with this technique images with "atomic resolution" can be obtained. However, lateral (shear) forces can distort some features in the image. Also, the forces normal for the tip-sample interaction can be high in air due to capillary forces from the adsorbed fluid layer on the sample surface. Additionally, the combination of lateral forces and high normal forces can result in reduced spatial resolution and may damage soft samples (i.e., biological samples, polymers, silicon) due to scraping between the tip and sample. These obstacles when using AFM Contact mode can be avoided by using TappingMode AFM or Non-contact AFM mode.

Tapping mode AFM operates by scanning a tip attached to the end of an oscillating cantilever across the sample surface [247]. The cantilever is oscillated at or slightly below its resonance frequency with an amplitude ranging typically from 20 nm to 100 nm. The tip lightly "taps" on the sample surface during scanning, contacting the surface at the bottom of its swing. The feedback loop maintains a constant oscillation amplitude by maintaining a constant root mean square (RMS) of the oscillation signal acquired by the split photodiode detector. The vertical position of the scanner at each (x, y) data point in order to maintain a constant "setpoint" amplitude is stored by the computer to form the topographic image of the sample surface. By maintaining a constant oscillation amplitude, a constant tip-sample interaction is maintained during imaging. Operation can take place in ambient and liquid environments. In liquid, the oscillation need not be at the cantilever resonance. When imaging in air, the typical amplitude of the oscillation

allows the tip to contact the surface through the adsorbed fluid layer without getting stuck. There are following examples of standard probes used for tapping mode: tapping mode etched silicon probes (also hardened ones), tapping mode focused ion beam (FIB) machined silicon probes and Olympus tapping tips. For instance, tapping mode etched silicon probes possess the following characteristics: spring constant 20 – 100 N/m; resonant frequency 200 – 400 kHz, nominal tip radius of curvature 5 – 10 nm. Thus, AFM tapping mode possesses higher lateral resolution on most samples (1 nm to 5 nm) and it is non-destructive for soft samples imaged in air due to lower forces. Also, lateral forces are virtually eliminated, so there is no scraping. But the scanning speed in tapping mode is slightly slower than in contact AFM mode.

In *Non-Contact mode* AFM no force is exerted on the sample surface [247]. The cantilever is oscillated at a frequency which is slightly above the cantilever's resonance frequency typically with an amplitude of a few nanometers (< 10nm), in order to obtain a signal from the cantilever. The tip does not contact the sample surface, but oscillates above the adsorbed fluid layer on the surface during scanning. The cantilever's resonant frequency is decreased by the van der Waals forces, which extend from 1 nm to 10 nm above the adsorbed fluid layer, and by other long range forces which extend above the surface. The decrease in resonant frequency causes the amplitude of oscillation to decrease. The feedback loop maintains a constant oscillation amplitude or frequency by vertically moving the scanner at each (x, y) data point until a "setpoint" amplitude or frequency is reached. The distance the scanner moves vertically at each (x, y) data point is stored by the computer to form the topographic image of the sample surface. However, applications for non-contact mode AFM imaging are limited due to several disadvantages. Firstly, it is the lower lateral resolution, limited by the tip-sample separation. Secondly, slower scan speed than in tapping mode and contact mode is used to avoid contacting the adsorbed fluid layer which often results in the tip getting stuck. Finally, non-contact mode is usually only operated on extremely hydrophobic samples, where the adsorbed fluid layer is at a minimum. If the fluid layer is too thick, the tip becomes trapped in the adsorbed fluid layer causing unstable feedback and scraping of the sample.

Very important parameters which can be evaluated by AFM image analysis are depth, height, width and angular values. Roughness measurements

can be performed over an entire image or a selected area. In this case, most common measurements are evaluation of the root mean square (RMS, R_q) roughness – standard deviation of the Z values within a given area:

Equation (6)
$$RMS = \sqrt{\frac{\sum_{i=1}^{N}(Z_i - Z_{Ave})^2}{N}} \; ,$$

where Z_{Ave} is the average Z value within the given area, Z_i is the current Z value and N is the number of points within a given area.

The mean roughness (R_a) represents an arithmetic average of the deviations from the center plane:

Equation (7)
$$R_a = \frac{\sum_{i=1}^{N}\left|Z_i - Z_{cp}\right|}{N} \; ,$$

where Z_{cp} is the Z value of the center plane, Z_i is the current Z value and N is the number of points within a given area;

R_{max} – the difference in height between the highest and lowest points on the surface relative to the mean plane;

Surface area – the three-dimensional area of a given region (the sum of the area of all of the triangles formed by three adjacent data points);

Surface area diff – the percentage increase of the three dimensional surface area over the two dimensional surface area.

All AFM-measurements were performed by using Dimension 3100 and Dimension V microscopes (Veeco, Digital Instruments, Inc., Santa Barbara, USA.) in tapping mode AFM. Obtained images were treated and analyzed with standard Veeco diNanoScope software 7.30 and WSxM 5.0 [248] software §.

2.2.2.3 Optical imaging instrument (MicroGlider)

With an optical imaging device such as MicroGlider (FRT, Fries Research & Technology GmbH, Bergisch Gladbach, Germany) it is possible to evaluate parameters like sample profile, topography, roughness, and coating thickness with enhanced accuracy **. Generally, the MicroGlider is a highly precise, multi-sensor measuring system for high flatness specification applications. This novel

---

§ WSxM software available from http://www.nanotec.es/products/wsxm/download.php (15.10.2013)
** Product info can be found at http://www.frt-gmbh.com/en/MicroGlider.aspx (15.10.2013)

optoelectronic device is based on a quasi-confocal, z-axis extended field. The instrument uses a chromatic white-light sensor (CWL), which is based on the principle of chromatic aberration of light. White-light is focused on the surface by a measuring head with a strongly wavelength-dependent focal length (chromatic aberration). The spectrum of the light scattered on the surface generates a peak in the spectrometer. The wavelength of this peak along with a calibration table reveals the distance from sensor to sample. The sensor works on transparent, highly reflective or even matt black surfaces. It is extremely fast and has virtually no edge effects. This method allows very high resolution due to a small spot and is suited for use in difficult ambient conditions. Due to its modified optical setup and its superluminescent diode, a high-resolution version of this sensor (CWL-HR) provides the highest lateral resolution of the family (sub-µm). Furthermore, it works on highly reflective as well as light absorbing and rough surfaces. It may even be used to measure the thicknesses of thin transparent films, as well as in nanotechnology or medical technology and life sciences.

This method can be used additionally to the AFM technique due to a large-scale vertical resolution (from 10 nm to 300 µm) of the optic imaging device. However, the lateral resolution is 1 – 2 µm (determined by the size of reflected light).

Samples with scanned area of 1x1 mm^2 and 0,26x0,26 mm^2 were investigated with the MicroGlider. The resolution of each image taken was 1000x1000 lines. The root mean square roughness was calculated from obtained images by using FRT Mark III software [††].

2.2.3 Wetting measurement techniques (Drop shape analysis)

Wettability is one of the most important interface properties that defines interactions between a solid interface and a liquid phase when they stay in contact. Usually, wettability can be characterized in terms of a contact angle. The term of contact angle and its different types have been already described in section 2.1.3.

[††] Trial version of Mark III software available at http://www.frt-gmbh.com/en/Mark-III.aspx (13.04.2013)

Generally the following methods are used for measuring the contact angle of a surface: static and dynamic sessile drop methods, dynamic Wilhelmy method and the single-fiber Wilhelmy method [249].

The dynamic Wilhelmy method can be used to calculate the average advancing and receding contact angles on solids of uniform geometry. Both sides of the investigated solid sample must have the same properties. The wetting force on the solid is measured as the solid is immersed in or withdrawn from a liquid of known surface tension. The single-fiber Wilhelmy method can be applied to single fibers for measuring the advancing and receding contact angles [249].

However, the most convenient is the static sessile drop method, where the angle formed between the liquid/solid interface and the liquid/vapor interface is measured using a microscope optical system, or with high-resolution cameras and software, to capture and analyze the contact angle. The dynamic sessile drop is similar to the static sessile drop but requires the drop to be modified. The largest contact angle possible without increasing its solid/liquid interfacial area is measured by adding volume dynamically (Figure 23). This maximum angle is the advancing angle, θ_{adv}. The volume is then removed to produce the smallest possible angle, the receding angle – θ_{rec}. The difference between the advancing and receding angles is the contact angle hysteresis. Additionally, the dynamic contact angle can also be measured for a drop travelling down a sloped flat surface as shown in Figure 23 [249].
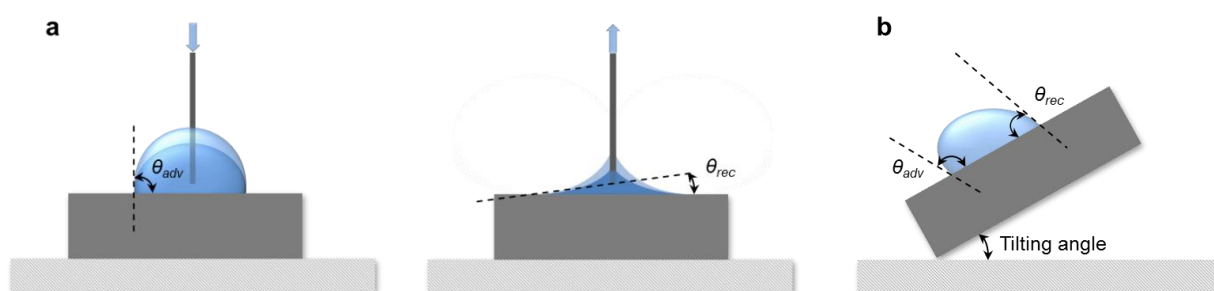

Figure 23. Different methods to measure the advancing and receding contact angle at solid surfaces: (a) dynamic sessile drop and (b) advancing drop method.

Static, apparent advancing and receding water contact angles were measured by the sessile drop method using a conventional drop shape analysis technique Krüss DSA 10 (Krüss, Hamburg, Germany). In these experiments de-

ionized reagent grade water was used. Volumes of the drops for apparent θ_{adv} and θ_{rec} were 20 – 30 µl and 10 – 20 µl respectively. Inflation and deflation of the liquid was controlled manually and the same constant speed was used in both cases. The average value of five measurements, made at different positions of the same sample, was adopted as the average value of contact angles of the investigated substrate. The error of the mean contact angle values, calculated as the standard deviation, did not exceed 2° and 4° for apparent advancing and receding contact angles, respectively. All contact angle measurements were carried out at (24 ± 0.5) °C and relative humidity of (40 ± 3) %, which were kept constant.

Contact angle values were evaluated with Krüss DSA software [‡‡]. Briefly, the basis for the determination of the contact angle is the image of the drop on the sample surface. In the Krüss DSA software the actual drop shape and the contact line (baseline) with the solid are first determined by the analysis of the grey level values of the image pixels. To describe this more accurate, by the software calculates the root of the secondary derivative of the brightness level to receive the point of greatest changes in brightness. The found drop shape is adapted to fit a mathematical model which is then used to calculate the contact angle. Therefore, various methods of calculating the contact angle differ in the mathematical model used for analyzing the drop shape. Either the complete drop shape, part of the drop shape, or only the area of phase contact is evaluated. For evaluation of the contact angles on hydrophobic and superhydrophobic surfaces tangent 1 and tangent 2 methods were used. In tangent 1 method the complete profile of a sessile drop is adapted to fit a general conic section equation. The derivative of this equation at the intersection point of the contour line with the baseline gives the slope at the 3-phase contact point and, as a result therefore, the contact angle. If dynamic contact angles are to be measured, this method should only be used when the drop shape is not distorted too much with the needle. In tangent 2 method part of the profile of a sessile drop which lies near the baseline is adapted to fit a polynomial function. The slope at the 3-phase contact point at the baseline and thus the contact angle are determined using

---

[‡‡] Some descriptions of the methods used in this program available at http://www.kruss.de/en/theory/measurements/contact-angle/measurement-contact-angle.html (14.04.2013)

iteratively adapted parameters. This function is the result of numerous theoretical simulations. The method is mathematically accurate, but is sensitive to distortions in the phase contact area caused by contaminants or surface irregularities on the sample surface. As only the contact area is evaluated, this method is also suitable for dynamic contact angles. Nevertheless, this method requires an excellent image quality, especially in the region of the phase contact point.

2.2.4 Other methods

Null-ellipsometry

Null-ellipsometry was used as an express method for the evaluation of the polymer layer thickness grafted from flat surfaces (usually silicon wafer).

In fact, ellipsometry is a well established non-destructive technique for characterization of thin films and surfaces. This technique allows a determination of optical constants and thicknesses in some cases within sub-nm accuracy of a layer system [250]. Ellipsometry uses the fact that the state of polarization of an incident beam changes upon reflection at a film covered surface. The change in the state of polarization can be described by two measurable quantities: Φ (amplitude parameter) and Δ (phase parameter), which, in turn, are related to the optical properties of the film. An ellipsometer, therefore, uses polarization optics to produce and analyze any desired state of polarization.

The basic components of an ellipsometer are light source, polarizer, analyzer and detector. Optionally, a compensator can be introduced into the system (Figure 24).
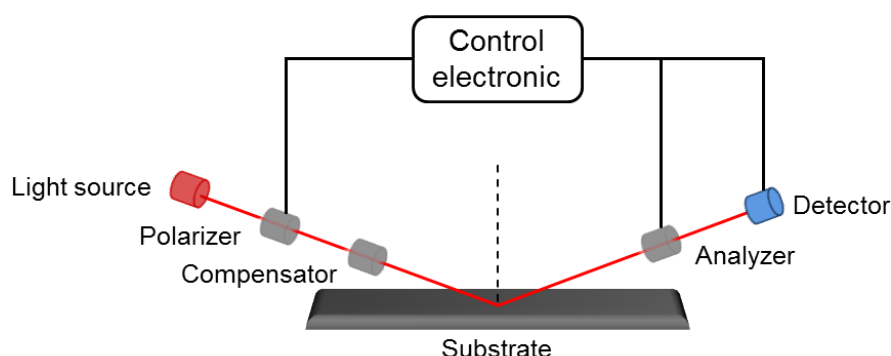

Figure 24. Simplified scheme of an ellipsometer.

Furthermore, a special ellipsometer setup is used in null-ellipsometry. Both analyzer and polarizer are rotating elements, and often a compensator is also included but fixed at ± 45°. In this case the angles of polarizer and analyzer are adjusted to achieve minimum intensity at the detector. Thus, the change in polarization introduced by the sample surface is compensated by the combined polarizer – compensator setting leading to linear polarized light upon reflection from the sample surface. With this signal compensation method a very high accuracy within the range of 0,01° to 0,05° for (Φ, Δ) can be achieved, since possible instrumental errors are eliminated due to relative measurements [251]. However, since the null-setting of the rotating elements depends on the wavelength, and the iterative adjustment of them is a relatively slow process, single-wavelength ellipsometers are most common when using this setup.

For ellipsometric measurements, the Multiskop (Optrel GbR, Sinzing, Germany) was used. All measurements were performed at the wavelength of 632.8 nm (light source: He-Ne laser) and with 70° angle of the light incident. Polymer thickness was evaluated with "Ellipsometry: simulation and data evaluation" software (Optrel GbR). General parameters for data evaluation were as follows: refractive index of the Si bottom layer n = 3,8858; extinction coefficient k = -0,0180; SiO_2 layer n = 3,8858; k = 0 and for the upper layer air n = 1; k = 0. Parameters for middle layers (including investigated polymer layer) were presented in specific experimental parts in chapter 3.

Thermogravimetric analysis (TGA)

Thermogravimetric analysis (TGA) was used to determine the amount of the grafted polymer layer onto the surface of synthesized and chemically modified silica particles. The number of initiator groups and polymer chains attached to the particle core was calculated, which allowed to estimate their density. TGA measurements were performed using a TGA Q 5000_{IR} thermal analyser (TA Instruments; Waters GmbH UB TA Instruments) at a heating rate of 10 K/min in air.

Gel permeation chromatography (GPC)

Polymers prepared by atom transfer radical polymerization (ATRP; polymerization conditions are described in specific experimental parts in chapter 4) in bulk solutions are characterized (M_n, M_w, PDI) by using Gradient HPLC HP Series 1100 (Pump, Autosampler, RI- and DA-detection) (Agilent

Technologies Inc., USA). Samples were prepared in chloroform and analyzed with UV254 or IR detectors.

Measurements of the electrophoretic mobility

The electrophoretic mobility was measured as a function of pH by using Zetasizer Nano ZS (Malvern Instruments, UK). The pH of the prepared suspensions was controlled by adding 0,1 M aqueous solutions of potassium hydroxide and hydrochloric acid. The samples were prepared as a dispersion of native or modified silica particles (2 mg) in 13 ml of 10^{-3} M sodium chloride solution. Three measurements were recorded for each sample at each value of pH. The ζ-potentials were calculated from the electrophoretic mobility using the Smoluchowsky equation [252].

Measurements of the surface area (BET)

Measurements of surface area were performed by using Quadrasorb SI station (Quantachorome Instruments, USA). Samples preliminary were dried in the vacuum oven at 150 °C and ca 20 mbar overnight. Surface area were calculated automatically from data of nitrogen adsorption-desorption by using BET theory [253].

3 Results and discussion

3.1 Preparation of complex colloidal particles

3.1.1 Introduction

Design of materials with controlled wetting properties is highly important for coating technology, microelectronics, biotechnology, and medicine. There are a number of approaches based on self-assembling monolayers [254], layer-by-layer technique [255], grafting of polymers [256], colloidal particles [257], which can be applied to control wetting properties of materials in a predictable way. Colloidal particles attract particular attention due to the possibility of large scale fabrication of superhydrophobic [258] and switchable surfaces at low cost. In fact, colloidal particles can simultaneously provide two properties required for the design of superhydrophobic materials: roughness and intrinsic hydrophobicity [100, 101]. Successful design of superhydrophobic surfaces requires, however, accurate control of these two parameters. For example, it was found that superhydrophobicity cannot be achieved using layers of densely packed smooth hydrophobic particles [21, 259], and fractal structures must be used [22]. One way to fabricate fractal structures is controlled aggregation of particles [22, 258, 260]. For this purpose, different types of modified silica particles can be used, including Janus silica particles [261]. Due to special functionalities on opposite sides, this type of particles could specifically aggregate with the formation of complex structures as well [262]. Another very elegant approach is based on the use of particles with complex geometrical structure, such as raspberry-like particles or diatomaceous earth.

In part 3.1 of the thesis, preparation and properties of complex colloidal particles are described. Section 3.1.2 delicates the synthesis and some properties of robust raspberry-like silica particles. Some examples of interfaces formed by using modified diatomaceous earth are shown in section 3.1.3.

3.1.2 Raspberry-like particles

Raspberry-like particles can be synthesized by physical adsorption [24, 263-265] or by chemical binding [266, 267] of small particles to the larger ones using silane chemistry. These methods are unable to provide proper

mechanical and chemical stability to the raspberry-like structures due to either weak linkage between the particles or solubility of the components, such as polystyrene latexes in organic solvents.

Dense grafted polymer layers – polymer brushes – as a mean to couple particles can be used to solve these problems (Figure 25). In particular, poly(glycidyl methacrylate) (PGMA) brush layer is a suitable coupling agent. Because of the presence of epoxy groups, PGMA is able to react with amino and carboxyl groups. Thin PGMA films were successfully applied for synthesis of monocomponent and mixed polymer brushes [268-272], as well as for immobilization of colloidal particles on textile surfaces [257]. The use of a thick PGMA grafted layer to couple inorganic particles is expected to provide proper stability to both mechanical treatment and organic solvents. As a result, we proposed a synthetic way of preparing such polymer brush-based robust raspberry-like particles with a grafted shell of poly(pentafluorostyrene), as well as further investigated the wetting properties of coatings based on them.

3.1.2.1 Materials

N,N,N',N'',N''-Pentamethyldiethylenetriamine (PMDTA, Aldrich, 99%), ethyl α-bromoisobutyrate (EBiB, Aldrich, 98%), 3-aminopropyltriethoxysilane (APS, ABCR, 97%), α-bromoisobutyryl bromide (Aldrich, 98%) anhydrous dichloromethane (99,5%, Sigma-Aldrich), ethylenediamine (99,5%, Aldrich), triethylamine (99%, Sigma-Aldrich), copper(II) bromide (Aldrich, 99,999%), anhydrous N,N-dimethylformamide (DMF, Sigma-Aldrich, 99,8%), water solution of hydrogen peroxide (30%, Merck), tetraethyl orthosilicate (TEOS, Aldrich, 99%), tetrahydrofuran (THF; Sigma-Aldrich, 99,9%), ammonium hydroxide 28 – 30 wt% solution of NH_3 in water (ACROS Organics), ethanol (VWR, 99,9%), tin(II) 2-ethylhexanoate (Aldrich, 95%), polished silicon wafers (diameter 95,5 – 100,5 mm, thickness 525 ± 15 μm, Silicon Material) were used as received. 2,3,4,5,6-Pentafluorostyrene (Aldrich, 99%) and glycidyl methacrylate (GMA, Aldrich, 97%) were distilled under nitrogen steam prior to the polymerization.

3.1.2.2 Experimental part

Synthesis of spherical silica particles (SP)

Small silica particles (100 nm, SP100) were prepared by one-step synthesis. Tetraethyl orthosilicate (TEOS, 1,5 ml) was added to the mixture of

50 ml of ethanol and 3 ml of saturated ammonia solution (28 – 30%). The reaction mixture was stirred at 700 rpm for 18 h. The particles were then centrifuged, washed several times with ethanol, and dried overnight in a vacuum oven. Large silica particles (ca. 1000 nm, SP1000) were prepared by a multistep synthesis as described in Table 1. After the last step, the particles were centrifuged, washed several times with ethanol and dried overnight in a vacuum oven.

Table 1. Amounts of chemicals used for the preparation of large silica particles.

Step	Amount of suspension from previous step, ml	Amount of used chemicals, ml			Size of the particles[*], nm
		EtOH	NH$_3$, H$_2$O solution	TEOS	
1 (SP100)	—	50	3	1,5	100 ± 10
2	25	175	12	6	210 ± 10
3	25	175	12	12[**]	410 ± 10
4 (SP1000)	50	350	24	24[**]	1020 ± 40

[*] The size of prepared particles was checked by SEM. Average values were calculated from SEM images.

[**] Total amount of TEOS added in the reaction mixture. TEOS was added in portion of 0,5 ml every 20 minutes untill the total volume was reached.

Small silica particles (ca. 50 nm, SP50) were prepared as follows. A mixture of 20 ml ethanol and 5 ml TEOS was added to the mixture of 125 ml ethanol and 10 ml saturated ammonia solution heated to 54 °C in an oil bath. After the addition of all components, the reaction mixture was stirred at 700 rpm at 54 °C for 24 h. The particles were centrifuged, washed several times with ethanol, and dried overnight in a vacuum oven. Size control of the particles has been done using SEM and the size of the particles was 53 ± 8 nm.

Modification of spherical silica particles by 3-aminopropyltriethoxysilane (SP100-NH2 and SP1000-NH2)

Dry spherical silica particles (either SP100 or SP1000, 0,5 g) were added to a 3% ethanol solution of 3-aminopropyltriethoxysilane (APS) and stirred for 20

h with a magnetic stirrer (600 rpm). After this, the particles were centrifuged and washed several times with ethanol to remove unreacted APS. Finally, APS-modified silica particles (either SP100-NH2 or SP1000-NH2) were dried in a vacuum oven at 60 °C.

The same procedure was also carried out for silica particles SP50 and SP210 and APS-modified particles SP50-NH2 and SP210-NH2.

Immobilization of the initiator for AGET-ATRP on large spherical silica particles (SP1000-BrIn)

0,5 g of dry SP1000-NH2 particles was dispersed in 50 ml of anhydrous dichloromethane. Then, 250 µl of α-bromoisobutyryl bromide and 500 µl of triethylamine were added to the suspension. The corresponding mixture was then stirred with a magnetic stirrer at 600 rpm for 10 h. The particles were centrifuged and washed several times with dichloromethane, distilled water, and ethanol. Finally, the purified particles were dried in a vacuum oven at 60 °C.

Grafting of glycidyl methacrylate (GMA) from large spherical particles (SP1000-PGMA)

1 g of dry SP1000-Br particles was dispersed in 10 ml of anhydrous N,N-dimethylformamide (DMF). Then, 10 ml of glycidyl methacrylate, 8 µl of a 0,1 M solution of copper(II) bromide in DMF, and 8 µl of a 0,5 M solution of N,N,N',N'',N''-pentamethyldiethylenetriamine in DMF were added. To remove the excess of oxygen, the reaction mixture was purged with nitrogen for 5 min. After the addition of tin(II) 2-ethylhexanoate (50 µl), the flask was heated up to 70 °C in an oil bath for 20 min. The particles were centrifuged and washed several times with DMF and ethanol after termination of the polymerization. Finally, poly(glycidyl methacrylate)-covered 1000 nm large silica particles (SP1000-PGMA) were dried in a vacuum oven at 40 °C. The "grafting from" approach for PGMA was performed without an initiator in solution (usually ethyl 2-bromo-2-methylpropionate used for polymerization in solution), and no free polymer was obtained. The determination of molecular weight of grafted polymer was not performed due to its complicity. Previous experiments [273] demonstrated that grafting density in this case is typically 0,1 – 0,3 chains/nm^2.

Preparation of a raspberry-like silica particles (RP100)

20 ml of suspension of small (100 nm) APS-modified silica particles (0,75 g) in ethanol were mixed with 25 ml of a suspension of SP-PGMA (0,5 g) in

ethanol. The reaction mixture was refluxed for 50 h. Non-bound small particles were separated from the reaction mixture by centrifugation. The obtained raspberry-like silica particles were washed several times with ethanol and then dried in a vacuum oven at 40 °C.

Other raspberry particles (either RP50 or RP210) can be synthesized in the same way by using amino-modified particles of the size 50 (SP50-NH2) or 210 nm (SP210-NH2) respectively, instead of small modified silica particles SP100-NH2.

Modification of the raspberry-like particles by ethylenediamine (RP100-NH2)

5 ml of ethylenediamine were added to 50 ml of a suspension of synthesized raspberry-like particles (RP, 0,5 g of particles in 50 ml of ethanol) and refluxed for 30 h. Then the particles were washed several times with ethanol and dichloromethane. The obtained RP100-NH2 particles were dried in a vacuum oven at 60 °C.

Immobilization of the AGET-ATRP initiator on raspberry-like particles (RP100-Br)

Initiator groups were immobilized on the surface of RP-NH2 particles in the same way as it was in the case of spherical particles.

Grafting of 2,3,4,5,6-pentafluorostyrene to raspberry-like particles (RP100-PPFS)

Copper(II) bromide (50 µl of a 0,1 M solution in DMF) and N,N,N',N'',N''-pentamethyldiethylenetriamine (50 µl of a 0,5 M solution in DMF) were added to a dispersion of RP-Br (0,15 g) in 2,3,4,5,6-pentafluorostyrene (PFS, 1,38 ml). After the addition of tin(II) 2-ethylhexanoate (150 µl) to the reaction mixture, the flask was heated to 70 °C in an oil bath. The polymerization was stopped after 35 min, and the particles were centrifuged and washed several times with DMF and ethanol.

The same procedure was used for the immobilization of PFS on 1000 nm large silica particles (SP1000-PPFS).

Preparation of flat surfaces based on silicon wafer modification

Generally, silicon wafers were used as support for the preparation of flat modified surfaces with different polymers and for further use as reference samples (i.e. for comprising of the wetting properties). First, silicon wafers were

cut in pieces of appropriate size and cleaned with dichloromethane in an ultrasonic bath for 15 minutes. Then the upper layer was oxidized by treating the wafers with mixture of a saturated ammonia solution, concentrated hydrogen peroxide and deionized water (volume ratio of each component 1:1:1) at 70 °C for 1 hour. Further modification with APS, α-bromoisobutyryl bromide and polymerization on flat surfaces were carried out the same way as for silica particles.

3.1.2.3 Properties of prepared raspberry particles and interfaces incorporated with them

Preparation of raspberry-like particles

In this work, possibilities to synthesize robust raspberry-like particles by chemical immobilization of 50, 100 and 210 nm large silica particles on 1 µm large ones were explored (Figure 25). Further modifications described in this thesis were done only with RP100 raspberry particles.

First, the approach suggested by Ming [267] was tested. This approach is based on coupling of small and large particles modified by silanes with amino and epoxy groups, respectively. Chemical reaction between amino and epoxy groups is expected to provide stable linking between the particles and allows fabrication of raspberry-like structures. Nonetheless, while the method does allow fabrication of raspberry-like particles, they are extremely fragile and quickly break apart after a few seconds of ultrasonication.

The reason for this poor stability is, most probably, the small contact area between large and small particles. In order to improve the stability of the raspberry-like particles, a thick layer of a reactive polymer poly(glycidyl methacrylate) (PGMA) was immobilized on the surface of large particles instead of a silane with epoxy groups.

In order to immobilize the PGMA brush layer, 1000 nm large silica particles were first modified by 3-aminopropyltriethoxysilane and, second, by α-bromoisobutyryl bromide as described in the experimental part, section 3.1.2.2. The PGMA layer was grafted to the surface of modified particles using activators generated by electron transfer atom-transfer radical polymerization (AGET-ATRP) [274]. The thickness of the PGMA layer, as evaluated from TGA results, was

found to be ca. 50 nm (Table 2). Similar to the silane with epoxy groups used by Ming, PGMA is able to react with amino groups.
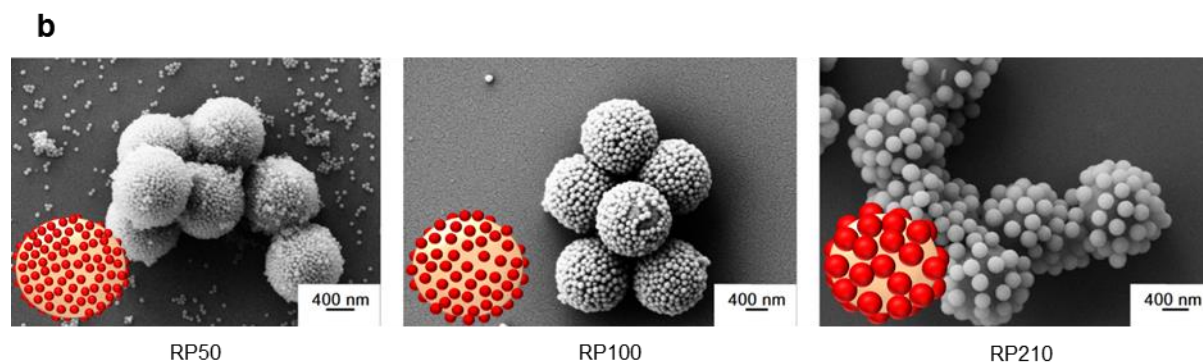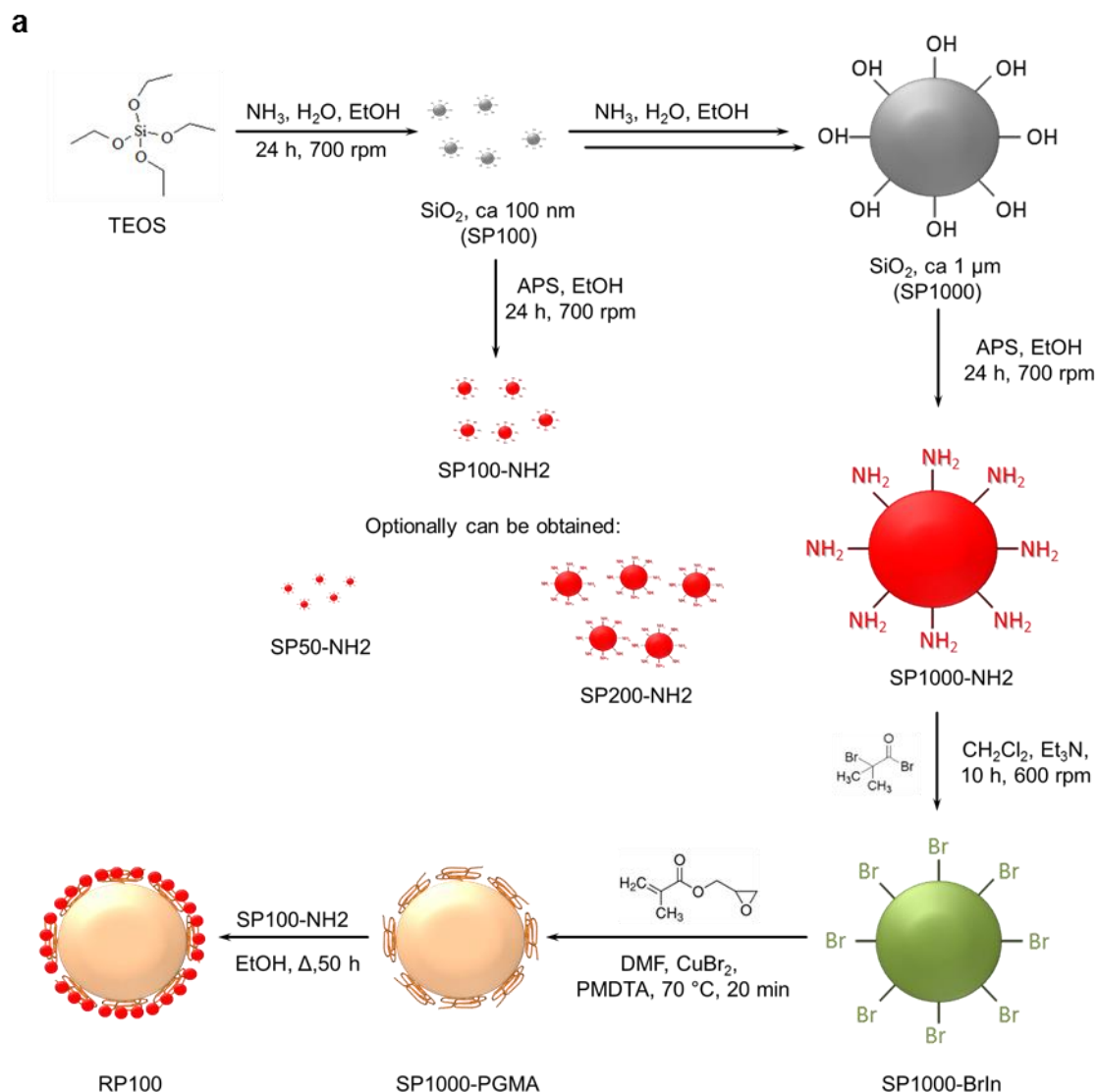

Figure 25. Raspberry-like silica particles: (a) Preparation; (b) SEM micrographs of raspberry-like particles with different sizes of side particles.

Raspberry-like particles were, therefore, prepared by linking 3-aminopropyltriethoxysilane-modified 100 nm large silica particles (SP100-NH2) to the surface of PGMA-modified 1000 nm large particles (SP1000-PGMA). Since the grafted PGMA layer is much thicker than silane monolayer, small particles can considerably immerse (by 30 – 50%, Figure 26) in the polymer layer, which allows a significant increase in the contact area between small and large particles.
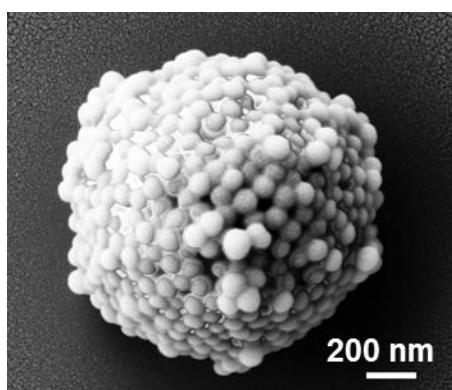

Figure 26. SEM image of a raspberry-like particle after synthesis (RP100).

As a result, the obtained raspberry-like particles are more stable than the ones produced using the Ming approach – more than 60% of small particles remain on the surface of the large ones after 20 min of exposure to an ultrasonic bath.

Polymer grafting: hydrophobization of raspberry particles

The obtained raspberry-like particles (RP100) were further used as substrates for immobilization of polymers. The particles were modified by ethylenediamine and α-bromoisobutyryl bromide in a stepwise manner in order to immobilize initiator groups. It was found that the raspberry-like particles remain stable after exposure to ethylenediamine, allowing a conclusion that there is no exchange reaction between ethylenediamine and epoxyamine adduct formed by PGMA (SP1000-PGMA) and APS (SP100-NH2). The possibility to immobilize polymers was demonstrated on the example of poly(pentafluorostyrene) (PPFS). Since this polymer is highly hydrophobic, the PPFS-modified raspberry-like

particles can be applied for the design of ultrahydrophobic coatings. PPFS was grafted on the surface of raspberry-like particles using AGET-ATRP (Figure 27).
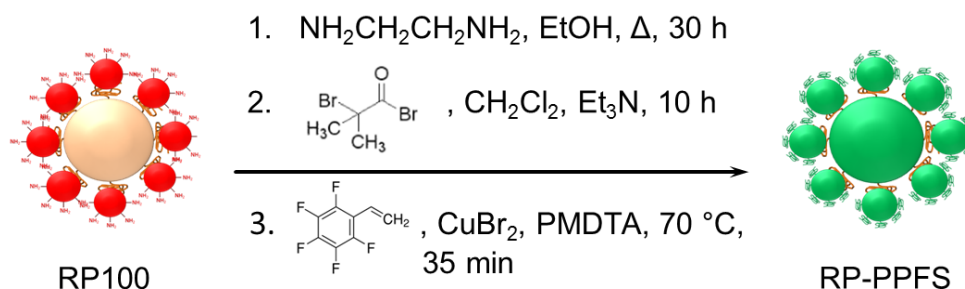

Figure 27. Scheme of modification of raspberry particles (RP100): hydrophobization with poly(pentafluorostyrene).

Wetting properties of the interfaces obtained from deposition of PPFS covered RP100 clearly indicate a successful grafting of PPFS (described below). However, because of the complex morphology of the raspberry-like particles, it is rather difficult to evaluate the hickness of the PPFS layer. In order to evaluate the thickness of the PPFS shell, a similar polymerization was performed on 1000 nm large spherical (SP1000-PPFS) particles at the same conditions which were used for the preparation of RP100-PPFS (Figure 28). Thickness of the PPFS layer, as evaluated using TGA results (Figure 29), had the value about 70 nm (sample SP-PPFS, Table 2). Moreover, raspberry-like particles retained their original structure after immobilization of the initiator and grafting of the polymer in an organic solvent at an elevated temperature. In fact, the same modification can be done with raspberry particles with different sizes of side particles as well as with different core size.
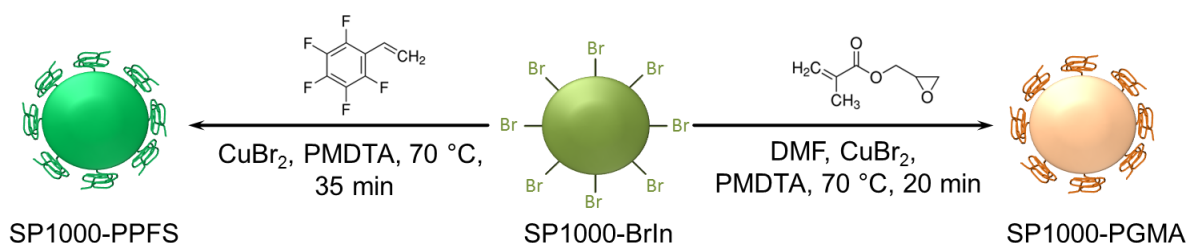
Figure 28. Scheme of polymerization on the surface of large silica particles for polymer thickness evaluation.
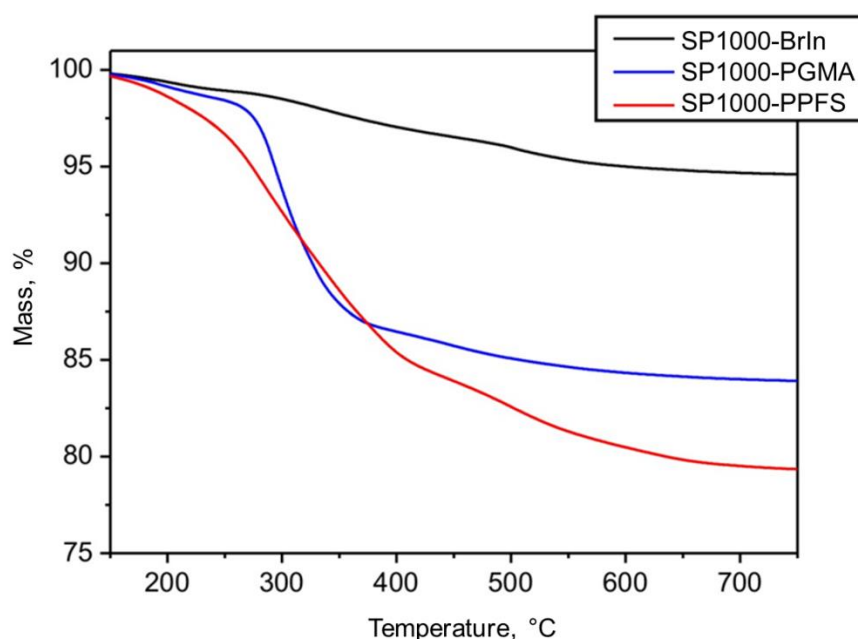
Figure 29. Thermogravimetric curves of spherical 1000 nm large silica particles with immobilized initiator (SP1000-BrIn, black), a grafted PGMA layer (SP1000-PGMA, blue) and reference sample with grafted PPFS (SP1000-PPFS, red).

Table 2. Results of termogravimetric analysis after different steps of modification.

Sample	Mass loss, %	Estimated thickness of polymer shell, H_{POL}, nm [*]
SP1000-BrIn	5,3	—
SP1000-PGMA	16,0	50
SP1000-PPFS	22	75

[*] Thickness of the grafted polymer layer was estimated by using the following equation:

Equation (8)
$$H_{POL} = \frac{R}{3} \frac{\rho_{SiO_2}}{\rho_{POL}} \frac{m_{POL} - m_{BrIn}}{100\% - m_{POL}},$$

where R is the radius of the particle, ρ_{SiO2} and ρ_{POL} are the mass densities of the silica and polymer, respectively, m_{POL} and m_{BrIn} are the values of the mass loss (%) in TGA experiments (calculated as a difference between mass loss at 750 °C and 120 °C).

Wetting properties of the interfaces incorporated with raspberry-like particles

Wetting properties were investigated and compared on layers formed by PPFS-modified spherical particles (SP1000-PPFS), raspberry-like particles right after modification with ethylenediamine (RP100-NH2), and raspberry-like particles before (RP100-BrIn) and after grafting of PPFS (RP100-PPFS). The particle layers were prepared by simple drying of the particle dispersion in THF on the surface of a silica wafer (Figure 30).
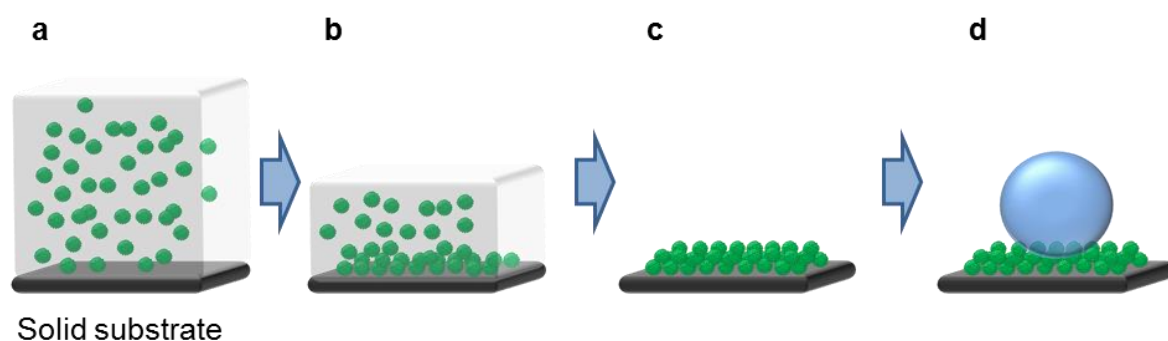
Figure 30. Scheme of the surface preparation by drying of the particle suspension: (a) deposition of the particle suspension in THF (100 µl; 17 mg/ml) on a silica wafer (1x1 cm^2); (b) drying of the suspension with (c) particle layer formation; (d) investigation of the wetting properties of obtained interfaces.

The obtained layers are unordered and possess a fractal structure, where two levels of roughness are formed by both the individual particles and the wavy morphology of the particle layer (Figure 31). It was found that RP-NH2 layers are strongly hydrophilic, because the water contact angle is below 20 °. On the other hand, SP1000-PPFS, RP100-BrIn, and RP100-PPFS layers are extremely hydrophobic: both apparent advancing and receding contact angles are in the range of 145 – 160° (Figure 32).

Figure 31. Scanning electron microscopy images of layers formed on silicon wafers after evaporation of the solvent from a particle dispersion: (a) raspberry-like particles with initiator (RP100-BrIn); (b) spherical particles with grafted PPFS (SP1000-PPFS), and (c) raspberry-like particles with PPFS (RP100-PPFS)

While SP1000-PPFS, RP100-BrIn, and RP100-PPFS layers appear similarly superhydrophobic, there are several differences between them. First, similar wetting properties of the layers formed by raspberry-like particles (RP100-BrIn and RP100-PPFS) and spherical ones (SP1000-PPFS) are due to the fractal character of the structures, which are obtained as a result of uncontrolled THF evaporation from the particle suspension (Figure 31). The nonfractal hexagonally ordered layers of highly hydrophobic spherical particles, as shown earlier, possess a considerable hysteresis of the water contact angles and, therefore, cannot be considered as superhydrophobic [21].

On the other hand, raspberry-like particles always form fractal structures, independently of the particle packing character. Secondly, RP100-BrIn particles, which are intrinsically hydrophilic (water contact angle on a flat surface with initiator groups is ca. 70°), form superhydrophobic layers similar to intrinsically hydrophobic RP-PPFS (static water contact angle on a flat surface modified with PPFS is 110°). This behavior cannot be explained using the equation of Cassie-Baxter, which predicts that ultrahydrophobic behavior is achievable only on intrinsically hydrophobic materials (CA > 90°). According to the model of Johnson and Dettre, this thermodynamically unfavorable behavior can be explained by the entrapment of a liquid drop in a metastable state [117, 275]. The difference in wetting properties between RP100-BrIn and RP100-PFS layers appears, when these particles are deposited on the water surface. The deposition was performed by drying of hexane dispersions (Figure 33). Particles without polymer (RP100-BrIn) quickly sink in water after a complete evaporation of hexane and reveal their intrinsic hydrophilic properties.
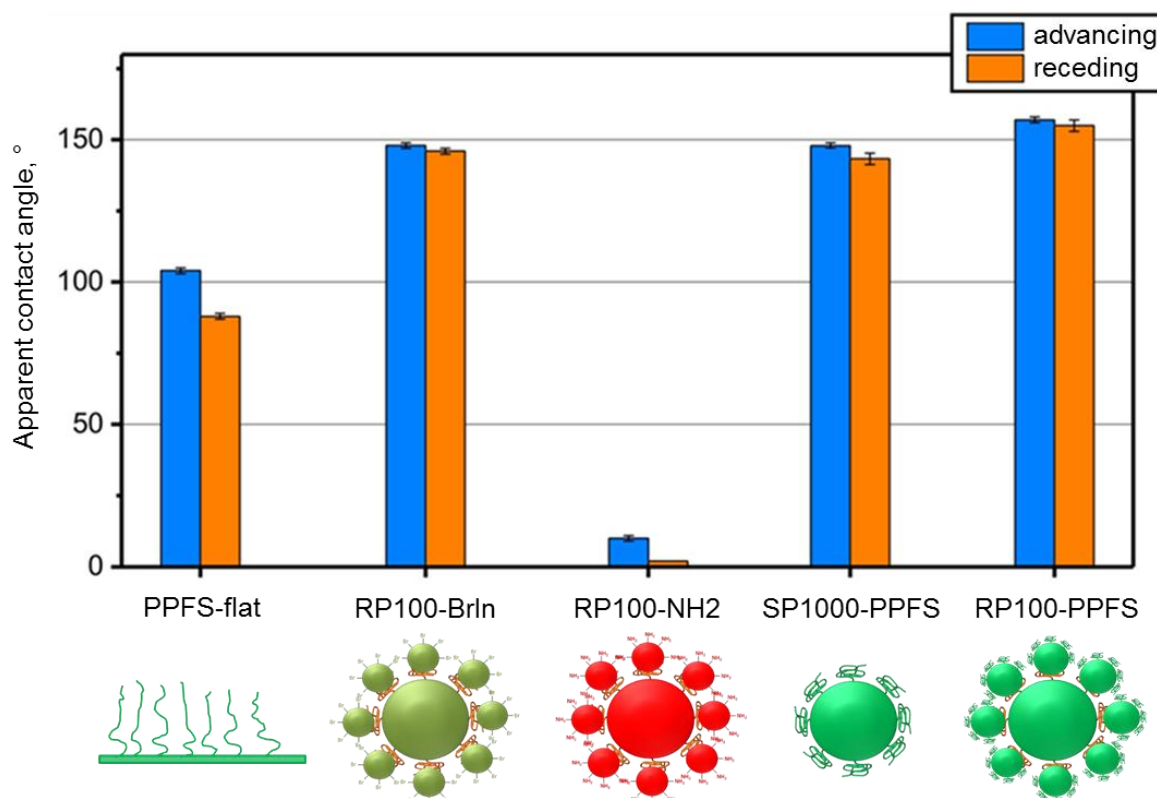
Figure 32. Values of advancing and receding water contact angles on flat silicon wafers with a grafted PPFS layer and layers formed by different particles.

On the other hand, particles with a grafted polymer (RP-PPFS) were floating on the water surface and could not sink even when force was applied. The particle multilayer floating on the water surface was superhydrophobic and could hold water droplets on the water surface (Figure 34a). Moreover, a water droplet can freely rotate on the particle layer and collect individual raspberry-like particles on its surface (Figure 34b).
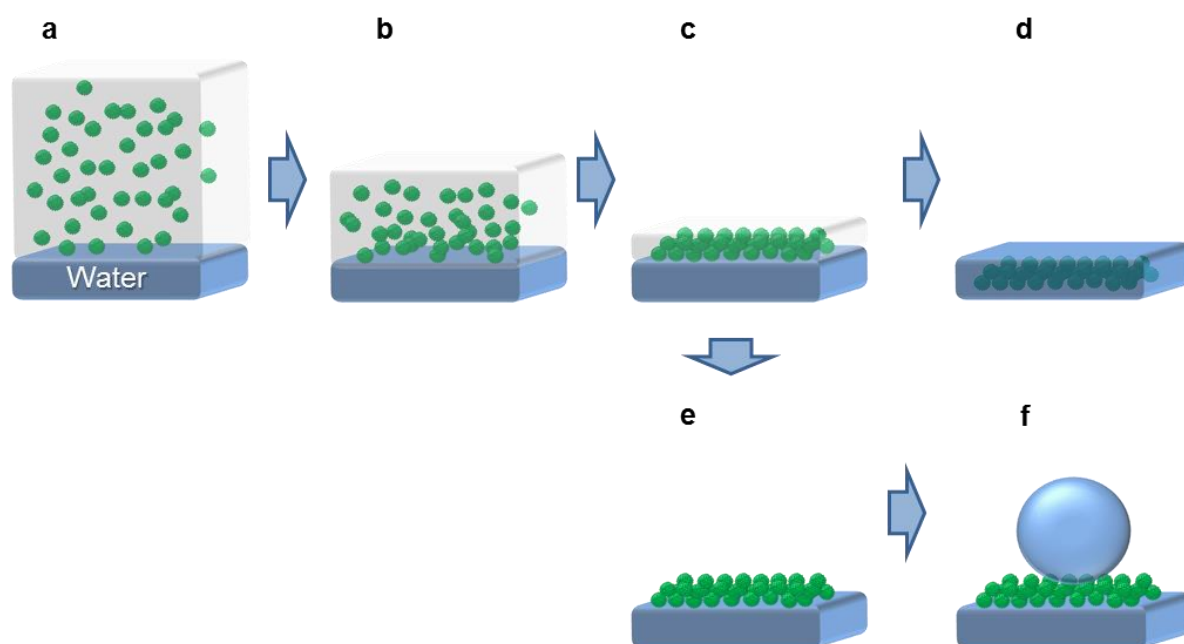
Figure 33. Scheme of deposition of raspberry particles (RP100-PPFS or RP100-BrIn) on a water interface in a Petri dish (diameter 9 cm) from a hexane dispersion (1 ml, 70 mg/ml in each dispersion case): (a) state of the system after deposition; (b) evaporation of hexane in air; (c) formation of the particle layers on the interface in a small amount of hexane; (e) formation of non-wetting layers of the PPFS modified raspberry-particles where (f) even a droplet of water stranded on it does not penetrate though; (d) formation of layers with RP100-BrIn, which became wet and the particles sank through.
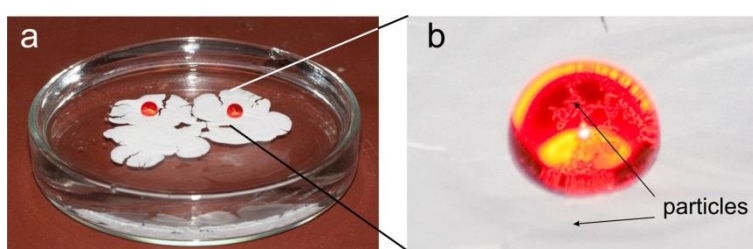
Figure 34. Photo images of water droplets colored with rhodamine 6G (a) on a layer of poly(pentafluorostyrene)-modified raspberry-like (RP100-PPFS) particles floating on the water surface; (b) some particles are obsereved on the water droplet in the zoomed image.

3.1.3 Diatomaceous earth

Diatomaceous earth (also known as diatomite, kieselguhr, tripolite; DE) is a yellow, white or light gray colored siliceous porous deposit from fossil opaline shells of diatoms [276]. Particle size of DE ranges from several hundreds of nanometers up to several hundreds of micrometers (Figure 35) and depends on the area of origin and industrial processing. Chemical composition of DE is typically following: 86 % silica, 5 % sodium, 3% magnesium and 2 % iron [277]. Generally, DE is using for water / waste water filtration and treatment [278, 279], coatings [280], as a material for supported catalysis [281], and in some other industrial areas due to its high porosity. Recently, Olivera et al [280] reported about exploitation of DE for the preparation of superhydrophobic surfaces by using fluorinated silanes and polystyrene as a matrix. However, silanes form thin (1-2 nm) film and mechanically unstable.
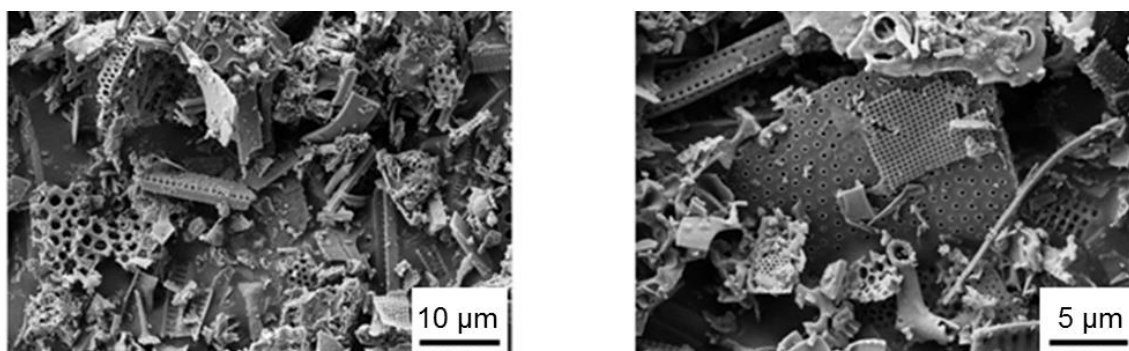
Figure 35. SEM micrographs of DE particles.

In this work, DE is also used for the preparation of superhydrophobic films and polymer-DE composites, but instead of using silanes for hydrophobization of DE, grafted polymers were used. Grafted polymers allow us to get a more robust material due to the physical interactions between the polymer chains in DE and / or the polymer matrix as, for instance, in the case of polymer-particle composite material. Initial modification of DE with an initiator for further polymerization was possible in a similar way as for raspberry-like silica particles (section 3.1.2) due to the high silica content in DE.

3.1.3.1 Materials

Additionally to the materials described in section 3.1.2.1, diatomaceous earth (D3877, Sigma-Aldrich) and 2 components epoxy based glue (UHU plus schnellfest 2-K-Epoxidharzkleber, 5 min) were used as received.

3.1.3.2 Experimental part

Modification and immobilization of polymer brushes on DE particles

DE was modified with APS and initiator for ATRP / AGET-ATRP. Modification steps were similar to the ones described in section 3.1.2.2 for RP. Hydrophobization of the DE particles was performed by using PFS (conditions were also similar as for RP)

3.1.3.3 Properties of surfaces incorporated with particles

First, the amount of grafted polymer on DE surface was estimated from TGA (Figure 36) and BET measurements.
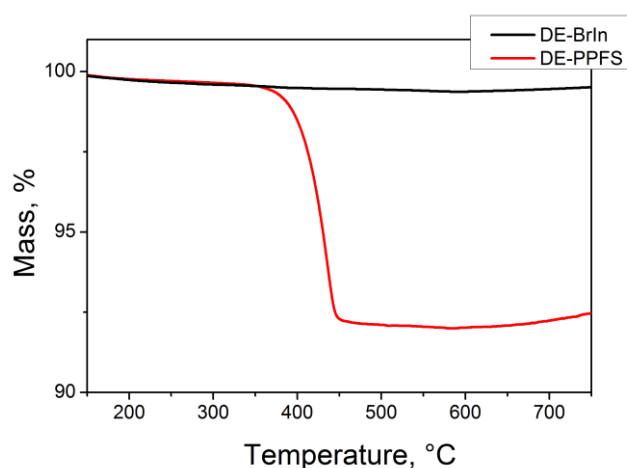
Figure 36. Thermogravimetric curves of DE particles with grafted PPFE layer (DE-PPFS, red) and reference sample with immobilized initiator (DE-BrIn, black).

The value of the surface area obtained from a BET experiment was – $S_{BET} = 4,826$ m^2/g. Thickness of the PPFS layer was estimated by using the Equation (9):

Equation (9)
$$H_{POL} = \frac{1}{S_{BET} \cdot \rho_{POL}} \frac{m_{POL} - m_{BrIn}}{100\% - m_{POL}},$$

where ρ_{POL} is the mass density of the polymer, m_{POL} and m_{BrIn} are the values of the mass loss (%) in TGA experiments (calculated as a difference between mass

loss at 750 °C and 120 °C). As a result, the value of PPFS-polymer shell is H_{POL} = 16 nm.

Hydrophobic DE particles (DE-PPFS) were used for the preparation of superhydrophobic films on the silicon wafer surface. This procedure was similar as for RP-PPFS particles (section 3.1.2.3, Figure 30): suspension of DE-PPFS in n-hexane (17 mg/ml) was placed on the surface of a silicon wafer (2x2 cm^2). The total amount of particles on the surface was 3,4 mg. Apparent water contact angles on the prepared surfaces were quite high: θ_{adv} = 152°, θ_{rec} = 151°.

Water droplets on the surface incorporated with DE-PPFS rotated and detached DE-PPFS particles (self-cleaning effect). At the same time the formation of so-called marble droplets [184, 282] was observed (Figure 37). The obtained marble droplets possess high sustainability and are destroyed only after several hours due to water evaporation.

DE-PPFS particles were incorporated with epoxy resin based on 2 component epoxy glue for the improvement of mechanical properties of the obtained particle film. First, two components of the glue were mixed and placed on a silicon wafer in order to form a thin layer. Second, DE-PPFS particles were deposited on top of the film with the thin layer.

After ca. 1 hour after the polymer film made of two components became hard, the excess of particles was removed and the surface was blown with nitrogen. The freshly prepared surface possessed high values of water contact angles: both advancing and receding angles were above 135°. Locally, areas of the obtained DE-PPFS-epoxy film possessed even superhydrophobicity (contact angles above 150°). However, because of the surface defects and inhomogeneous distribution of the particles, the obtained surface in whole cannot be considered as superhydrophobic. But mechanical properties are improved: particles were not released from the film and remained in the polymer top layer (Figure 38).

a

b

c
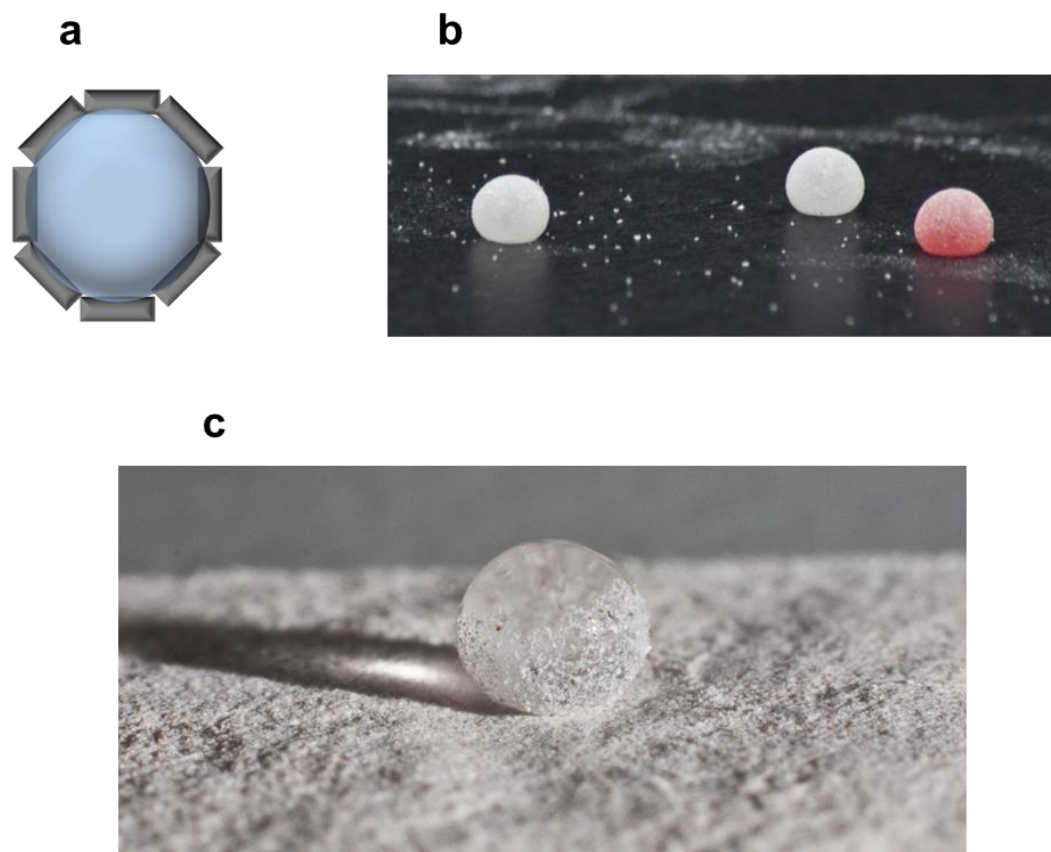
Figure 37. Marble droplets: schematic image of a marble droplet in section (a); marble droplets (one of them colored with rhodamine 6G) on a paper surface (b); formation of marble droplet on the surface with DE-PPFS particles.

a

b

c
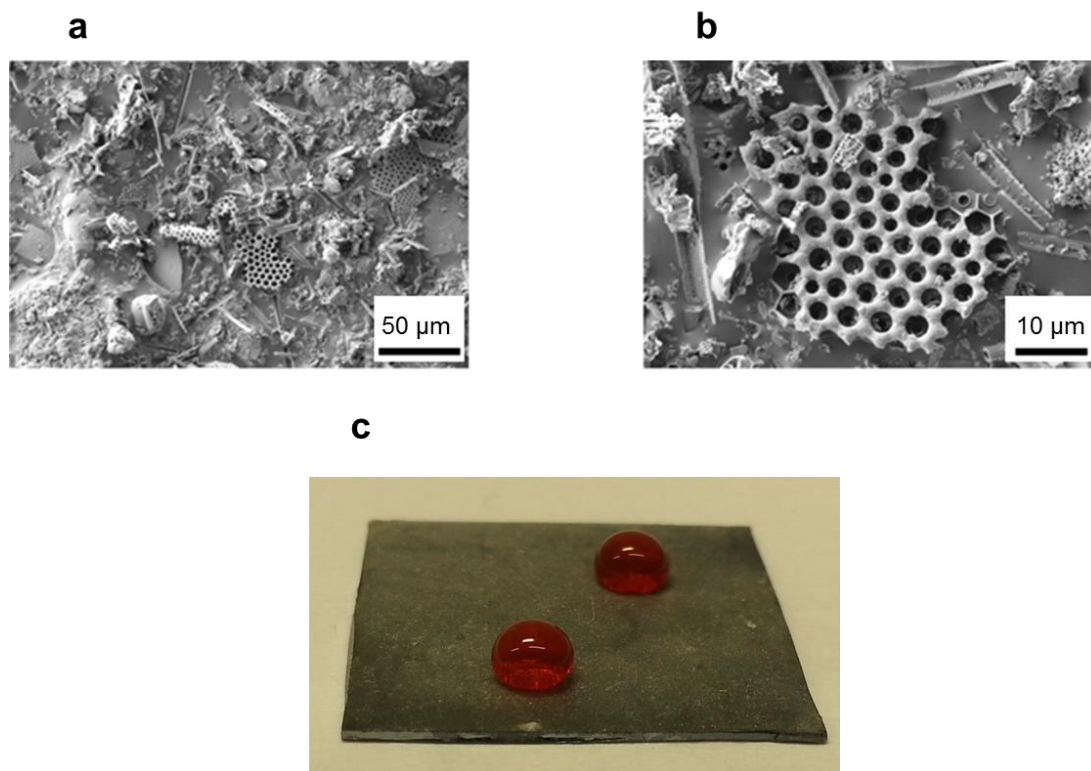
Figure 38. DE-PPFS – epoxy resin composite: SEM micrographs of DE-PPFS particles incorporated into epoxy resin matrix (a, b), water droplets colored with rhodamine 6G on the surface of epoxy-resin incorporated with DE-PPFS particles.

3.1.4 Conclusions

Applicability of particles with complex geometry, such as raspberry-like particles and diatomaceous earth, for the design of superhydrophobic surfaces was demonstrated. First, a new route for the fabrication of mechanically and solvent-resistant raspberry-like particles was developed. The approach is based on using polymer brushes as a mean to couple small inorganic particles with larger ones. Raspberry-like particles retain their structure after ultrasonication and exposure to organic solvents which allows their use as substrates for immobilization of polymer chains. Finally, the fabrication of superhydrophobic surfaces using raspberry-like particles with immobilized poly(pentafluorostyrene) was demonstrated. Additionally, the developed robust raspberry-like particles may be suitable as substrates for immobilization of stimuli-responsive brushes as well. Thus, these switchable functional colloidal particles are promising candidates for the design of waterborne superhydrophobic coatings.

Furthermore, it was shown that not only raspberry-like particles, but also diatomaceous earth, which occurs in nature, can be used for the preparation of superhydrophobic layers. In this case, the main component – DE – is quite cheap and suitable for the same modification process and hydrophobization as RPs.

Finally, an example of a composite polymer-DE system was shown. Such kind of composites may be used for the preparation of hydrophobic and superhydrophobic surfaces on a large scale.

3.2 Switchable self-repairable surfaces based on colloidal particles

3.2.1 Introduction

Surfaces with switchable/adaptive behavior [4, 256, 283-288] are of growing interest for the design of microfluidic devices [289-291], sensors [9, 292-294], functional coatings [6, 11, 295, 296], logical devices [297], and for biotechnological applications [16, 298-301]. To date, stimuli-responsive surfaces were designed mainly using self-assembled monolayers, polymer brushes [7], or using metal oxides [8]. Exposure of these materials to environmental stimuli (solvent, pH, temperature, and light) changes the composition in the topmost layer that affects their surface properties, including adhesion, friction and wetting.

Recently, it was found that the switching range of wetting properties of stimuli-responsive surfaces could be dramatically increased using rough substrates. According to the equations of Wenzel [100, 302, 303] and Cassie [101, 302] (chapter 2, section 2.1.3), roughness "enhances" intrinsic wetting properties of materials and makes hydrophilic / hydrophobic materials even more hydrophilic / hydrophobic, respectively. Using this principle, Minko et al., for example, fabricated mixed hydrophobic – hydrophilic brushes grafted to rough substrates, which demonstrate a very broad switching range between absolute wetting (water contact angle is close to 0°) and superhydrophobicity (water contact angle is more than 150°) [6]. On the other hand, surface roughness and, therefore, wetting properties of composite hydrogels can be switched by deformation [295]. Some other examples of preparation methods of the surfaces with switchable wetting behavior are given in section 2.1.5.

In this work, a novel approach for the design of surfaces, where both chemical composition and roughness can be switched by external stimuli, was suggested. The approach is based on the use of hydrophilic particles deposited on a surface of hydrophobic oil, the melting point of which is slightly higher than the ambient temperature. At this point, paraffin wax with a melting point around 54 °C, incorporated with small silica particles was used. The degree of particle immersion in the molten wax layer is determined by the interfacial forces, which depend on the environment, namely, dry or aqueous. Therefore, roughness, as well as hydrophobicity / hydrophilicity, of the particle-wax surface can be

reversibly switched by applying dry and aqueous media. Moreover, the obtained morphologies can be "frozen" by cooling down below the melting point of wax. Properties of such surfaces are described in section 3.2.4. General procedures for preparation particle-wax switchable surfaces are presented in section 3.2.3.

Due to their roughness, particle-oil surfaces can even possess superhydrophobic properties. Examples of this kind of surfaces present in section 3.3.

3.2.2 Materials

Additionally to the materials described in section 3.1.2.1 paraffin wax (mp 58 – 62 °C; Aldrich) and hexadecane (anhydrous, ≥ 99%, Sigma-Aldrich) were used as received.

3.2.3 Experimental part

Preparation and modification of silica particles

Silica particles with the size of 200 nm were prepared by a two-step synthesis, according to the procedure described in section 3.1.2.2. Modification of the particles was made by using 3-aminopropyltriethoxysilane (section 3.1.2.2).

Preparation of paraffin wax-particle mixtures and films based on them

Particle-wax mixtures were prepared by the following procedure. Native or APS-modified particles (100 mg) were dispersed in chloroform (10 ml) at room temperature. Then paraffin wax (2 g, mp 58 – 62 °C) was added, the system was heated up to 60 °C and sonicated for 15 min. Hot water (40 ml) was added to the particle-paraffin wax mixture after evaporation (at a rotary evaporator) of chloroform. The mixture was stirred and after 30 minutes rapidly cooled by pouring out in liquid nitrogen (temperature ca -196 °C). The obtained so-called particle-wax colloidosomes (round paraffin wax particles covered with silica particles) were filtered out and dried in the vacuum oven (40 °C, 15 mbar) during 12 h. Paraffin wax-particle films were prepared by melting the colloidosomes on the surface of water. Briefly, 4 ml of Millipore water were placed in glass vial (inner diameter ca 4 cm) and carefully heated up to 70 °C. 150 mg of particle-wax colloidosomes were placed on the surface and after melting them, the water was cooled down. Due to the ability of the particles to migrate to the interfaces for the

reduction of surface energy (discussed in section 3.2.4), two types of surfaces, so-called "water" (interface water-wax) and "air" (interface wax-air) annealed surfaces, incorporated with particles were obtained.

3.2.4 Particles at wax-air and wax-water interfaces

Behavior of native and 3-aminopropyltriethoxysilane (APS)-modified 200 nm large silica particles on the wax surface was investigated. It was previously shown, that particles with partial wettability in two immiscible fluid phases can adsorb strongly at the interface between them [304]. In general case, gravity effects play an important role in the location of the particle in a particular phase in two phase – particles systems (Figure 39), where the particle density is larger than that of water and oil, and interface can deform due to gravity [305].
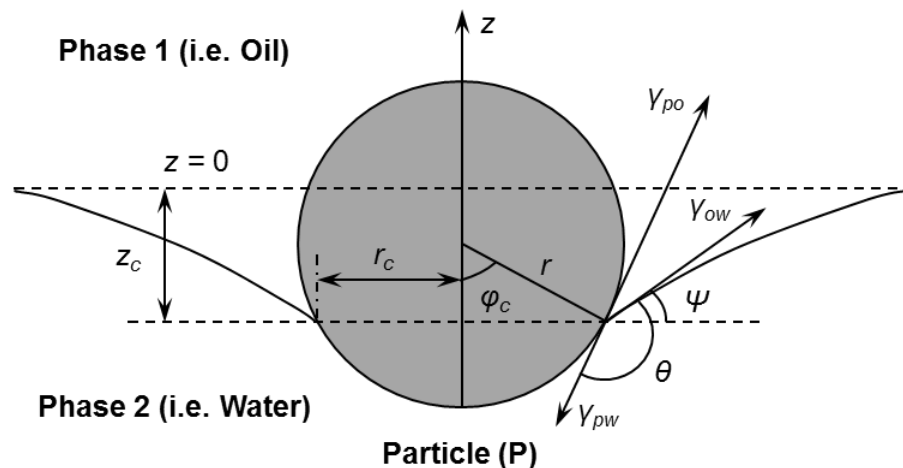
Figure 39. Heavy solid spherical particle with radius r and contact angle θ (depends on the surface free energies at the particle-water, γ_{pw}, particle-oil, γ_{po}, and oil-water, γ_{ow}, interface) in equilibrium at the two phases interface (i.e. oil-water interface) levelled at $z = 0$ far from the particle. The three-phase contact line with radius r_c is depressed at depth z_c below the zero level. Angles φ_c and Ψ determine the position of the three-phase contact line due to gravity effect [305].

Nevertheless, it was also shown, that for a sufficiently small particle the deformation of the fluid interface caused by gravity is very small and can be neglected. In this case, the fluid interface can be considered as flat up to the three-phase contact line (Figure 40). However, deformation can also exist in this case due to a non-uniform wetting of the particle surface [305-308].

Thus, the effect of gravity was not considered for 200 nm silica particles used in this work.
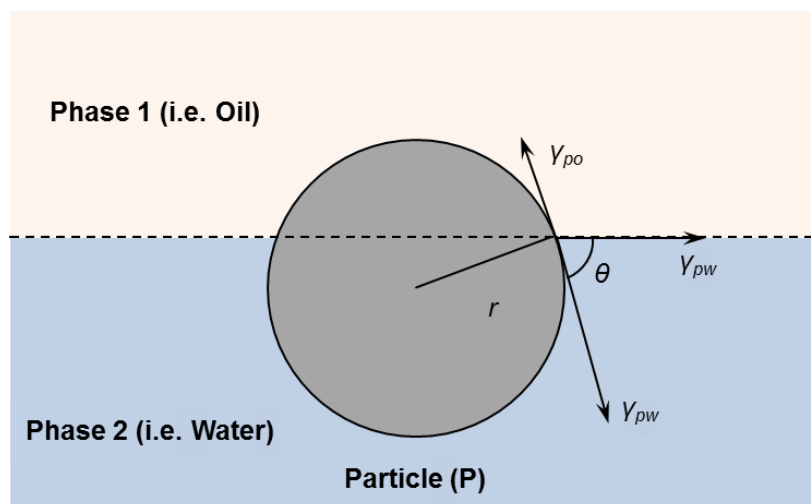
Figure 40. Small solid spherical particle with radius *r* and contact angle *θ* attached to a planar oil-water interface in its equilibrium state.

The particle-wax films were prepared by melting of wax-particle colloidosomes on the water surface. One side (upper one) is, therefore, annealed in dry conditions (in air) and another side (lower one) is annealed in aqueous environment (Figure 41).
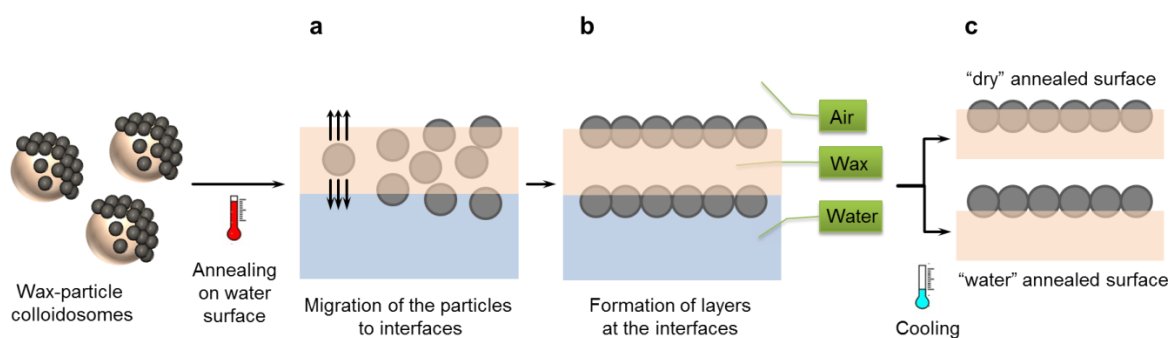
Figure 41. Scheme of the experiment of melting wax-particle colloidosomes on the water surface. Particles have a tendency to adsorb on either air / oil (melted paraffin wax) or oil / water interfaces (a) with a formation of particles layers at the interfaces (b) in the equilibrium state. After cooling the system and wax solidification two types of surfaces, so-called "dry" annealed and "water" annealed, were obtained (c).

It was found, that both native and APS-modified silica particles almost completely immersed into wax at the wax-air interface (after annealing on air). On the other hand, both kinds of particles, as it was expected from contact angle measurements data (Table 3), should be only slightly immersed in wax at the

water-wax interface (after annealing under water). In this case, the height of the particle cap above the wax surface normalized to the particle radius (h^*) was calculated by the using formula $h^* = 1 + \cos\theta$ [21] from contact angle measurements ($h^* = 1{,}91$ and $h^* = 1{,}64$ for native and APS-modified silica particles, respectively; Table 3). These calculated data from the measurements of apparent contact angles of hexadecane are in good qualitative correlation with the previously obtained results [309] (Table 4).
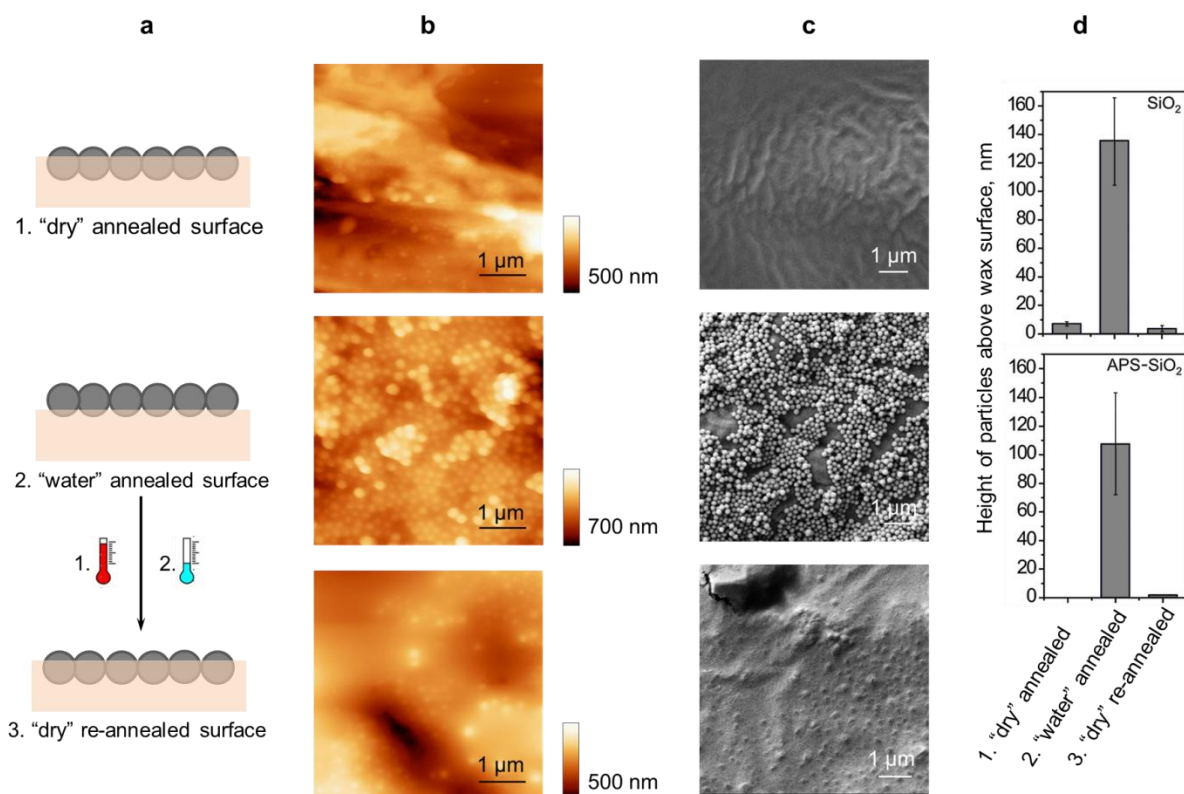
Figure 42. Immersion of native silica particles into wax after annealing the sample in air ("dry" annealing), annealing in water and re-annealing in air after initially annealing in water. General scheme of experiment (a); AFM images (b) and SEM micrographs (c) of the prepared surfaces. Comprising values of the particles height above the wax surface for native silica and APS-modified particles (d) for different types of surfaces (1-3).

However, values of the normalized height of the particle cap above the wax surface (h^*) obtained by AFM-technique are slightly different (Table 4). This quantitative difference of h^* between AFM results and calculated from contact angle measurements can be explained by the intrinsic roughness of the particles and the difference between advancing and receding contact angles of wax on the particle surface (Figure 42).

77

Table 3. Experimentally measured values of contact angles at different flat interfaces.

Flat surface	Interface	Contact angle, °	
		Water (θ)	Hexadecane (apparent value, θ') [*]
APS-modified silicon wafer	APS(NH_2-SiO_2)-water-air	70	
Cleaned silicon wafer	SiO_2-water-air	43	
Wax melted on silicon wafer	wax-water-air	107	
Cleaned silicon wafer	SiO_2-hexadecane-air		0
Cleaned silicon wafer	SiO_2-hexadecane-water		155
APS-modified silicon wafer	APS(NH_2-SiO_2)-hexadecane-air		0
APS-modified silicon wafer	APS(NH_2-SiO_2)-hexadecane-water		130

[*] Hexadecane was used as an oil phase in some experiments for measuring the contact angle due to the low melting point of hexadecane (mp 18 °C) comparing to wax (mp 58 – 62 °C) and its chemical resemblance with wax.

Table 4. Values of the immersion degree of native and APS-modified silica particles in wax depending on the environment.

Particles	Annealing conditions	Height of the particle cap above the wax surface normalized to the particle radius, h^*		
		AFM	Contact angle*	Lit. [309]
SiO$_2$	dry (in air)	0,1	0	
	water	1,3	1,91	1,8
APS-SiO$_2$	dry (in air)	0	0	
	water	1,1	1,64	1,5

* h^* values were estimated by using the following equation $h^* = 1 + \cos\theta$ [21] from the contact angle results (Table 3).

Next, theoretical and experimental investigations of the wetting properties of composite wax-particle surfaces was carried out. The wetting properties of these surfaces were determined by several parameters: hydrophilicity and surface roughness provided by particles, as well as hydrophobicity of wax. Although there are many models, which may be used for simulation of the wetting behavior of wax surfaces with particles, a modified Cassie-Baxter Equation (10) was used. This choice is justified by the recent experimental findings [21, 22, 259], where it was demonstrated, that this modification of Cassie-Baxter equation provides the best agreement with the experimental results for the wetting behavior on surfaces made of colloidal particles. For simplicity, only the case when the water droplets collapsed on the surface was considered. Therefore, the liquid completely fills the grooves between the particle and the collapsed drop. Thus, the Cassie-Baxter equation can be modified as follows:

Equation (10) $\quad\quad \cos\theta = f_{particle}^{wax} r_{particle}^{wax} \cos\theta_{particle}^{wax} + (1 - f_{particle}^{wax}) \cos\theta_{wax}^{water}$,

where $\cos\theta_{particle}^{wax}$ and $\cos\theta_{wax}^{water}$ are the intrinsic water contact angles on the surfaces of particles and wax, respectively (Table 3, values for water-air interfaces); $f_{particle}^{wax} = n\pi R_p^2 \left(2h^* - h^{*2}\right)$ is the area fraction of particles on the surface of wax; $r_{particle}^{wax} = \dfrac{2}{2 - h^*}$ is the roughness factor of the particle cap above the wax surface; h^* is normalized height of the particle cap above the wax surface

(Table 4, values estimated from AFM measurements); $\theta_{wax}^{air\_or\_water}$ is the intrinsic contact angle of wax on the particle surface in air or aqueous environment (Table 3, values for hexadecane-air or water interfaces); $n = \dfrac{N}{S}$ is the number of particles (*N*) per area (*S*); $n_{max} = \dfrac{1}{2\sqrt{3}R_p^2}$ is the maximum number density of particles on the surface, which corresponds to closely packed particles. The performed simulations demonstrate that the native and APS-modified particle wax surfaces provide different wetting properties after annealing in air and in water, and that the particle-wax surface is hydrophilic after annealing in water and is hydrophobic after annealing in air. The contrast between hydrophilic and hydrophobic states increases with the density of particles on the surface (Figure 43).
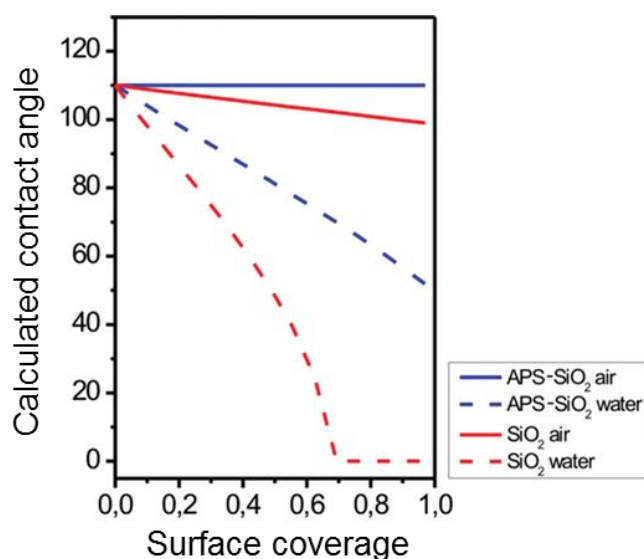
Figure 43. Calculated water contact angles on native (red lines) and APS-modified (blue lines) wax-particle surfaces after annealing in air ("dry"-annealing)

Experimental investigations of the wetting properties of the obtained wax-particle layers after annealing in different media was performed using water contact angle measurements (Figure 44). Both advancing (θ_{adv}) and receding (θ_{rec}) water contact angles were measured in order to characterize the wetting properties of the obtained surfaces. It was found that the wax-particle surfaces

are more hydrophilic after annealing under water (θ_{adv} = 60 – 70°, θ_{rec} = 10 – 20°)

then after annealing in air (θ_{adv} = 100 – 110°, θ_{rec} = 90 – 95°, Figure 44a, b). Due

to a small contact angle hysteresis, water droplets are flexible on the wax-particle

surface annealed in air and can be removed by slight shaking. On the other hand,

water droplets remain strongly pinned to the wax-particle surface after annealing

under water. A control experiment and investigations of wetting properties of wax

without particles, annealed in air and in water, was performed. The wax surface

becomes slightly more hydrophilic after annealing in aqueous environment, which

is seen from the decrease in the receding contact angle. The values for receding

contact angles are θ_{rec} = 90° and θ_{rec} = 70° after annealing in air and in water,

respectively (Figure 44c). The values of advancing water contact angles on the

wax surfaces annealed in dry and aqueous environment are nearly the same:

θ_{adv} = 100 – 105°. Therefore, the difference in wetting properties of the wax-

particle surface annealed at different conditions (air or water) originates from the

different degree of particles immersion into wax.
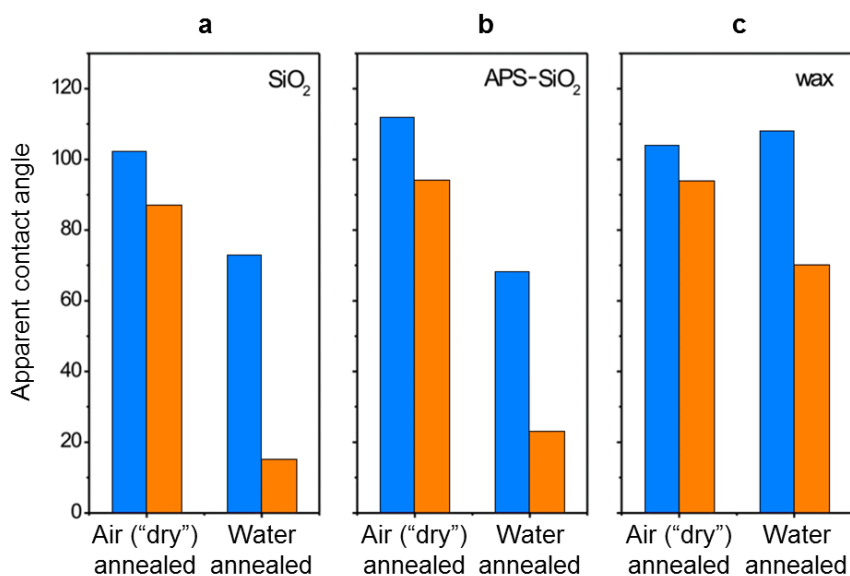
Figure 44. Wetting properties of particle-wax surfaces after annealing in air (air or "dry" annealed) and under water (water annealed). Advancing (blue) and receding (orange) contact angles for surfaces prepared with native silica particles-wax (a), APS-modified silica particles-wax (b) and reference wax sample (c) after annealing in different environments.

The possibility of reversibly switching the wetting properties of the particle-wax surfaces was experimentally tested. The hydrophilic wax-particle film, which was preliminary annealed in water, was used for the switching experiments. This film was then melted in air ("dry" annealing). It was found that the particle-wax film switches into hydrophobic state after annealing in air (Figure 45, state 2). The second annealing under water switches the surface back into the hydrophilic state (Figure 45, state 3). Further re-annealings in air and under water switch the layer in hydrophilic and hydrophobic states, respectively. Thus, the wax-particle layer demonstrates a fully reversible switching of wetting properties after annealing in dry (air) and aqueous environments.
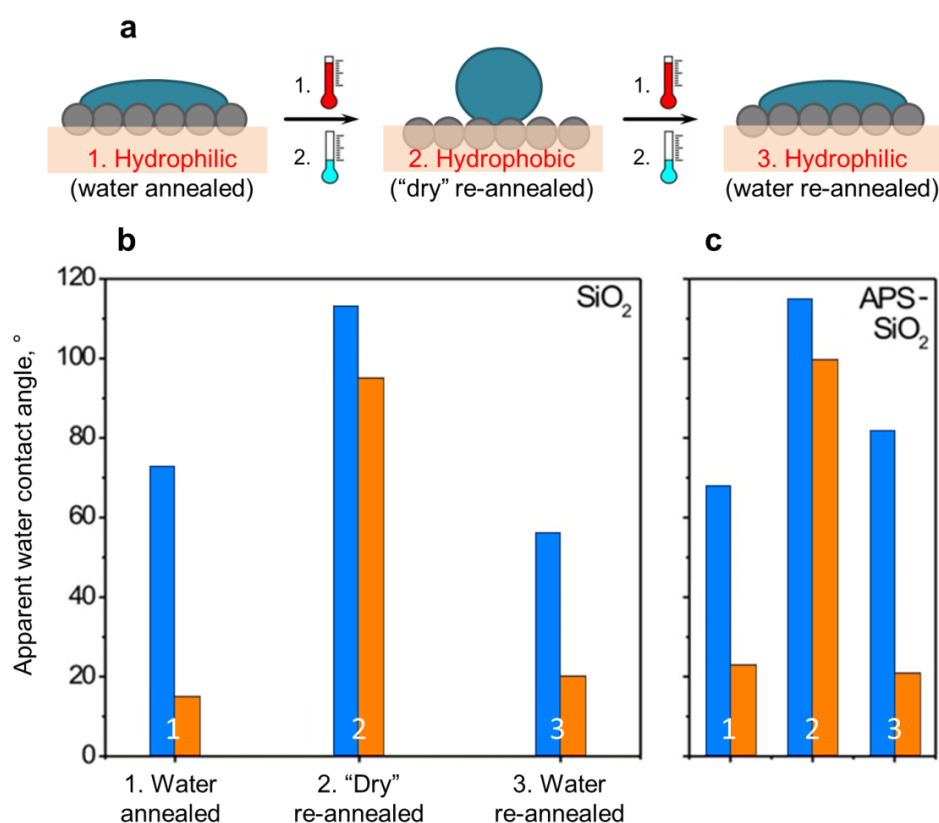
Figure 45. Reversible switching of wetting properties of particle-wax surfaces by sequential annealing in different environments. General scheme of experiment (a): state 1 – initially hydrophilic surface prepared by water annealing of particle-wax mixtures; state 2 – hydrophobic surface after "dry" re-annealing of surface 1; and state 3 – re-annealing under water of surface 2. Values of advancing (blue) and receding (orange) contact angles in these experiments for native silica particle-wax surfaces (b) and for APS-modified silica particle-wax surfaces (c) in three different states.

Applicability of the developed stimuli-responsive surfaces for hydrophilic-hydrophobic patterning was also demonstrated. In order to obtain a pattern (Figure 46b), a particle-wax film, which was preliminary switched to the hydrophilic state by annealing in water, was used. By locally approaching the heat source (in our experiments a hot needle was used) to the surface with no direct contact between them, the wetting of the surface can be switched from hydrophilic to hydrophobic (Figure 46). In fact, it was observed that water readily wets areas where no heat source was applied (hydrophilic areas), whereas water does not wet the areas where the heat was applied (hydrophobic area). In this way, different structures can be introduced to the sample surface for further usage.
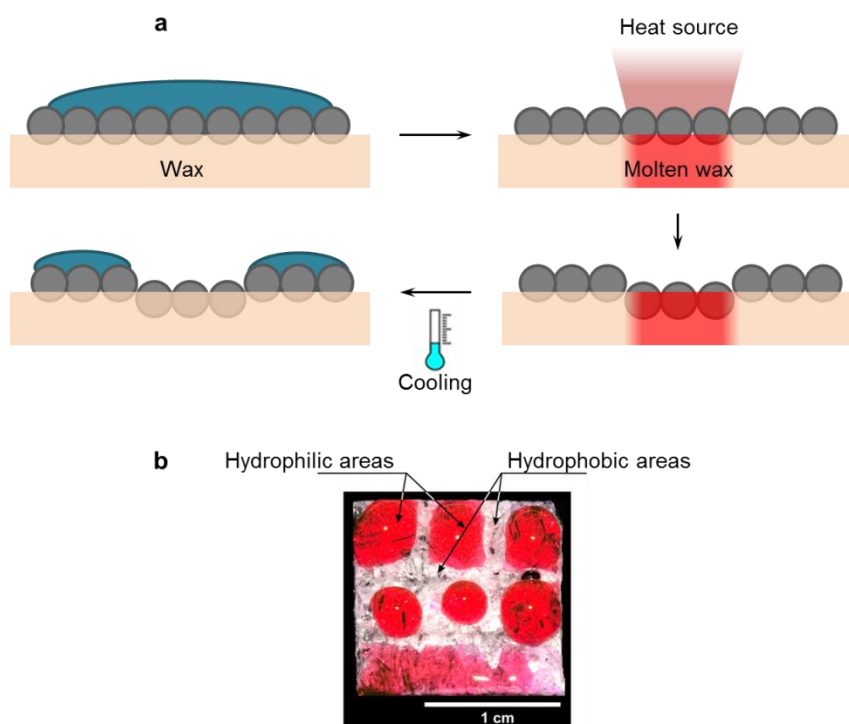
Figure 46. Hydrophobic/hydrophilic patterning of APS-modified silica particle-wax surface using locally applied heat source (i.e. hot needle). Scheme of experiment (a): the surface, initially switched to hydrophilic state by annealing under water, locally melted due to heat from the source. After cooling, the water (colored with rhodamine 6G) selectively wets the hydrophilic areas and does not wet the re-melted areas (b).

The investigated particle-wax surfaces also possess a moderate repairability and, in compliance with classification in section 2.1.2, can be classified as self-healing films. In fact, particles are localized not only at the

surface, but also inside the wax. After damage, which can involve a partial or full removal of the surface layer, these films may lose the initial wetting properties. However, morphology and the related wetting behavior can be easily restored by re-melting of the film under water in order to get back the hydrophilic properties or in air to obtain a hydrophobic film, due to the ability of the particles to migrate to the interface with reducing of the surface energy (some similar examples discussed in section 2.1.2). This ability of the particles was utilized for the preparation of superhydrophobic surfaces (section 3.3.4).

3.2.5 Conclusion

A novel approach for the design of stimuli-responsive surfaces was developed. This approach is based on hydrophobic waxy surfaces with incorporated hydrophilic particles. It was demonstrated, that the degree of particle immersion in the liquid oil layer depends on the environment (dry (air) or aqueous (water)) during the annealing of the wax-particle composite. Thus, roughness as well as hydrophobicity / hydrophilicity of the particle-wax surface can be switched in dry and aqueous environments, as well as it can be frozen by cooling down below the melting point of the wax. The possibility to pattern wax-particle surfaces using locally applied heat (in our experiments – warm needle) was also demonstrated. Moreover, the patterning can also be performed using localized heating by a laser beam.

Particle-wax blend possesses also reparability: due to particles distributed also inside of wax, after damaging of the surface layer and re-annealing (under water or in air) initial properties of the film (depending on annealing environment) can be easily restored. Finally, the developed approach can find broad applications in the design of switchable surfaces for offset printing of pigments, proteins, as well as cells.

3.3 Self-repairable superhydrophobic surfaces based on colloidal particles

3.3.1 Introduction

The design of coatings with superhydrophobic properties is a highly challenging task, because superhydrophobicity allows a reduction of surface contamination, wear, and corrosion. There are many approaches for the fabrication of superhydrophobic surfaces, including the ones based on photolithography [310], self-assembly [311], microcontact printing [312], layer-by-layer technique [313], controlled polymerization [314], and hydrolysis [315], as well as fabrics [118] and colloidal particles [22, 186, 258, 262, 267]. In section 2.1.3 some examples of such kind of surfaces are given.

Unfortunately, most of the superhydrophobic materials suffer from low durability: once the surface is mechanically damaged, it loses its superhydrophobic behavior. Therefore, the development of materials with durable and / or self-repairable superhydrophobic properties is very important. One group of approaches for the preparation of self-repairable superhydrophobic surfaces includes an encapsulation of a hydrophobic low-molecular weight compound in cavities [180] or pores [182], and superhydrophobicity can be restored after treatment with oxygen plasma.

Colloidal particles are particularly attractive for large-scale fabrication of superhydrophobic [258] and switchable surfaces at low cost, as it was already mentioned in this work. In fact, colloidal particles can simultaneously provide two properties required for the design of superhydrophobic materials: roughness and intrinsic hydrophobicity [100, 101]. The successful design of superhydrophobic surfaces requires, however, an accurate control of these two parameters. For example, it was found that superhydrophobicity cannot be achieved by using layers of densely packed, smooth hydrophobic particles [21, 259], and fractal structures must be used [22, 24, 258, 260, 263-265].

In this part of thesis, the effect of spontaneous segregation of colloidal particles at an oily surface for the design of novel materials with self-repairable superhydrophobic surfaces is shown. Perfluorodecane is used, in this case as an oil phase, and the particles are located on its surface, which in order provides superhydrophobicity of the surface. Once the surface is damaged, it can recover

its superhydrophobic properties after (re)melting of the hydrophobic perfuorodecane due to the migration of colloidal particles from the bulk to the newly formed surface (Figure 47). Properties of such surfaces are presented in section 3.3.4.

General procedures for the preparation of particle-pefluorodecane superhydrophobic surfaces are presented in section 3.3.3.

Further improvement of the mechanical properties of the obtained particle-wax composites for outdoor utilization may be needed. It the last part of this chapter, namely in section 3.3.5, an example of polymer-particle composite material and its properties are presented.

3.3.2 Materials

Additionally to the materials described in sections 3.1.2.1 and 3.2.2, 1-iodo-1H,1H,2H,2H-perfluorodecane (96%, Aldrich) and Sylgard 184 silicone elastomer kit (DOW corning) were used as received.

3.3.3 Experimental part

Preparation of perfluorodecane-particle mixtures and films based on them.

1-Iodo-1H,1H,2H,2H-perfluorodecane (PFD) with mp 54 – 58 °C was used as a bulk material for the preparation of superhydrophobic films. Mixtures with 50 mg, 100 mg, 150 mg and 200 mg amino-covered 200 nm silica particles and 1 g of PFD were prepared. The appropriate amount of particles was mixed with PFD, the mixture was heated up to 60 °C in a water bath and sonicated for 10 minutes. Thin and thick films of PFD incorporated with particles were prepared on silicon wafers by melting the PFD-particle mixtures.

For impregnation experiment 3-mm-thick porous polypropylene film was used. Particle-PFD mixture (ca 100 mg) was melted on the film (ca 1,5x1,5 cm, thickness ca 1 mm) in order to test wetting properties of obtained composite material.

Preparation of PDMS-particle mixtures and films based on them.

Mixture of 0,2 g APS-modified silica particles with 1 ml chloroform and 1 ml (ca 1,14 g) of elastomer (base) from Sylgard 184 Silicone Elastomer Kit preliminary stirred overnight at 900 rpm on magnetic stirrer was used for

preparation of polymer-particle composite films. For this purpose 0,4 ml of initial mixture was placed into 3 ml glass vial and 40 µl of curing agent was added. A portion (0,2 ml) of reaction mixture was placed on silicon wafer (ca 2x2 cm) in order to obtain ca 0,5 – 1 mm thick film. After it wafer with polymer-particle mixture was placed in vacuum oven at 80 °C and ca 20 mbar for 1 h. Then wafer was removed from the oven and heated to 250 °C for 1 min. After cooling solid polymer-particle film was obtained.

At the same manner reference polymer film on silicon wafer was obtain: 1 ml of the base was mixed with 1 ml chloroform overnight. To 0,4 ml of the mixture 40 µl of curing agent was added. 0,2 ml of the reaction mixture was filmed on 2x2 cm silicon wafer and placed into vacuum oven at 80 °C and ca 20 mbar for 1 h. After wafer removing and its cooling to room temperature reference PDMS-film was obtained. In order to correspond to the procedure for particle-PDMS film, obtained PDMS-film was heated on air at 250 °C for 1 min though this step for the preparation of PDMS-film was not necessary.

3.3.4 Particles on a perfluorodecane surface

The same approach, as discussed in section 3.2.4, based on colloidal particles incorporated with a hydrophobic waxy-matrix, may be used for the preparation of superhydrophobic self-repairable films (Figure 47).
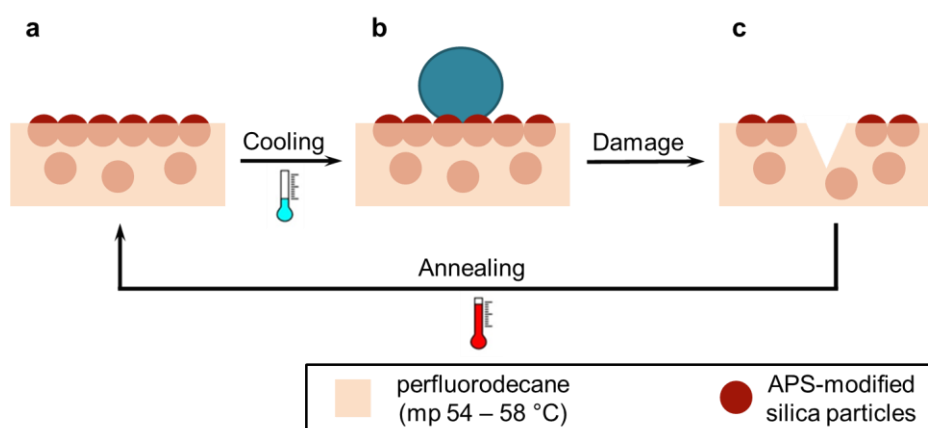
Figure 47. Schematic illustration of a material based on a particle-wax matrix with self-repairable superhydrophobicity. Superhydrophobic surface formed by colloidal particles incorporated with perfluorodecane (a, b). Particles may be removed by mechanical damage partially or fully from the surface layer (c). Re-melting of the film leads to a migration of the particles to the surface and their reorganization with restoring of the initial surface properties (a).

In our experiments, a mixture of PFD and 200 nm large 3-aminopropyltriethyxy silane (APS)-modified silica particles was used. The PFD itself is a highly hydrophobic waxy solid with a melting point around 60 °C, crystalline structure and, due to this, PFD forms rough, fractal surfaces in solid state (Figure 48a ; root mean square roughness R_q = 2 − 3 µm, fractal dimension D = 2,2 – 2,3 – data were evaluated from MicroGlider measurements). Due to the specific fractal rough structure of the surface, the advancing and receding contact angles on the surface of this material are slightly higher (θ_{adv}^{PFD} = 127°, θ_{rec}^{PFD} = 95°, Figure 49a) than that on the surface of smooth perfluorinated silanes [310]. Apparently, according to the Wenzel and Cassie−Baxter equationsEquation (2) – Equation (3), roughness increases the hydrophobicity of the surface.

Figure 48. Morphology of rough surfaces formed with pure PFD (a) and PFD-particles (b, c, d) after different treatment steps: PFD-particle blend (b); damaged surface (c) –top layer was almost removed by cutting; healed PFD-particle surface after annealing at 60 °C (mp of PFD) for several seconds (d)

Superhydrophobic behavior appears, when PFD is mixed with moderately hydrophilic APS-modified silica particles (intrinsic advancing water contact angle on a flat APS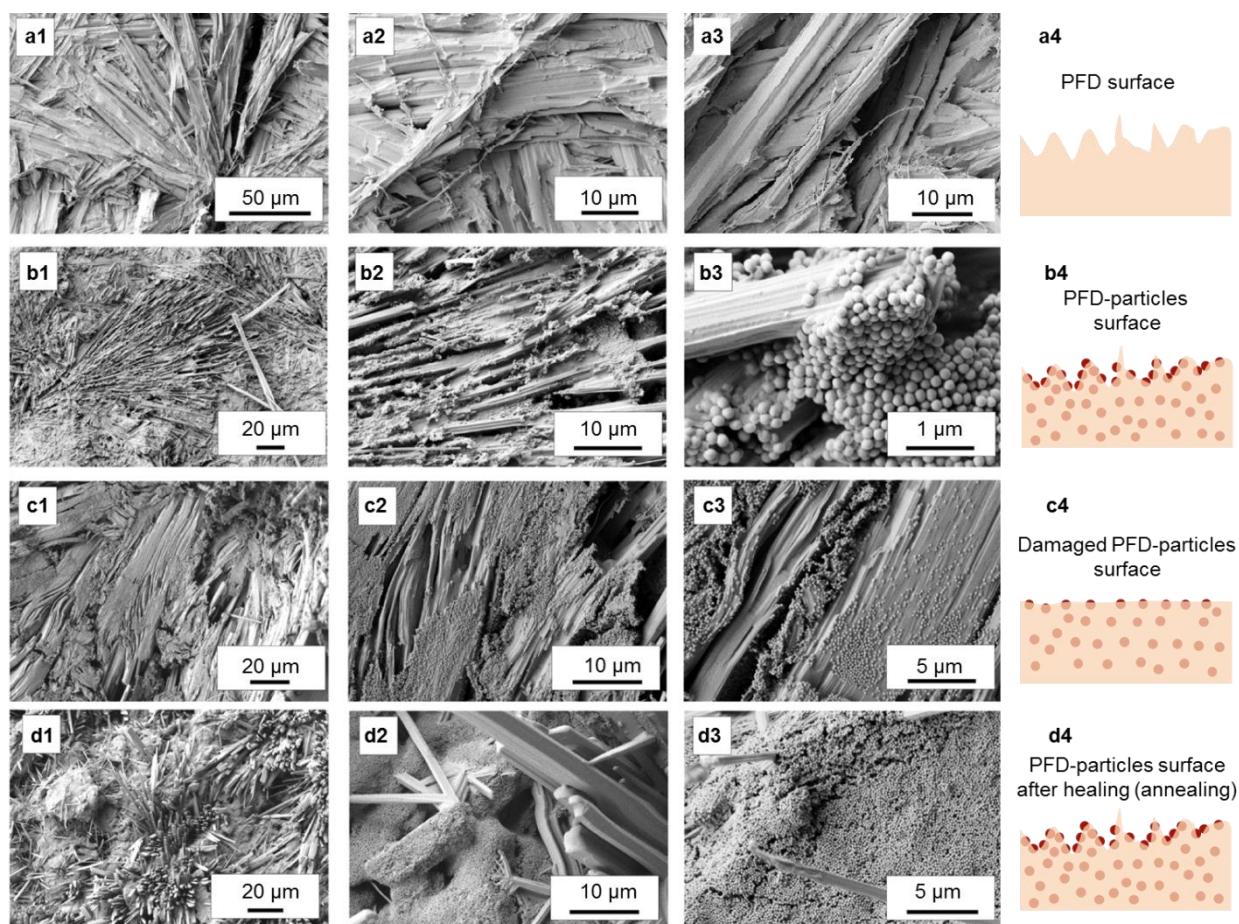-modified silicon wafer is $\theta_{adv}^{APS-flat}$ = 70°). After annealing in air, the surface of the wax−particle blend with a typical thickness of 2 – 3 mm becomes superhydrophobic: both advancing and receding contact angles are very high ($\theta_{adv}^{PFD-particles}$ = 153°, $\theta_{rec}^{PFD-particles}$ = 152°, Figure 49b). Water droplets in this case may easily roll out from the surface, and in some experiments, due to this fact, a self-cleaning effect was demonstrated by collecting some dust particles from the surface. Superhydrophobicity was observed for particle−PFD blends with the mass fraction of particles being 5% or more. The reason for this superhydrophobic behavior is hierarchically rough morphology formed by particles, which are segregated at the surface of PFD crystallites (Figure 48b). The values of roughness and fractal dimension of PFD with and without particles, as obtained by MicroGlider, are, however, the same because the resolution of the MicroGlider is ca. 1 µm, which is insufficient to image silica particles. Contrary to APS-modified silica particles, native ones strongly immerse into PFD and do not affect its hydrophobicity.

Both segregation of hydrophilic particles at the PFD-air interface and the formation of superhydrophobic surfaces are unexpected. Firstly, PFD completely wets the surface of APS-modified silica wafers and, thus, PFD also wets APS-modified particles, as well as their aggregates. Thereby, particles and their aggregates should be completely immersed into the PFD matrix. It was assumed that the particles are most probably expelled from the wax during crystallization. Secondly, the addition of intrinsically hydrophilic modified silica particles leads to superhydrophobic properties. According to the equations of Wenzel Equation (2) and Cassie−Baxter Equation (3), which predict equilibrium contact angle corresponding to a global minimum of energy, roughness amplifies the intrinsic properties and makes hydrophobic and hydrophilic surfaces even more hydrophobic and hydrophilic, respectively. Contrary to our expectations, hydrophilic APS-modified surface of the particles became more hydrophobic. This contradictory effect can be explained by an entrapment of the water droplet in energetically metastable states [117, 275], which occurs on moderately hydrophobic surfaces and results in superhydrophobic behavior [316].
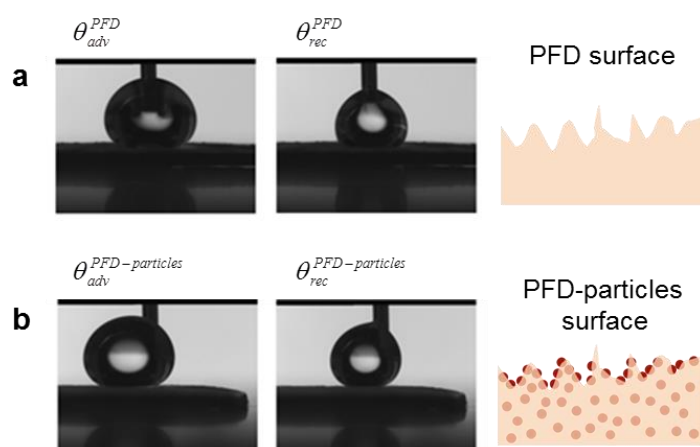
Figure 49. Water droplet profiles on PFD-surface (a) and on the surface of PFD-particle blend (b).

The healing properties of the superhydrophobic composite surfaces formed by PFD and particles were tested. First, superhydrophobic surfaces were prepared by melting the particles with PFD. The topmost surface layer (0.1−0.2 mm) was completely removed by a razor blade (Figure 48c). As a result, the surface density of colloidal particles decreased (Figure 48c3), and the values of advancing and receding contact angles simultaneously decreased (Figure 50) to the values corresponding to the surface of pure PFD ($\theta_{adv}^{PFD-particles,damaged}$ = 120°, $\theta_{rec}^{PFD-particles,damaged}$ = 100°). Melting of the particle-PFD composite for 30 seconds at 60 °C (slightly above the melting point of PFD), followed by cooling, resulted in restoration of the superhydrophobic surface with very high values of advancing and receding contact angles ($\theta_{adv}^{PFD-particles}$ = 149°, $\theta_{rec}^{PFD-particles}$ = 148°, Figure 50). Colloidal particles segregated at the interface and the morphology of the recovered surface was similar to that before damage (Figure 48d). Reproducibility of the observed phenomenon even after multiple damage-heating cycles was also demonstrated (Figure 50).
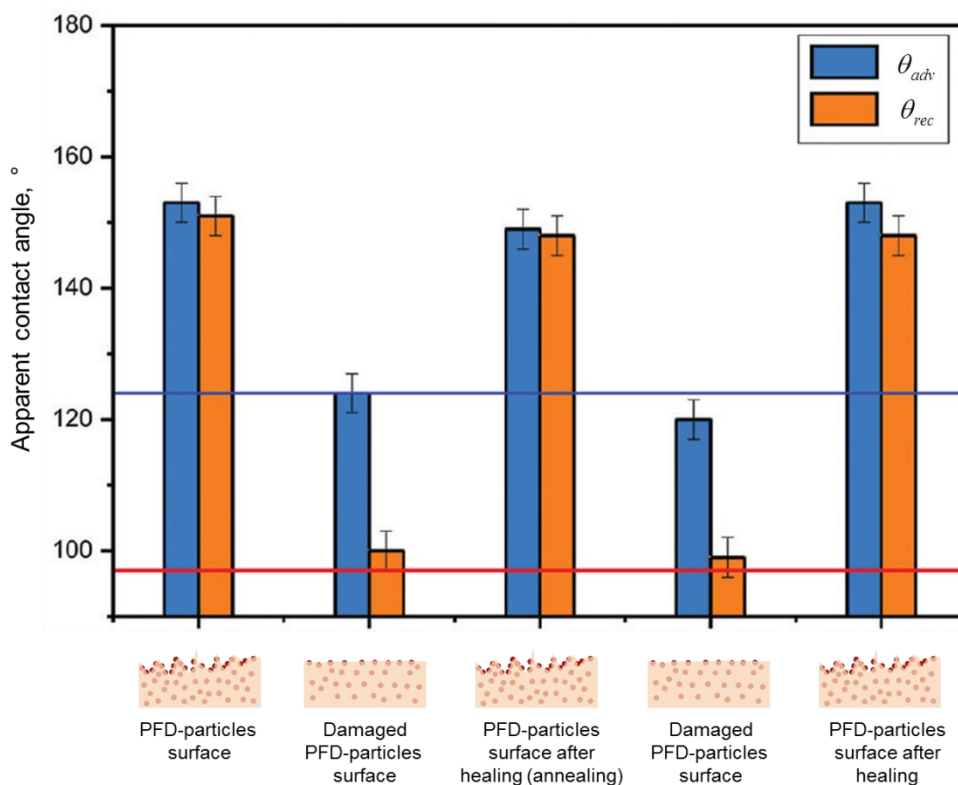
Figure 50. Water contact angle on PFD-particle surface after different stages of treatment (damage and healing).

Unfortunately, the investigated PFD−particle composite material is brittle. However, mechanical properties can be improved by using porous materials as scaffolds, with the particle−PFD blend soaked in it. For this purpose, a 3-mm-thick porous polypropylene film with an average pore size of 100 μm was used for the impregnation experiment. The formed surface demonstrated moderate repairing superhydrophobic properties: the surface of the film was superhydrophobic and the scratched film recovered its superhydrophobicity after heating and annealing it several seconds at 60 °C (the results were identical to those presented in Figure 50). The film could be easily deformed by bending or twisting without breaking. Thus, the possibility of preparation of the material that combines the rigidity of the polymer scaffold with the self-repairing properties of the particle-PFD blend was also shown.

3.3.5 Particles on a polymer surface

Another option for the improvement of the particle – PFD (or particle-wax) composite properties is utilization of polymer materials instead of wax. For our experiments, it was decided to explore commercially available PDMS (Sylgard

184 silicone elastomer kit) due to the simplicity of the film preparation and initial hydrophobicity of PDMS. Also, PDMS is an amorphous polymer and forms a flat surface after curing, what was observed for the reference PDMS-sample (Figure 51).

The addition of particles affects the curing ability of the curing agent, therefore, an additional amount of the curing agent was used (in accordance with the preparation procedure for the PDMS film, 1:10 ratio of curing agent : base should be used; in our experiments ratio 1:5 was used) and additional heating was required. It can be explained, that the particles affect the reaction ability of the curing agent during heating, but after annealing for a short time at 250 °C a particle-PDMS film was obtained.

It was found, that the particles almost immersed into the polymer: only about 20 nm particle cap was above the surface (Figure 51). So the height of the particle cap above the wax surface normalized to the particle radius (h^*) in this case is slightly higher than for a particle-wax surface (for PDMS – APS-modified particles $h^* = 0{,}2$ for wax – APS-modified particles $h^* = 0$, Table 4).

Further, wetting properties of the obtained films were investigated. PDMS film without particles possesses hydrophobic properties with quite high advancing and receding contact angles ($\theta_{adv}^{PDMS} = 120°$, $\theta_{rec}^{PDMS} = 91°$, Figure 52). Addition of the particles results in an increase of both values of contact angles: $\theta_{adv}^{PDMS-particles} = 137°$, $\theta_{rec}^{PDMS-particles} = 110°$, Figure 52. This fact can be explained by an of increased roughness of the surface and is in good correlation with the previously obtained results for particle-wax and APS-modified particle-PFD systems.
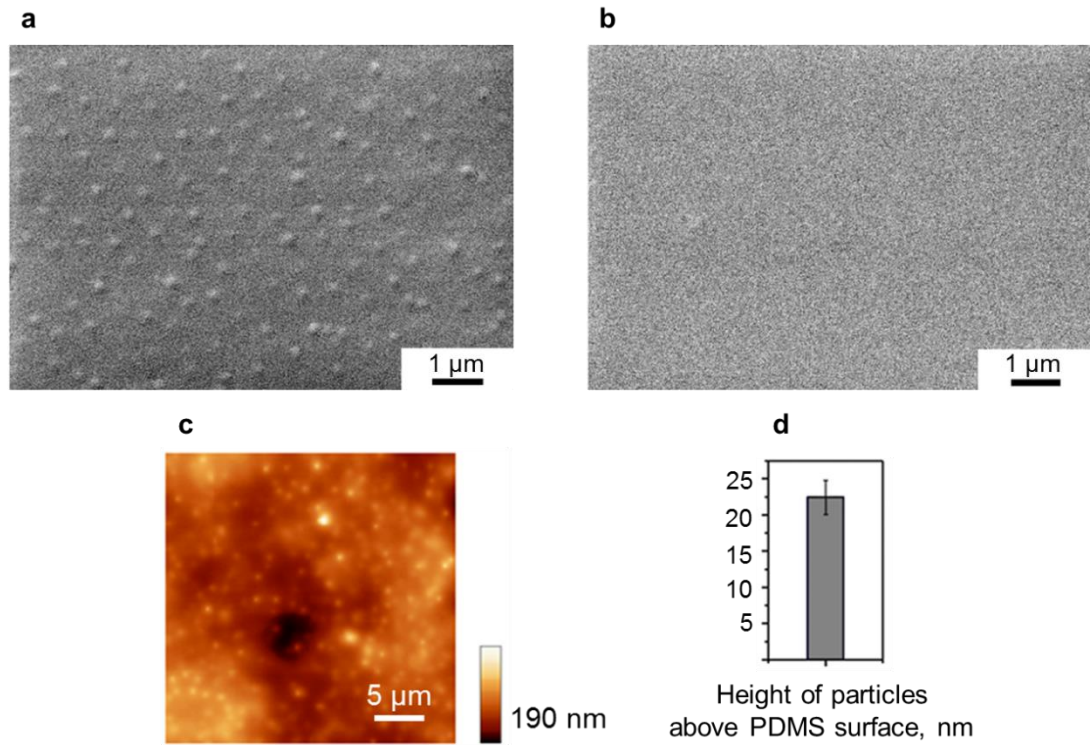
Figure 51. APS-modified particle-PDMS surface and reference PDMS surface: SEM images (a, b); AFM image (c) and the height of the particle cap above the PDMS surface evaluated from AFM measurements (d)
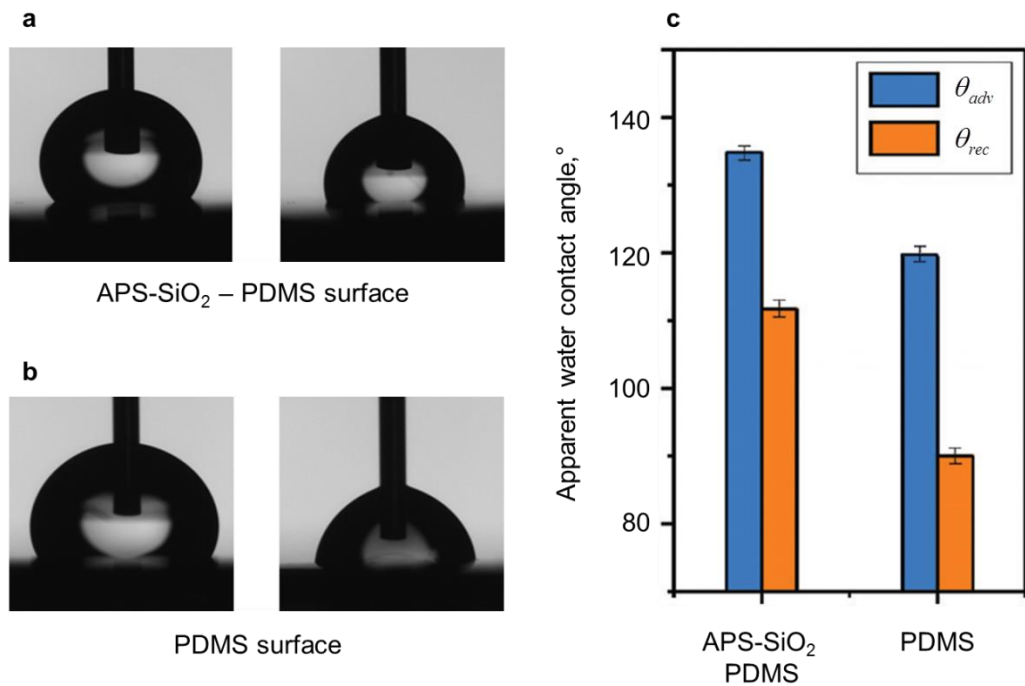
Figure 52. Wetting properties of APS-modified particles incorporated with PDMS and reference PDMS surfaces: water drop profiles on a particle-PDMS surface (a) and PDMS surface (b); water contact angles on investigated surfaces (c).

Although PMDS is not crystalline comparing to wax and PFD, superhydrophobic properties were unfortunately not observed, in this case. On the other hand, mechanically obtained films are much more stable than particle-wax or particle-PFD films.

3.3.6 Conclusion

An approach for the design of surfaces with self-repairing superhydrophobic properties based on incorporation of amino-modified colloidal particles into hydrophobic matrix, namely perfluorodecane, was developed. The particles spontaneously segregate at the air-PFD interface during annealing with a formation of hierarchical fractal structures on the surface. After damage (superhydrophobicity does not occur in this case) the surface can easily recover initial superhydrophobic properties after re-melting, due to the migration of particles to the newly formed surface. Obtained composite can be classified as a non-autonomic self-healing material with intrinsic capability. Though nanoparticles using in the developing of self-healing materials considered in literature as non-autonomic extrinsic self-healing, particles in blends with PFD define wetting properties of material itself and cannot be considered as extrinsic additive.

The investigated particle-PFD blends are considered as model systems. Two possible ways of improving the mechanical properties of the obtained films were investigated. One of these approaches is based on the encapsulation of particle-oil blends into a porous material. Second method involves using a polymer matrix instead of oil.

4 Summary and outlook

The aim of this thesis was to design a self-repairable material with superhydrophobic and switchable properties using colloidal particles. Specific goals were the synthesis of colloidal particles and the preparation of functional surfaces incorporated with the obtained particles, which exhibit a repairable switching behavior and repairable superhydrophobicity. In order to achieve these goals, first, methods of preparation of simple and functional colloidal particles were developed. Second, the behavior of particles at surfaces of easy fusible solid materials, namely, paraffin wax or perfluorodecane, was investigated. This chapter summarizes the obtained results and presents an outlook for further developments.

First, methods for the synthesis of colloidal particles with different shapes were developed. Mechanically- and solvent-resistant raspberry-like particles were synthesized by coupling small particles to a bigger core utilizing polymer brushes. The obtained raspberry-like structures possess high durability and do not break down under ultrasonication and exposure to organic solvents. Furthermore, applicability of raspberry-like particles after their hydrophobization for the fabrication of superhydrophobic surfaces was demonstrated. Potentially, the developed robust raspberry-like particles may be suitable substrates for immobilization of stimuli-responsive brushes as well, and obtained switchable functional colloidal particles are promising candidates for the design of waterborne superhydrophobic coatings (Figure 53).
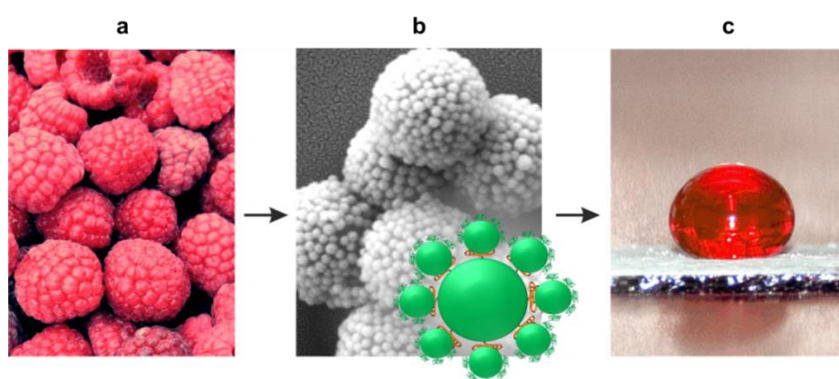

Figure 53. Raspberry (a), raspberry-like particles (b) and superhydrophobic film based on raspberry particles (c).

It was shown, that not only complex raspberry-like particles, but also diatomaceous earth, fossil soft shells of hard-shell algae, can be used for the preparation of superhydrophobic surfaces. The main advantages of diatomaceous earth particles are their hierarchical shape and affordability. Similar to raspberry-like particles, diatomaceous earth can be modified by grafted polymers. Immobilization of a polymer shell has certain advantages comparing to the widely-used silane modification. Due to a greater thickness of the polymer, the obtained polymer layer is more stable and robust than a silane monolayer with similar chemical functionality. An example of polymer-modified diatomaceous earth particles was shown. Such kinds of materials can be used for the preparation of hydrophobic and superhydrophobic surfaces on a large scale.

Second, a novel approach for the design of stimuli-responsive surfaces, based on native and amino-modified silica particles incorporated in a hydrophobic matrix with a slightly low melting point – paraffin wax – was developed. It was found that the degree of particle immersion in the liquid oil layer depends on the environment, dry (air) or aqueous (water), during annealing of the wax-particle composites. Thus, roughness as well as hydrophobicity / hydrophilicity of the particle-wax surface can be switched by annealing in different environments with further cooling and solidification of the composite. The possibility to pattern wax-particle surfaces using locally applied heat was also demonstrated. Moreover, patterning can also be performed using localized heating by a laser beam. The developed approach can find broad applications in the design of switchable surfaces for offset printing of pigments, proteins, as well as cells.

Third, a similar approach was used for the design of surfaces with self-repairing superhydrophobic properties. In this case, the composites are based on perfluorodecane and amino-modified colloidal particles. The particles spontaneously segregate at the air-perfluorodecane interface during annealing with the formation of hierarchical fractal structures on the surface. After damage and loss of superhydrophobicity the surface can easily recover initial superhydrophobic properties by re-melting: due to the migration of particles to the newly formed surface. Ultimately, full reparability of the surface properties was demonstrated (Figure 54).
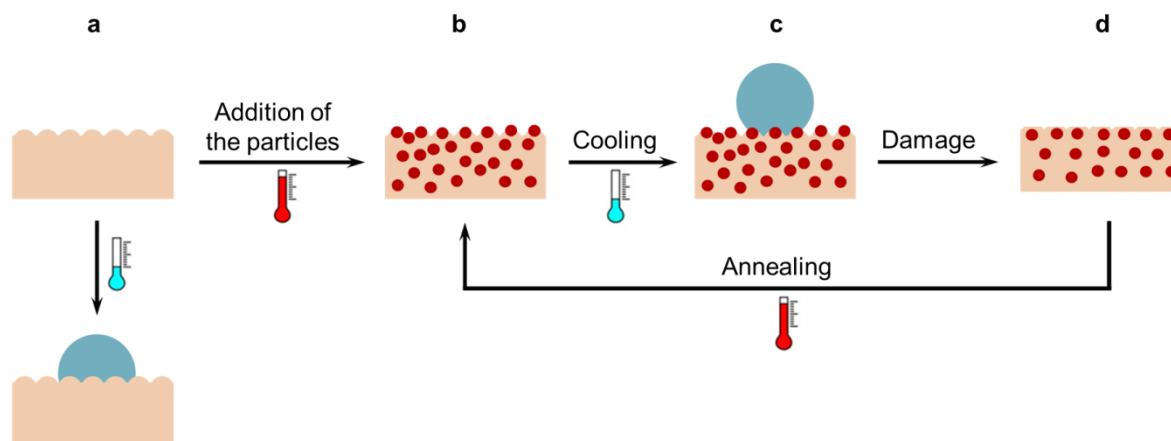
Figure 54. Schematic illustration of the concept of self-repairable material based on colloidal particle-PFD blends. Particles on the surface provide additional roughness and the initially hydrophobic surface (a) becomes superhydrophobic (c). Superhydrophobicity can be restored (b) after damage (d) by annealing of the particle-perfluorodecane composite.

The obtained particle-wax and particle-perflurodecane composites can be classified as non-autonomic self-healing materials with intrinsic capability of self-healing. Even though nanoparticles used for the development of self-healing materials are considered in literature as non-autonomic extrinsic self-healing, additives particles in blends with fusible solids, which define the wetting properties of the material itself cannot be considered as an extrinsic additive.

The investigated particle-wax and particle-perfluorodecane blends are considered as model systems for the study of the behavior of particles on the surfaces. Two possible ways of improving the mechanical properties of the obtained composites were investigated. One of these approaches is based on the encapsulation of particle-oil blends into a porous material. This approach allowed us, for instance, to get a superhydrophobic material with improved mechanical properties. Similar approach may also be used for the preparation of advanced switchable surfaces. The second method is based on using a polymer matrix instead of fusible wax. This approach is promising for the preparation of durable superhydrophobic films. It is also expected that the same approach can be used to obtain switchable surfaces, but the switching trigger would be higher in this case, comparing to the particle-paraffin wax systems.

Outlook

Further efforts should be focused on systems that have a higher potential and applicability as a self-repairing material. A possible example of such a system would be one based on a polymer with an encapsulated mixture of droplets of monomer and particles. Damage of the surface would lead to the release of the particles, which, as we have shown, would segregate at the monomer−air interface. Curing of the monomer would then complete the healing process.

On the other hand, utilization of particles received from natural sources instead of complex synthetic particles (diatomaceous earth, for instance) as well as polymer brushes, which can be synthesized from a monomer obtained from plant oil, i.e. stearyl methacrylate, is very attractive. In this case, surfaces with excellent properties may be acquired at low costs.

Further improvement of this approach, ultimately obtaining not only a superhydrophobic self-repairable material, but also one with switchable wetting properties, may be achieved by using dipolar particles, which are also known as Janus particles. Generally, Janus particles should migrate to the interface and orient there in order to minimize the free energy in the same manner as colloidal particles described in this work. This behavior can be investigated by using mixtures of Janus particles and paraffin wax with a low melting point. But in this case not only surface topology will be changed during annealing in different environments, but also the orientation of particles on the surface (Figure 55).
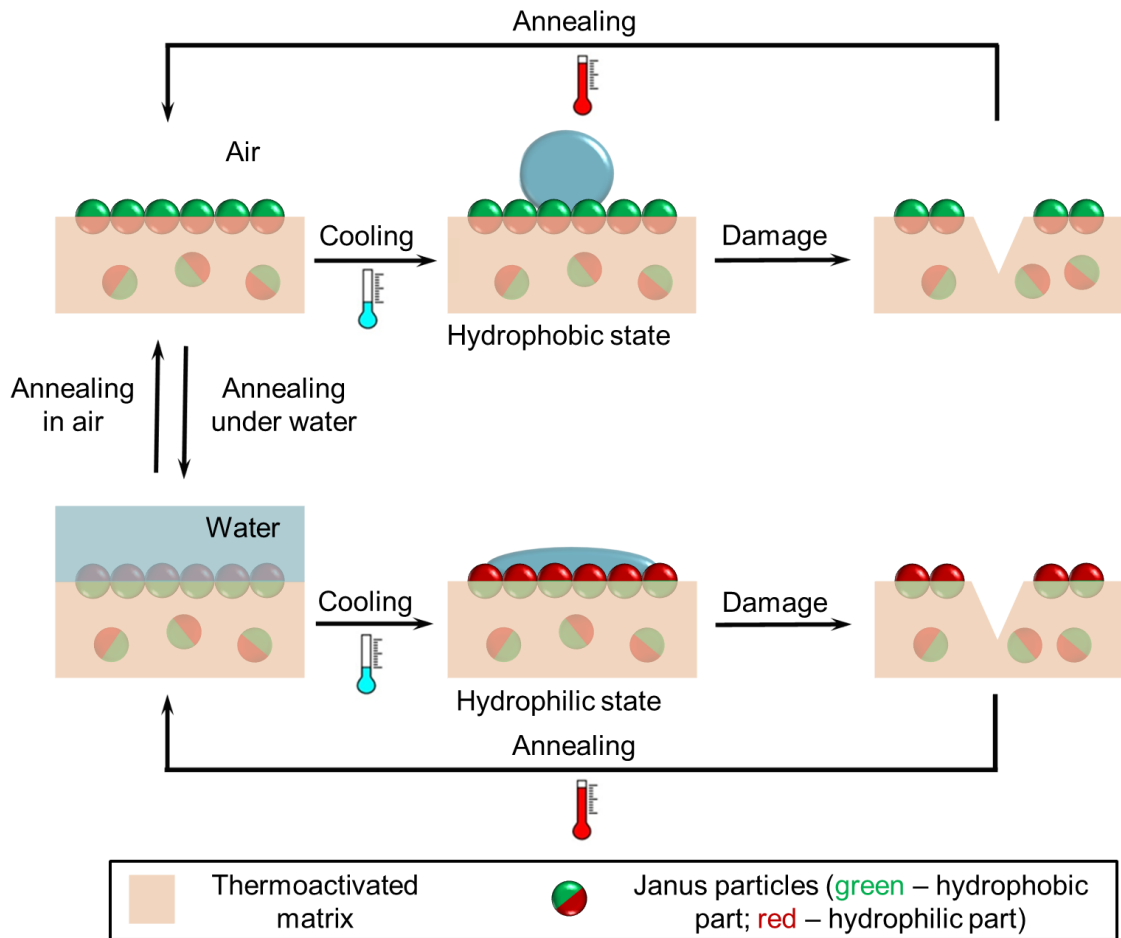
Figure 55. Scheme of switchable surfaces based on Janus particle-thermo-activated matrix. Schematic of damage repair in two different states: for renewal of initial surface properties annealing should be performed in air for a hydrophobic surface and under water – for hydrophilic.

According to this and the results obtained in this work, a surface incorporated with Janus particles may possess more hydrophobicity (even superhydrophobicity) and hydrophilicity comparing to composites, consisting of simple colloidal particles and wax. Substitution of the wax matrix with a polymer with self-repairable properties leads to the formation of a composite with fully self-repairable switchable properties.

5 List of abbreviations

AFM	Atom force microscopy
AGET-ATRP	Atom generated electron transfer atom transfer radical polymerization
APS	(3-Aminopropyl)triethoxysilane
ATRP	Atom transfer radical polymerization
BET theory	Brunauer-Emmett-Teller theory
BSE	Backscattered electrones
CA	Contact angles, °
Δ	Phase parameter (ellipsometry)
DE	Diatomaceous earth
DMF	Dimethylformamide
DNA	Deoxyribonucleic acid
FAS	Fluorinated alkyl silane
FD-POSS	Fluorinated-decyl polyhedral oligomeric silsesquioxane
FIB	Focused ion beam
GMA	Glycidyl methacrylate
GPC	Gel-permeation chromatography
EBiB	Ethyl α-bromoisobutyrate
n	Refractive index
k	Extinction coefficient
LCST	Lower critical solution temperature, °C
PAA	Poly(acrylic acid)
PAH	Poly(allylamine hydrochloride)
PC	Personal computer
PDMS	Poly(dimethyl siloxane)
PGMA	Poly(glycidyl methacrylate)
PFD	1-Iodo-1H,1H,2H,2H-perfluorodecane
PFS	2,3,4,5,6-Pentafluorostyrene
PMDTA	N,N,N',N'',N''-Pentamethyldiethylenetriamine
PNIPAAm	Poly(N-isopropylacrylamide)

PPFS	Poly(2,3,4,5,6-pentafluorostyrene)
POTS	1H,1H,2H,2H-perfluorooctyltriethoxysilane
PSFD	Phase space filtered detection
R_a	Mean roughness, µm
RMS (R_q)	Root mean square roughness, µm
RP	Raspbery-like particle (-s)
r_s	Roughness factor
SAM	Self-assembled monolayer
SE	Secondary electrones
SEM	Scanning electron microscopy
SFM	Scanning force microscopy
SP	Silica particle (-s)
SPEEK	Sulfonated poly(ether ether ketone)
THF	Tetrahydrofuran
Φ	Amplitude parameter (ellipsometry)
θ	Static contact angle, °
θ_{adv}	Advancing contact angle, °
θ_{flat}	Contact angle on flat surface, °
θ_{rec}	Receding contact angle, °
TEOS	Tetraethyl orthosilicate
TGA	Thermogravimetric analysis
UV	Ultraviolet

6. References

1.   Hager, M. D.; Greil, P.; Leyens, C.; van der Zwaag, S.; Schubert, U. S., Self-Healing Materials. *Advanced Materials* **2010,** 22, (47), 5424-5430.
2.   Koch, K.; Bhushan, B.; Jung, Y. C.; Barthlott, W., Fabrication of artificial Lotus leaves and significance of hierarchical structure for superhydrophobicity and low adhesion. *Soft Matter* **2009,** 5, (7), 1386-1393.
3.   Barthlott, W.; Neinhuis, C., Purity of the sacred lotus, or escape from contamination in biological surfaces. *Planta* **1997,** 202, (1), 1-8.
4.   Luzinov, I.; Minko, S.; Tsukruk, V. V., Adaptive and responsive surfaces through controlled reorganization of interfacial polymer layers. *Progress in Polymer Science* **2004,** 29, (7), 635-698.
5.   Minko, S.; Müller, M.; Usov, D.; Scholl, A.; Froeck, C.; Stamm, M., Lateral versus Perpendicular Segregation in Mixed Polymer Brushes. *Physical Review Letters* **2002,** 88, (3), 035502.
6.   Minko, S.; Müller, M.; Motornov, M.; Nitschke, M.; Grundke, K.; Stamm, M., Two-Level Structured Self-Adaptive Surfaces with Reversibly Tunable Properties. *Journal of the American Chemical Society* **2003,** 125, (13), 3896-3900.
7.   Senaratne, W.; Andruzzi, L.; Ober, C. K., Self-Assembled Monolayers and Polymer Brushes in Biotechnology: Current Applications and Future Perspectives. *Biomacromolecules* **2005,** 6, (5), 2427-2448.
8.   Wang, R.; Hashimoto, K.; Fujishima, A.; Chikuni, M.; Kojima, E.; Kitamura, A.; Shimohigoshi, M.; Watanabe, T., Light-induced amphiphilic surfaces. *Nature* **1997,** 388, (6641), 431-432.
9.   Ionov, L.; Minko, S.; Stamm, M.; Gohy, J.-F.; Jérôme, R.; Scholl, A., Reversible Chemical Patterning on Stimuli-Responsive Polymer Film: Environment-Responsive Lithography. *Journal of the American Chemical Society* **2003,** 125, (27), 8302-8306.
10.   Rühe, J.; Ballauff, M.; Biesalski, M.; Dziezok, P.; Gröhn, F.; Johannsmann, D.; Houbenov, N.; Hugenberg, N.; Konradi, R.; Minko, S.; Motornov, M.; Netz, R.; Schmidt, M.; Seidel, C.; Stamm, M.; Stephan, T.; Usov, D.; Zhang, H., Polyelectrolyte Brushes. In *Polyelectrolytes with Defined Molecular Architecture I*, Schmidt, M., Ed. Springer Berlin Heidelberg: 2004; Vol. 165, pp 79-150.
11.   Lahann, J.; Mitragotri, S.; Tran, T.-N.; Kaido, H.; Sundaram, J.; Choi, I. S.; Hoffer, S.; Somorjai, G. A.; Langer, R., A Reversibly Switching Surface. *Science* **2003,** 299, (5605), 371-374.
12.   Katz, E.; Sheeney-Haj-Ichia, L.; Basnar, B.; Felner, I.; Willner, I., Magnetoswitchable Controlled Hydrophilicity/Hydrophobicity of Electrode Surfaces Using Alkyl-Chain-Functionalized Magnetic Particles: Application for Switchable Electrochemistry. *Langmuir* **2004,** 20, (22), 9714-9719.
13.   Ichimura, K.; Oh, S.-K.; Nakagawa, M., Light-Driven Motion of Liquids on a Photoresponsive Surface. *Science* **2000,** 288, (5471), 1624-1626.
14.   Nath, N.; Chilkoti, A., Creating "Smart" Surfaces Using Stimuli Responsive Polymers. *Advanced Materials* **2002,** 14, (17), 1243-1247.
15.   Edahiro, J.-i.; Sumaru, K.; Tada, Y.; Ohi, K.; Takagi, T.; Kameda, M.; Shinbo, T.; Kanamori, T.; Yoshimi, Y., In Situ Control of Cell Adhesion Using Photoresponsive Culture Surface. *Biomacromolecules* **2005,** 6, (2), 970-974.

16.   Huber, D. L.; Manginell, R. P.; Samara, M. A.; Kim, B.-I.; Bunker, B. C., Programmed Adsorption and Release of Proteins in a Microfluidic Device. *Science* **2003,** 301, (5631), 352-354.

17.   Lee, J. Y.; Buxton, G. A.; Balazs, A. C., Using nanoparticles to create self-healing composites. *The Journal of Chemical Physics* **2004,** 121, (11), 5531-5540.

18.   Gupta, S.; Zhang, Q.; Emrick, T.; Balazs, A. C.; Russell, T. P., Entropy-driven segregation of nanoparticles to cracks in multilayered composite polymer structures. *Nat Mater* **2006,** 5, (3), 229-233.

19.   Tyagi, S.; Lee, J. Y.; Buxton, G. A.; Balazs, A. C., Using Nanocomposite Coatings To Heal Surface Defects. *Macromolecules* **2004,** 37, (24), 9160-9168.

20.   Ogihara, H.; Okagaki, J.; Saji, T., A Facile Fabrication of Superhydrophobic Films by Electrophoretic Deposition of Hydrophobic Particles. *Chemistry Letters* **2009,** 38, (2), 132-133.

21.   Synytska, A.; Ionov, L.; Dutschk, V.; Stamm, M.; Grundke, K., Wetting on Regularly Structured Surfaces from "Core−Shell" Particles: Theoretical Predictions and Experimental Findings. *Langmuir* **2008,** 24, (20), 11895-11901.

22.   Synytska, A.; Ionov, L.; Grundke, K.; Stamm, M., Wetting on Fractal Superhydrophobic Surfaces from "Core−Shell" Particles: A Comparison of Theory and Experiment. *Langmuir* **2009,** 25, (5), 3132-3136.

23.   Boinovich, L.; Emelyanenko, A., Principles of Design of Superhydrophobic Coatings by Deposition from Dispersions. *Langmuir* **2009,** 25, (5), 2907-2912.

24.   Qian, Z.; Zhang, Z.; Song, L.; Liu, H., A novel approach to raspberry-like particles for superhydrophobic materials. *Journal of Materials Chemistry* **2009,** 19, (9), 1297-1304.

25.   Volkov, A. G.; Adesina, T.; Markin, V. S.; Jovanov, E., Kinetics and Mechanism of Dionaea muscipula Trap Closing. *Plant Physiology* **2008,** 146, (2), 694-702.

26.   Zwaag, S., An Introduction to Material Design Principles: Damage Prevention versus Damage Management Self Healing Materials. In *Self Healing Materials. An Alternative Approach to 20 Centuries of Materials Science*, Zwaag, S., Ed. Springer, Dordrecht, The Netherlands: 2007; Vol. 100, pp 1-18.

27.   Yuan, Y. C.; Yin, T.; Rong, M. Z.; Zhang, M. Q., Self healing in polymers and polymer composites. Concepts, realization and outlook: A review. *Express Polymer Letters* **2008,** 2, (4), 238-250.

28.   Ghosh, S. K., Self-Healing Materials: Fundamentals, Design Strategies, and Applications. In *Self-Healing Materials: Fundamentals, Design Strategies, and Applications*, Wiley-VCH Verlag GmbH & Co. KGaA, Weinheim, Gemany: 2009; pp 1-28.

29.   Osswald, T. A.; Menges, G., Failure and Damage of Polymers. In *Materials Science of Polymers for Engineers. 3rd Edition* Carl Hanser Verlag GmbH & Co. KG, Munich, Germany: 2012; pp 423-487.

30.   Wu, D. Y.; Meure, S.; Solomon, D., Self-healing polymeric materials: A review of recent developments. *Progress in Polymer Science* **2008,** 33, (5), 479-522.

31.   Yousefpour, A.; Hojjati, M.; Immarigeon, J.-P., Fusion Bonding/Welding of Thermoplastic Composites. *Journal of Thermoplastic Composite Materials* **2004,** 17, (4), 303-341.

32.   Wool, R. P.; O'Connor, K. M., A theory crack healing in polymers. *Journal of Applied Physics* **1981,** 52, (10), 5953-5963.

33.   Wool, R. P.; O'Connor, K. M., Time dependence of crack healing. *Journal of Polymer Science: Polymer Letters Edition* **1982,** 20, (1), 7-16.

34.   Ageorges, C.; Ye, L.; Hou, M., Advances in fusion bonding techniques for joining thermoplastic matrix composites: a review. *Composites Part A: Applied Science and Manufacturing* **2001,** 32, (6), 839-857.

35.   Boiko, Y. M.; Guérin, G.; Marikhin, V. A.; Prud'homme, R. E., Healing of interfaces of amorphous and semi-crystalline poly(ethylene terephthalate) in the vicinity of the glass transition temperature. *Polymer* **2001,** 42, (21), 8695-8702.

36.   Shen, J.-S.; Harmon, J. P.; Lee, S., Thermally-induced Crack Healing in Poly(Methyl Methacrylate). *Journal of Materials Research* **2002,** 17, (06), 1335-1340.

37.   Jud, K.; Kausch, H. H.; Williams, J. G., Fracture mechanics studies of crack healing and welding of polymers. *J Mater Sci* **1981,** 16, (1), 204-210.

38.   Kim, H. J.; Lee, K.-J.; Lee, H. H., Healing of fractured polymers by interdiffusion. *Polymer* **1996,** 37, (20), 4593-4597.

39.   Avramova, N., Study of the healing process of polymers with different chemical structure and chain mobility. *Polymer* **1993,** 34, (9), 1904-1907.

40.   Lin, C. B.; Lee, S.; Liu, K. S., Methanol-Induced crack healing in poly(methyl methacrylate). *Polymer Engineering & Science* **1990,** 30, (21), 1399-1406.

41.   Wang, P.-P.; Lee, S.; Harmon, J. P., Ethanol-induced crack healing in poly(methyl methacrylate). *Journal of Polymer Science Part B: Polymer Physics* **1994,** 32, (7), 1217-1227.

42.   Chen, J.-S.; Ober, C. K.; Poliks, M. D., Characterization of thermally reworkable thermosets: materials for environmentally friendly processing and reuse. *Polymer* **2002,** 43, (1), 131-139.

43.   Stubblefield, M. A.; Yang, C.; Pang, S.-S.; Lea, R. H., Development of heat-activated joining technology for composite-to-composite pipe using prepreg fabric. *Polymer Engineering & Science* **1998,** 38, (1), 143-149.

44.   Paul, J.; Jones, R., Repair of impact damaged composites. *Engineering Fracture Mechanics* **1992,** 41, (1), 127-141.

45.   Gan, L.-H.; Ye, L.; Mai, Y.-W., Optimum design of cross-sectional profiles of pultruded box beams with high ultimate strength. *Composite Structures* **1999,** 45, (4), 279-288.

46.   Zhang, H.; Motipalli, J.; Lam, Y. C.; Baker, A., Experimental and finite element analyses on the post-buckling behaviour of repaired composite panels. *Composites Part A: Applied Science and Manufacturing* **1998,** 29, (11), 1463-1471.

47.   Chotard, T. J.; Pasquiet, J.; Benzeggagh, M. L., Residual performance of scarf patch-repaired pultruded shapes initially impact damaged. *Composite Structures* **2001,** 53, (3), 317-331.

48.   Hosur, M. V.; Vaidya, U. K.; Myers, D.; Jeelani, S., Studies on the repair of ballistic impact damaged S2-glass/vinyl ester laminates. *Composite Structures* **2003,** 61, (4), 281-290.

49.   Zimmerman, K. B.; Liu, D., An experimental investigation of composite repair. *Experimental Mechanics* **1996,** 36, (2), 142-147.

50.   Abdelouahab, J. B.; Bouardi, A. E.; Granger, R.; Vergnaud, J. M., Repairing broken thermoset pieces using diffusional pretreatment and cure with uncured resin. *Polymers and Polymer Composites* **2001,** 9, (8), 515-522.

51.   Jud, K.; Kausch, H. H., Load transfer through chain molecules after interpenetration at interfaces. *Polymer Bulletin* **1979,** 1, (10), 697-707.

52.   Chung, C.-M.; Roh, Y.-S.; Cho, S.-Y.; Kim, J.-G., Crack Healing in Polymeric Materials via Photochemical [2+2] Cycloaddition. *Chemistry of Materials* **2004,** 16, (21), 3982-3984.

53.   Kunihiko, T.; Mitsuru, T.; Haruo, U., Self-repairing mechanism of plastics. *Science and Technology of Advanced Materials* **2003,** 4, (5), 435.

54.   Imaizumi, K.; Ohba, T.; Ikeda, Y.; Takeda, K., Self-Repairing Mechanism of Polymer Composite. *Materials science research international* **2001,** 7, (4), 249-253.

55.   Chipara, M.; Wooley, K., Molecular self-healing processes in polymers. *MRS Proceedings* **2004,** 851, NN4.3.

56.   Lee, J.-Y.; Zhang, Q.; Emrick, T.; Crosby, A. J., Nanoparticle Alignment and Repulsion during Failure of Glassy Polymer Nanocomposites. *Macromolecules* **2006,** 39, (21), 7392-7396.

57.   Zako, M.; Takano, N., Intelligent Material Systems Using Epoxy Particles to Repair Microcracks and Delamination Damage in GFRP. *Journal of Intelligent Material Systems and Structures* **1999,** 10, (10), 836-841.

58.   Hayes, S. A.; Jones, F. R.; Marshiya, K.; Zhang, W., A self-healing thermosetting composite material. *Composites Part A: Applied Science and Manufacturing* **2007,** 38, (4), 1116-1120.

59.   Hayes, S. A.; Zhang, W.; Branthwaite, M.; Jones, F. R., Self-healing of damage in fibre-reinforced polymer-matrix composites. *Journal of The Royal Society Interface* **2007,** 4, (13), 381-387.

60.   Dry, C., Passive tunable fibers and matrices. *International Journal of Modern Physics B* **1992,** 6, (15-16), 2763-2771.

61.   Dry, C., Passive Smart Materials for Sensing and Actuation. *Journal of Intelligent Material Systems and Structures* **1993,** 4, (3), 420-425.

62.   Dry, C., Procedures developed for self-repair of polymer matrix composite materials. *Composite Structures* **1996,** 35, (3), 263-269.

63.   Bleay, S. M.; Loader, C. B.; Hawyes, V. J.; Humberstone, L.; Curtis, P. T., A smart repair system for polymer matrix composites. *Composites Part A: Applied Science and Manufacturing* **2001,** 32, (12), 1767-1776.

64.   Pang, J. W. C.; Bond, I. P., A hollow fibre reinforced polymer composite encompassing self-healing and enhanced damage visibility. *Composites Science and Technology* **2005,** 65, (11–12), 1791-1799.

65.   Li, V. C.; Lim, Y. M.; Chan, Y.-W., Feasibility study of a passive smart self-healing cementitious composite. *Composites Part B: Engineering* **1998,** 29, (6), 819-827.

66.   White, S. R.; Sottos, N. R.; Geubelle, P. H.; Moore, J. S.; Kessler, M. R.; Sriram, S. R.; Brown, E. N.; Viswanathan, S., Autonomic healing of polymer composites. *Nature* **2001,** 409, (6822), 794-797.

67.   Brown, E. N.; Kessler, M. R.; Sottos, N. R.; White, S. R., In situ poly(urea-formaldehyde) microencapsulation of dicyclopentadiene. *Journal of Microencapsulation* **2003,** 20, (6), 719-730.

68.   Brown, E. N.; White, S. R.; Sottos, N. R., Microcapsule induced toughening in a self-healing polymer composite. *J Mater Sci* **2004,** 39, (5), 1703-1710.

69.   Brown, E. N.; White, S. R.; Sottos, N. R., Retardation and repair of fatigue cracks in a microcapsule toughened epoxy composite—Part II: In situ self-healing. *Composites Science and Technology* **2005,** 65, (15–16), 2474-2480.

70.   Brown, E. N.; White, S. R.; Sottos, N. R., Retardation and repair of fatigue cracks in a microcapsule toughened epoxy composite – Part I: Manual infiltration. *Composites Science and Technology* **2005,** 65, (15–16), 2466-2473.

71.   Jones, A. S.; Rule, J. D.; Moore, J. S.; White, S. R.; Sottos, N. R., Catalyst Morphology and Dissolution Kinetics of Self-Healing Polymers. *Chemistry of Materials* **2006,** 18, (5), 1312-1317.

72.   Kessler, M. R.; Sottos, N. R.; White, S. R., Self-healing structural composite materials. *Composites Part A: Applied Science and Manufacturing* **2003,** 34, (8), 743-753.

73.   Lee, J. K.; Hong, S. J.; Liu, X.; Yoon, S. H., Characterization of dicyclopentadiene and 5-ethylidene-2-norbornene as self-healing agents for polymer composite and its microcapsules. *Macromol. Res.* **2004,** 12, (5), 478-483.

74.   Liu, X.; Lee, J. K.; Yoon, S. H.; Kessler, M. R., Characterization of diene monomers as healing agents for autonomic damage repair. *Journal of Applied Polymer Science* **2006,** 101, (3), 1266-1272.

75.   Rule, J. D.; Brown, E. N.; Sottos, N. R.; White, S. R.; Moore, J. S., Wax-Protected Catalyst Microspheres for Efficient Self-Healing Materials. *Advanced Materials* **2005,** 17, (2), 205-208.

76.   Rule, J. D.; Moore, J. S., ROMP Reactivity of endo- and exo-Dicyclopentadiene. *Macromolecules* **2002,** 35, (21), 7878-7882.

77.   Kessler, M. R.; White, S. R., Self-activated healing of delamination damage in woven composites. *Composites Part A: Applied Science and Manufacturing* **2001,** 32, (5), 683-699.

78.   Kessler, M. R.; White, S. R., Cure kinetics of the ring-opening metathesis polymerization of dicyclopentadiene. *Journal of Polymer Science Part A: Polymer Chemistry* **2002,** 40, (14), 2373-2383.

79.   Cho, S. H.; Andersson, H. M.; White, S. R.; Sottos, N. R.; Braun, P. V., Polydimethylsiloxane-Based Self-Healing Materials. *Advanced Materials* **2006,** 18, (8), 997-1000.

80.   Chen, Y.; Wang, Q., Preparation, properties and characterizations of halogen-free nitrogen–phosphorous flame-retarded glass fiber reinforced polyamide 6 composite. *Polymer Degradation and Stability* **2006,** 91, (9), 2003-2013.

81.   Cosco, S.; Ambrogi, V.; Musto, P.; Carfagna, C., Urea-Formaldehyde Microcapsules Containing an Epoxy Resin: Influence of Reaction Parameters on the Encapsulation Yield. *Macromolecular Symposia* **2006,** 234, (1), 184-192.

82.   Yuan, L.; Liang, G.; Xie, J.; Li, L.; Guo, J., Preparation and characterization of poly(urea-formaldehyde) microcapsules filled with epoxy resins. *Polymer* **2006,** 47, (15), 5338-5349.

83.   Harreld, J. H.; Wong, M. S.; Hansma, P. K.; Morse, D. E.; Stucky, G. D. Self-healing organosiloxane materials containing reversible and energy-dispersive crosslinking domains. Regents of the University of California (Oakland, CA). US: 6783709 B2. 2004.

84.   Eisenberg, A.; Rinaudo, M., Polyelectrolytes and ionomers. *Polymer Bulletin* **1990,** 24, (6), 671-671.

85.   Chen, X.; Dam, M. A.; Ono, K.; Mal, A.; Shen, H.; Nutt, S. R.; Sheran, K.; Wudl, F., A Thermally Re-mendable Cross-Linked Polymeric Material. *Science* **2002,** 295, (5560), 1698-1702.

86.   Chen, X.; Wudl, F.; Mal, A. K.; Shen, H.; Nutt, S. R., New Thermally Remendable Highly Cross-Linked Polymeric Materials. *Macromolecules* **2003,** 36, (6), 1802-1807.

87.   Liu, Y.-L.; Chen, Y.-W., Thermally Reversible Cross-Linked Polyamides with High Toughness and Self-Repairing Ability from Maleimide- and Furan-Functionalized Aromatic Polyamides. *Macromolecular Chemistry and Physics* **2007,** 208, (2), 224-232.

88.   Liu, Y.-L.; Hsieh, C.-Y., Crosslinked epoxy materials exhibiting thermal remendablility and removability from multifunctional maleimide and furan compounds. *Journal of Polymer Science Part A: Polymer Chemistry* **2006,** 44, (2), 905-913.

89.   Higaki, Y.; Otsuka, H.; Takahara, A., Dynamic Formation of Graft Polymers via Radical Crossover Reaction of Alkoxyamines. *Macromolecules* **2004,** 37, (5), 1696-1701.

90.   Higaki, Y.; Otsuka, H.; Takahara, A., A Thermodynamic Polymer Cross-Linking System Based on Radically Exchangeable Covalent Bonds. *Macromolecules* **2006,** 39, (6), 2121-2125.

91.   Otsuka, H.; Aotani, K.; Higaki, Y.; Amamoto, Y.; Takahara, A., Thermal Reorganization and Molecular Weight Control of Dynamic Covalent Polymers Containing Alkoxyamines in Their Main Chains. *Macromolecules* **2007,** 40, (5), 1429-1434.

92.   Yamaguchi, G.; Higaki, Y.; Otsuka, H.; Takahara, A., Reversible Radical Ring-Crossover Polymerization of an Alkoxyamine-Containing Dynamic Covalent Macrocycle. *Macromolecules* **2005,** 38, (15), 6316-6320.

93.   Yamaguchi, M.; Ono, S.; Terano, M., Self-repairing property of polymer network with dangling chains. *Materials Letters* **2007,** 61, (6), 1396-1399.

94.   Varghese, S.; Lele, A.; Mashelkar, R., Metal-ion-mediated healing of gels. *Journal of Polymer Science Part A: Polymer Chemistry* **2006,** 44, (1), 666-670.

95.   Varghese, S.; Lele, A. K.; Srinivas, D.; Mashelkar, R. A., Role of Hydrophobicity on Structure of Polymer−Metal Complexes. *The Journal of Physical Chemistry B* **2001,** 105, (23), 5368-5373.

96.   Lendlein, A.; Kelch, S., Shape-Memory Polymers. *Angewandte Chemie International Edition* **2002,** 41, (12), 2034-2057.

97.   Ni, W.; Cheng, Y.-T.; Grummon, D. S., Recovery of microindents in a nickel--titanium shape-memory alloy: A ``self-healing'' effect. *Applied Physics Letters* **2002,** 80, (18), 3310-3312.

98.   Ni, W.; Cheng, Y.-T.; Grummon, D. S., Wear resistant self-healing tribological surfaces by using hard coatings on NiTi shape memory alloys. *Surface and Coatings Technology* **2006,** 201, (3–4), 1053-1057.

99.   Young, T., An Essay on the Cohesion of Fluids. *Philosophical Transactions of the Royal Society of London* **1805,** 95, 65-87.

100.   Wenzel, R. N., Resistance of solid surfaces to wetting by water. *Industrial & Engineering Chemistry* **1936,** 28, (8), 988-994.

101.   Cassie, A. B. D.; Baxter, S., Wettability of porous surfaces. *Transactions of the Faraday Society* **1944,** 40, (0), 546-551.

102.   Giacomello, A.; Meloni, S.; Chinappi, M.; Casciola, C. M., Cassie–Baxter and Wenzel States on a Nanostructured Surface: Phase Diagram, Metastabilities,

and Transition Mechanism by Atomistic Free Energy Calculations. *Langmuir* **2012,** 28, (29), 10764-10772.

103. Onda, T.; Shibuichi, S.; Satoh, N.; Tsujii, K., Super-Water-Repellent Fractal Surfaces. *Langmuir* **1996,** 12, (9), 2125-2127.

104. Shibuichi, S.; Onda, T.; Satoh, N.; Tsujii, K., Super Water-Repellent Surfaces Resulting from Fractal Structure. *The Journal of Physical Chemistry* **1996,** 100, (50), 19512-19517.

105. Extrand, C. W., Model for Contact Angles and Hysteresis on Rough and Ultraphobic Surfaces. *Langmuir* **2002,** 18, (21), 7991-7999.

106. Extrand, C. W., Contact Angles and Hysteresis on Surfaces with Chemically Heterogeneous Islands. *Langmuir* **2003,** 19, (9), 3793-3796.

107. Wang, B.; Zhang, Y.; Shi, L.; Li, J.; Guo, Z., Advances in the theory of superhydrophobic surfaces. *Journal of Materials Chemistry* **2012,** 22, (38), 20112-20127.

108. Chibowski, E., Surface free energy of a solid from contact angle hysteresis. *Advances in Colloid and Interface Science* **2003,** 103, (2), 149-172.

109. Extrand, C. W.; Kumagai, Y., An Experimental Study of Contact Angle Hysteresis. *Journal of Colloid and Interface Science* **1997,** 191, (2), 378-383.

110. Gennes, P.-G. d.; Brochard-Wyart, F.; Quere, D., *Capillarity and Wetting Phenomena. Drops, Bubbles, Pearls, Waves*. Springer-Verlag: 2004.

111. Tadmor, R., Line Energy and the Relation between Advancing, Receding, and Young Contact Angles. *Langmuir* **2004,** 20, (18), 7659-7664.

112. Tadmor, R.; Yadav, P. S., As-placed contact angles for sessile drops. *Journal of Colloid and Interface Science* **2008,** 317, (1), 241-246.

113. Hyungmo, K.; Moo Hwan, K.; Joonwon, K., Wettability of dual-scaled surfaces fabricated by the combination of a conventional silicon wet-etching and a ZnO solution method. *Journal of Micromechanics and Microengineering* **2009,** 19, (9), 095002.

114. Jeong, H. E.; Kwak, M. K.; Park, C. I.; Suh, K. Y., Wettability of nanoengineered dual-roughness surfaces fabricated by UV-assisted capillary force lithography. *Journal of Colloid and Interface Science* **2009,** 339, (1), 202-207.

115. Gupta, P.; Ulman, A.; Fanfan, S.; Korniakov, A.; Loos, K., Mixed Self-Assembled Monolayers of Alkanethiolates on Ultrasmooth Gold Do Not Exhibit Contact-Angle Hysteresis. *Journal of the American Chemical Society* **2004,** 127, (1), 4-5.

116. Deng, X.; Mammen, L.; Butt, H.-J.; Vollmer, D., Candle Soot as a Template for a Transparent Robust Superamphiphobic Coating. *Science* **2012,** 335, (6064), 67-70.

117. Johnson Rulon, E.; Dettre Robert, H., Contact Angle Hysteresis. In *Contact Angle, Wettability, and Adhesion*, AMERICAN CHEMICAL SOCIETY: 1964; Vol. 43, pp 112-135.

118. Choi, W.; Tuteja, A.; Chhatre, S.; Mabry, J. M.; Cohen, R. E.; McKinley, G. H., Fabrics with Tunable Oleophobicity. *Advanced Materials* **2009,** 21, (21), 2190-2195.

119. Deng, B.; Cai, R.; Yu, Y.; Jiang, H.; Wang, C.; Li, J.; Li, L.; Yu, M.; Li, J.; Xie, L.; Huang, Q.; Fan, C., Laundering Durability of Superhydrophobic Cotton Fabric. *Advanced Materials* **2010,** 22, (48), 5473-5477.

120. Gao, L.; McCarthy, T. J., "Artificial Lotus Leaf" Prepared Using a 1945 Patent and a Commercial Textile. *Langmuir* **2006,** 22, (14), 5998-6000.

121. Zhou, H.; Wang, H.; Niu, H.; Gestos, A.; Wang, X.; Lin, T., Fluoroalkyl Silane Modified Silicone Rubber/Nanoparticle Composite: A Super Durable, Robust Superhydrophobic Fabric Coating. *Advanced Materials* **2012,** 24, (18), 2409-2412.

122. Zimmermann, J.; Reifler, F. A.; Fortunato, G.; Gerhardt, L.-C.; Seeger, S., A Simple, One-Step Approach to Durable and Robust Superhydrophobic Textiles. *Advanced Functional Materials* **2008,** 18, (22), 3662-3669.

123. Bhushan, B.; Jung, Y. C.; Koch, K., Self-Cleaning Efficiency of Artificial Superhydrophobic Surfaces. *Langmuir* **2009,** 25, (5), 3240-3248.

124. Bhushan, B.; Jung, Y. C.; Koch, K., Micro-, nano- and hierarchical structures for superhydrophobicity, self-cleaning and low adhesion. *Philosophical Transactions of the Royal Society A: Mathematical,*
Physical and Engineering Sciences **2009,** 367, (1894), 1631-1672.

125. Bhushan, B.; Koch, K.; Jung, Y. C., Fabrication and characterization of the hierarchical structure for superhydrophobicity and self-cleaning. *Ultramicroscopy* **2009,** 109, (8), 1029-1034.

126. Blossey, R., Self-cleaning surfaces [mdash] virtual realities. *Nat Mater* **2003,** 2, (5), 301-306.

127. Fürstner, R.; Barthlott, W.; Neinhuis, C.; Walzel, P., Wetting and Self-Cleaning Properties of Artificial Superhydrophobic Surfaces. *Langmuir* **2005,** 21, (3), 956-961.

128. Nakajima, A.; Hashimoto, K.; Watanabe, T.; Takai, K.; Yamauchi, G.; Fujishima, A., Transparent Superhydrophobic Thin Films with Self-Cleaning Properties. *Langmuir* **2000,** 16, (17), 7044-7047.

129. Sas, I.; Gorga, R. E.; Joines, J. A.; Thoney, K. A., Literature review on superhydrophobic self-cleaning surfaces produced by electrospinning. *Journal of Polymer Science Part B: Polymer Physics* **2012,** 50, (12), 824-845.

130. Gao, X.; Yan, X.; Yao, X.; Xu, L.; Zhang, K.; Zhang, J.; Yang, B.; Jiang, L., The Dry-Style Antifogging Properties of Mosquito Compound Eyes and Artificial Analogues Prepared by Soft Lithography. *Advanced Materials* **2007,** 19, (17), 2213-2217.

131. Cao, L.; Jones, A. K.; Sikka, V. K.; Wu, J.; Gao, D., Anti-Icing Superhydrophobic Coatings. *Langmuir* **2009,** 25, (21), 12444-12448.

132. Guo, P.; Zheng, Y.; Wen, M.; Song, C.; Lin, Y.; Jiang, L., Icephobic/Anti-Icing Properties of Micro/Nanostructured Surfaces. *Advanced Materials* **2012,** 24, (19), 2642-2648.

133. Jung, S.; Dorrestijn, M.; Raps, D.; Das, A.; Megaridis, C. M.; Poulikakos, D., Are Superhydrophobic Surfaces Best for Icephobicity? *Langmuir* **2011,** 27, (6), 3059-3066.

134. Kim, P.; Wong, T.-S.; Alvarenga, J.; Kreder, M. J.; Adorno-Martinez, W. E.; Aizenberg, J., Liquid-Infused Nanostructured Surfaces with Extreme Anti-Ice and Anti-Frost Performance. *ACS Nano* **2012,** 6, (8), 6569-6577.

135. Kulinich, S. A.; Farhadi, S.; Nose, K.; Du, X. W., Superhydrophobic Surfaces: Are They Really Ice-Repellent? *Langmuir* **2010,** 27, (1), 25-29.

136. Mishchenko, L.; Hatton, B.; Bahadur, V.; Taylor, J. A.; Krupenkin, T.; Aizenberg, J., Design of Ice-free Nanostructured Surfaces Based on Repulsion of Impacting Water Droplets. *ACS Nano* **2010,** 4, (12), 7699-7707.

137. Meuler, A. J.; McKinley, G. H.; Cohen, R. E., Exploiting Topographical Texture To Impart Icephobicity. *ACS Nano* **2010,** 4, (12), 7048-7052.

138. Pan, Q.; Liu, J.; Zhu, Q., A Water Strider-Like Model with Large and Stable Loading Capacity Fabricated from Superhydrophobic Copper Foils. *ACS Applied Materials & Interfaces* **2010,** 2, (7), 2026-2030.

139. Pan, Q.; Wang, M., Miniature Boats with Striking Loading Capacity Fabricated from Superhydrophobic Copper Meshes. *ACS Applied Materials & Interfaces* **2009,** 1, (2), 420-423.

140. Zhao, Y.; Tang, Y.; Wang, X.; Lin, T., Superhydrophobic cotton fabric fabricated by electrostatic assembly of silica nanoparticles and its remarkable buoyancy. *Applied Surface Science* **2010,** 256, (22), 6736-6742.

141. Guo, Z.; Zhou, F.; Hao, J.; Liu, W., Stable Biomimetic Super-Hydrophobic Engineering Materials. *Journal of the American Chemical Society* **2005,** 127, (45), 15670-15671.

142. Zhang, F.; Zhao, L.; Chen, H.; Xu, S.; Evans, D. G.; Duan, X., Corrosion Resistance of Superhydrophobic Layered Double Hydroxide Films on Aluminum. *Angewandte Chemie International Edition* **2008,** 47, (13), 2466-2469.

143. Liu, H.; Szunerits, S.; Xu, W.; Boukherroub, R., Preparation of Superhydrophobic Coatings on Zinc as Effective Corrosion Barriers. *ACS Applied Materials & Interfaces* **2009,** 1, (6), 1150-1153.

144. Ishizaki, T.; Masuda, Y.; Sakamoto, M., Corrosion Resistance and Durability of Superhydrophobic Surface Formed on Magnesium Alloy Coated with Nanostructured Cerium Oxide Film and Fluoroalkylsilane Molecules in Corrosive NaCl Aqueous Solution. *Langmuir* **2011,** 27, (8), 4780-4788.

145. Ishizaki, T.; Sakamoto, M., Facile Formation of Biomimetic Color-Tuned Superhydrophobic Magnesium Alloy with Corrosion Resistance. *Langmuir* **2011,** 27, (6), 2375-2381.

146. Genzer, J.; Efimenko, K., Recent developments in superhydrophobic surfaces and their relevance to marine fouling: a review. *Biofouling* **2006,** 22, (5), 339-360.

147. Li, J.; Shi, L.; Chen, Y.; Zhang, Y.; Guo, Z.; Su, B.-l.; Liu, W., Stable superhydrophobic coatings from thiol-ligand nanocrystals and their application in oil/water separation. *Journal of Materials Chemistry* **2012,** 22, (19), 9774-9781.

148. Wang, C.-F.; Tzeng, F.-S.; Chen, H.-G.; Chang, C.-J., Ultraviolet-Durable Superhydrophobic Zinc Oxide-Coated Mesh Films for Surface and Underwater–Oil Capture and Transportation. *Langmuir* **2012,** 28, (26), 10015-10019.

149. Wang, C.; Yao, T.; Wu, J.; Ma, C.; Fan, Z.; Wang, Z.; Cheng, Y.; Lin, Q.; Yang, B., Facile Approach in Fabricating Superhydrophobic and Superoleophilic Surface for Water and Oil Mixture Separation. *ACS Applied Materials & Interfaces* **2009,** 1, (11), 2613-2617.

150. Zhu, Q.; Pan, Q.; Liu, F., Facile Removal and Collection of Oils from Water Surfaces through Superhydrophobic and Superoleophilic Sponges. *The Journal of Physical Chemistry C* **2011,** 115, (35), 17464-17470.

151. Guix, M.; Orozco, J.; García, M.; Gao, W.; Sattayasamitsathit, S.; Merkoçi, A.; Escarpa, A.; Wang, J., Superhydrophobic Alkanethiol-Coated Microsubmarines for Effective Removal of Oil. *ACS Nano* **2012,** 6, (5), 4445-4451.

152. Feng, L.; Zhang, Z.; Mai, Z.; Ma, Y.; Liu, B.; Jiang, L.; Zhu, D., A Super-Hydrophobic and Super-Oleophilic Coating Mesh Film for the Separation of Oil and Water. *Angewandte Chemie International Edition* **2004,** 43, (15), 2012-2014.

153. Bhushan, B.; Koch, K.; Jung, Y. C., Nanostructures for superhydrophobicity and low adhesion. *Soft Matter* **2008,** 4, (9), 1799-1804.

154. Cottin-Bizonne, C.; Barrat, J.-L.; Bocquet, L.; Charlaix, E., Low-friction flows of liquid at nanopatterned interfaces. *Nat Mater* **2003,** 2, (4), 237-240.

155. Ou, J.; Perot, B.; Rothstein, J. P., Laminar drag reduction in microchannels using ultrahydrophobic surfaces. *Physics of Fluids* **2004,** 16, (12), 4635-4643.

156. Xue, Y.; Chu, S.; Lv, P.; Duan, H., Importance of Hierarchical Structures in Wetting Stability on Submersed Superhydrophobic Surfaces. *Langmuir* **2012,** 28, (25), 9440-9450.

157. Han, J. T.; Xu; Cho, K., Diverse Access to Artificial Superhydrophobic Surfaces Using Block Copolymers. *Langmuir* **2005,** 21, (15), 6662-6665.

158. Shirtcliffe, N. J.; McHale, G.; Newton, M. I.; Chabrol, G.; Perry, C. C., Dual-Scale Roughness Produces Unusually Water-Repellent Surfaces. *Advanced Materials* **2004,** 16, (21), 1929-1932.

159. Lau, K. K. S.; Bico, J.; Teo, K. B. K.; Chhowalla, M.; Amaratunga, G. A. J.; Milne, W. I.; McKinley, G. H.; Gleason, K. K., Superhydrophobic Carbon Nanotube Forests. *Nano Letters* **2003,** 3, (12), 1701-1705.

160. Huang, Y.-H.; Wu, J.-T.; Yang, S.-Y., Direct fabricating patterns using stamping transfer process with PDMS mold of hydrophobic nanostructures on surface of micro-cavity. *Microelectronic Engineering* **2011,** 88, (6), 849-854.

161. Hwang, H. S.; Lee, S. B.; Park, I., Fabrication of raspberry-like superhydrophobic hollow silica particles. *Materials Letters* **2010,** 64, (20), 2159-2162.

162. Kinoshita, H.; Ogasahara, A.; Fukuda, Y.; Ohmae, N., Superhydrophobic/superhydrophilic micropatterning on a carbon nanotube film using a laser plasma-type hyperthermal atom beam facility. *Carbon* **2010,** 48, (15), 4403-4408.

163. Guo, Z.-G.; Fang, J.; Hao, J.-c.; Liang, Y.-m.; Liu, W.-m., A Novel Approach to Stable Superhydrophobic Surfaces. *ChemPhysChem* **2006,** 7, (8), 1674-1677.

164. Mumm, F.; van Helvoort, A. T. J.; Sikorski, P., Easy Route to Superhydrophobic Copper-Based Wire-Guided Droplet Microfluidic Systems. *ACS Nano* **2009,** 3, (9), 2647-2652.

165. Ganbavle, V. V.; Bangi, U. K. H.; Latthe, S. S.; Mahadik, S. A.; Rao, A. V., Self-cleaning silica coatings on glass by single step sol–gel route. *Surface and Coatings Technology* **2011,** 205, (23–24), 5338-5344.

166. Latthe, S. S.; Imai, H.; Ganesan, V.; Rao, A. V., Superhydrophobic silica films by sol–gel co-precursor method. *Applied Surface Science* **2009,** 256, (1), 217-222.

167. Rao, A. V.; Latthe, S. S.; Kappenstein, C.; Ganesan, V.; Rath, M. C.; Sawant, S. N., Wetting behavior of high energy electron irradiated porous superhydrophobic silica films. *Applied Surface Science* **2011,** 257, (7), 3027-3032.

168. Sanjay, S. L.; Hirashima, H.; Rao, A. V., TEOS based water repellent silica films obtained by a co-precursor sol–gel method. *Smart Materials and Structures* **2009,** 18, (9), 095017.

169. Ma, M.; Mao, Y.; Gupta, M.; Gleason, K. K.; Rutledge, G. C., Superhydrophobic Fabrics Produced by Electrospinning and Chemical Vapor Deposition. *Macromolecules* **2005,** 38, (23), 9742-9748.

170. Zhang, X.; Guo, Y.; Zhang, P.; Wu, Z.; Zhang, Z., Superhydrophobic CuO@Cu2S nanoplate vertical arrays on copper surfaces. *Materials Letters* **2010,** 64, (10), 1200-1203.

171.	Ionov, L.; Synytska, A., Self-healing superhydrophobic materials. *Physical Chemistry Chemical Physics* **2012,** 14, (30), 10497-10502.

172.	Xue, C.-H.; Ma, J.-Z., Long-lived superhydrophobic surfaces. *Journal of Materials Chemistry A* **2013,** 1, (13), 4146-4161.

173.	Verho, T.; Bower, C.; Andrew, P.; Franssila, S.; Ikkala, O.; Ras, R. H. A., Mechanically Durable Superhydrophobic Surfaces. *Advanced Materials* **2011,** 23, (5), 673-678.

174.	Su, C.; Xu, Y.; Gong, F.; Wang, F.; Li, C., The abrasion resistance of a superhydrophobic surface comprised of polyurethane elastomer. *Soft Matter* **2010,** 6, (24), 6068-6071.

175.	Li, J.; Liu, X.; Ye, Y.; Zhou, H.; Chen, J., A simple solution-immersion process for the fabrication of superhydrophobic cupric stearate surface with easy repairable property. *Applied Surface Science* **2011,** 258, (5), 1772-1775.

176.	Li, J.; Wan, H.; Ye, Y.; Zhou, H.; Chen, J., One-step process for the fabrication of superhydrophobic surfaces with easy repairability. *Applied Surface Science* **2012,** 258, (7), 3115-3118.

177.	Wu, W.; Wang, X.; Liu, X.; Zhou, F., Spray-Coated Fluorine-Free Superhydrophobic Coatings with Easy Repairability and Applicability. *ACS Applied Materials & Interfaces* **2009,** 1, (8), 1656-1661.

178.	Yang, J.; Zhang, Z.; Men, X.; Xu, X.; Zhu, X., A simple approach to fabricate regenerable superhydrophobic coatings. *Colloids and Surfaces A: Physicochemical and Engineering Aspects* **2010,** 367, (1–3), 60-64.

179.	Zhu, X.; Zhang, Z.; Men, X.; Yang, J.; Wang, K.; Xu, X.; Zhou, X.; Xue, Q., Robust superhydrophobic surfaces with mechanical durability and easy repairability. *Journal of Materials Chemistry* **2011,** 21, (39), 15793-15797.

180.	Li, Y.; Li, L.; Sun, J., Bioinspired Self-Healing Superhydrophobic Coatings. *Angewandte Chemie International Edition* **2010,** 49, (35), 6129-6133.

181.	Wang, H.; Xue, Y.; Ding, J.; Feng, L.; Wang, X.; Lin, T., Durable, Self-Healing Superhydrophobic and Superoleophobic Surfaces from Fluorinated-Decyl Polyhedral Oligomeric Silsesquioxane and Hydrolyzed Fluorinated Alkyl Silane. *Angewandte Chemie International Edition* **2011,** 50, (48), 11433-11436.

182.	Wang, X.; Liu, X.; Zhou, F.; Liu, W., Self-healing superamphiphobicity. *Chemical Communications* **2011,** 47, (8), 2324-2326.

183.	Liu, Q.; Wang, X.; Yu, B.; Zhou, F.; Xue, Q., Self-Healing Surface Hydrophobicity by Consecutive Release of Hydrophobic Molecules from Mesoporous Silica. *Langmuir* **2012,** 28, (13), 5845-5849.

184.	Aussillous, P.; Quere, D., Liquid marbles. *Nature* **2001,** 411, (6840), 924-927.

185.	Larmour, I. A.; Saunders, G. C.; Bell, S. E. J., Sheets of Large Superhydrophobic Metal Particles Self Assembled on Water by the Cheerios Effect. *Angewandte Chemie International Edition* **2008,** 47, (27), 5043-5045.

186.	Kim, S.-H.; Lee, S. Y.; Yang, S.-M., Janus Microspheres for a Highly Flexible and Impregnable Water-Repelling Interface. *Angewandte Chemie International Edition* **2010,** 49, (14), 2535-2538.

187.	Liu, Y.; Mu, L.; Liu, B.; Kong, J., Controlled Switchable Surface. *Chemistry – A European Journal* **2005,** 11, (9), 2622-2631.

188.	Chaudhury, M. K.; Whitesides, G. M., How to Make Water Run Uphill. *Science* **1992,** 256, (5063), 1539-1541.

189.	Liu, X.; Liang, Y.; Zhou, F.; Liu, W., Extreme wettability and tunable adhesion: biomimicking beyond nature? *Soft Matter* **2012,** 8, (7), 2070-2086.

190.   Raphael, E.; De Gennes, P. G., Rubber-rubber adhesion with connector molecules. *The Journal of Physical Chemistry* **1992,** 96, (10), 4002-4007.

191.   Ruths, M.; Johannsmann, D.; Rühe, J.; Knoll, W., Repulsive Forces and Relaxation on Compression of Entangled, Polydisperse Polystyrene Brushes. *Macromolecules* **2000,** 33, (10), 3860-3870.

192.   Berman, A.; Steinberg, S.; Campbell, S.; Ulman, A.; Israelachvili, J., Controlled microtribology of a metal oxide surface. *Tribology Letters* **1998,** 4, (1), 43-48.

193.   Klein, J.; Kumacheva, E.; Mahalu, D.; Perahia, D.; Fetters, L. J., Reduction of frictional forces between solid surfaces bearing polymer brushes. *Nature* **1994,** 370, (6491), 634-636.

194.   Aksay, I. A.; Trau, M.; Manne, S.; Honma, I.; Yao, N.; Zhou, L.; Fenter, P.; Eisenberger, P. M.; Gruner, S. M., Biomimetic Pathways for Assembling Inorganic Thin Films. *Science* **1996,** 273, (5277), 892-898.

195.   Galaev, I. Y.; Mattiasson, B., 'Smart' polymers and what they could do in biotechnology and medicine. *Trends in Biotechnology* **1999,** 17, (8), 335-340.

196.   Zhao, B.; Moore, J. S.; Beebe, D. J., Surface-Directed Liquid Flow Inside Microchannels. *Science* **2001,** 291, (5506), 1023-1026.

197.   Crevoisier, G. d.; Fabre, P.; Corpart, J.-M.; Leibler, L., Switchable Tackiness and Wettability of a Liquid Crystalline Polymer. *Science* **1999,** 285, (5431), 1246-1249.

198.   Abbott, N. L.; Gorman, C. B.; Whitesides, G. M., Active Control of Wetting Using Applied Electrical Potentials and Self- Assembled Monolayers. *Langmuir* **1995,** 11, (1), 16-18.

199.   Byloos, M.; Al-Maznai, H.; Morin, M., Phase Transitions of Alkanethiol Self-Assembled Monolayers at an Electrified Gold Surface. *The Journal of Physical Chemistry B* **2001,** 105, (25), 5900-5905.

200.   Prins, M. W. J.; Welters, W. J. J.; Weekamp, J. W., Fluid Control in Multichannel Structures by Electrocapillary Pressure. *Science* **2001,** 291, (5502), 277-280.

201.   Xin, B.; Hao, J., Reversibly switchable wettability. *Chemical Society Reviews* **2010,** 39, (2), 769-782.

202.   Sakai, N.; Wang, R.; Fujishima, A.; Watanabe, T.; Hashimoto, K., Effect of Ultrasonic Treatment on Highly Hydrophilic TiO2 Surfaces. *Langmuir* **1998,** 14, (20), 5918-5920.

203.   Stevens, N.; Priest, C. I.; Sedev, R.; Ralston, J., Wettability of Photoresponsive Titanium Dioxide Surfaces. *Langmuir* **2003,** 19, (8), 3272-3275.

204.   Feng, X.; Zhai, J.; Jiang, L., The Fabrication and Switchable Superhydrophobicity of TiO2 Nanorod Films. *Angewandte Chemie International Edition* **2005,** 44, (32), 5115-5118.

205.   Feng, X.; Feng, L.; Jin, M.; Zhai, J.; Jiang, L.; Zhu, D., Reversible Super-hydrophobicity to Super-hydrophilicity Transition of Aligned ZnO Nanorod Films. *Journal of the American Chemical Society* **2003,** 126, (1), 62-63.

206.   Sun, R.-D.; Nakajima, A.; Fujishima, A.; Watanabe, T.; Hashimoto, K., Photoinduced Surface Wettability Conversion of ZnO and TiO2 Thin Films. *The Journal of Physical Chemistry B* **2001,** 105, (10), 1984-1990.

207.   Wang, S.; Feng, X.; Yao, J.; Jiang, L., Controlling Wettability and Photochromism in a Dual-Responsive Tungsten Oxide Film. *Angewandte Chemie International Edition* **2006,** 45, (8), 1264-1267.

208. Lim, H. S.; Kwak, D.; Lee, D. Y.; Lee, S. G.; Cho, K., UV-Driven Reversible Switching of a Roselike Vanadium Oxide Film between Superhydrophobicity and Superhydrophilicity. *Journal of the American Chemical Society* **2007,** 129, (14), 4128-4129.

209. Lim, H. S.; Han, J. T.; Kwak, D.; Jin, M.; Cho, K., Photoreversibly Switchable Superhydrophobic Surface with Erasable and Rewritable Pattern. *Journal of the American Chemical Society* **2006,** 128, (45), 14458-14459.

210. Oh, S.-K.; Nakagawa, M.; Ichimura, K., Photocontrol of liquid motion on an azobenzene monolayer. *Journal of Materials Chemistry* **2002,** 12, (8), 2262-2269.

211. Liu, X.; Cai, M.; Liang, Y.; Zhou, F.; Liu, W., Photo-regulated stick-slip switch of water droplet mobility. *Soft Matter* **2011,** 7, (7), 3331-3336.

212. Rosario, R.; Gust, D.; Hayes, M.; Jahnke, F.; Springer, J.; Garcia, A. A., Photon-Modulated Wettability Changes on Spiropyran-Coated Surfaces. *Langmuir* **2002,** 18, (21), 8062-8069.

213. Cooper, C. G. F.; MacDonald, J. C.; Soto, E.; McGimpsey, W. G., Non-Covalent Assembly of a Photoswitchable Surface. *Journal of the American Chemical Society* **2004,** 126, (4), 1032-1033.

214. Driscoll, P. F.; Purohit, N.; Wanichacheva, N.; Lambert, C. R.; McGimpsey, W. G., Reversible Photoswitchable Wettability in Noncovalently Assembled Multilayered Films. *Langmuir* **2007,** 23, (26), 13181-13187.

215. Abbott, S.; Ralston, J.; Reynolds, G.; Hayes, R., Reversible Wettability of Photoresponsive Pyrimidine-Coated Surfaces. *Langmuir* **1999,** 15, (26), 8923-8928.

216. Kidoaki, S.; Ohya, S.; Nakayama, Y.; Matsuda, T., Thermoresponsive Structural Change of a Poly(N-isopropylacrylamide) Graft Layer Measured with an Atomic Force Microscope. *Langmuir* **2001,** 17, (8), 2402-2407.

217. Liang; Feng, X.; Liu, J.; Rieke, P. C.; Fryxell, G. E., Reversible Surface Properties of Glass Plate and Capillary Tube Grafted by Photopolymerization of N-Isopropylacrylamide. *Macromolecules* **1998,** 31, (22), 7845-7850.

218. Yim, H.; Kent, M. S.; Huber, D. L.; Satija, S.; Majewski, J.; Smith, G. S., Conformation of End-Tethered PNIPAM Chains in Water and in Acetone by Neutron Reflectivity. *Macromolecules* **2003,** 36, (14), 5244-5251.

219. Yim, H.; Kent, M. S.; Mendez, S.; Balamurugan, S. S.; Balamurugan, S.; Lopez, G. P.; Satija, S., Temperature-Dependent Conformational Change of PNIPAM Grafted Chains at High Surface Density in Water. *Macromolecules* **2004,** 37, (5), 1994-1997.

220. Liu, X.; Ye, Q.; Yu, B.; Liang, Y.; Liu, W.; Zhou, F., Switching Water Droplet Adhesion Using Responsive Polymer Brushes. *Langmuir* **2010,** 26, (14), 12377-12382.

221. Sun, T.; Wang, G.; Feng, L.; Liu, B.; Ma, Y.; Jiang, L.; Zhu, D., Reversible Switching between Superhydrophilicity and Superhydrophobicity. *Angewandte Chemie International Edition* **2004,** 43, (3), 357-360.

222. Gil, E. S.; Hudson, S. M., Stimuli-reponsive polymers and their bioconjugates. *Progress in Polymer Science* **2004,** 29, (12), 1173-1222.

223. Wang, J.; Hu, J.; Wen, Y.; Song, Y.; Jiang, L., Hydrogen-Bonding-Driven Wettability Change of Colloidal Crystal Films: From Superhydrophobicity to Superhydrophilicity. *Chemistry of Materials* **2006,** 18, (21), 4984-4986.

224. Azzaroni, O.; Brown, A. A.; Huck, W. T. S., Tunable Wettability by Clicking Counterions Into Polyelectrolyte Brushes. *Advanced Materials* **2007,** 19, (1), 151-154.

225. Zhou, F.; Hu, H.; Yu, B.; Osborne, V. L.; Huck, W. T. S.; Liu, W., Probing the Responsive Behavior of Polyelectrolyte Brushes Using Electrochemical Impedance Spectroscopy. *Analytical Chemistry* **2006,** 79, (1), 176-182.

226. Shen, Y.; Zhang, Y.; Zhang, Q.; Niu, L.; You, T.; Ivaska, A., Immobilization of ionic liquid with polyelectrolyte as carrier. *Chemical Communications* **2005,** 0, (33), 4193-4195.

227. Zhang, Y.; Shen, Y.; Yuan, J.; Han, D.; Wang, Z.; Zhang, Q.; Niu, L., Design and Synthesis of Multifunctional Materials Based on an Ionic-Liquid Backbone. *Angewandte Chemie International Edition* **2006,** 45, (35), 5867-5870.

228. Boyes, S. G.; Brittain, W. J.; Weng, X.; Cheng, S. Z. D., Synthesis, Characterization, and Properties of ABA Type Triblock Copolymer Brushes of Styrene and Methyl Acrylate Prepared by Atom Transfer Radical Polymerization. *Macromolecules* **2002,** 35, (13), 4960-4967.

229. Jennings, G. K.; Brantley, E. L., Physicochemical Properties of Surface-Initiated Polymer Films in the Modification and Processing of Materials. *Advanced Materials* **2004,** 16, (22), 1983-1994.

230. Liao, K.-S.; Fu, H.; Wan, A.; Batteas, J. D.; Bergbreiter, D. E., Designing Surfaces with Wettability That Varies in Response to Solute Identity and Concentration. *Langmuir* **2008,** 25, (1), 26-28.

231. Qing, G.; Sun, T., Chirality-Triggered Wettability Switching on a Smart Polymer Surface. *Advanced Materials* **2011,** 23, (14), 1615-1620.

232. Sun, T.; Qing, G., Biomimetic Smart Interface Materials for Biological Applications. *Advanced Materials* **2011,** 23, (12), H57-H77.

233. Choi, I. S.; Chi, Y. S., Surface Reactions On Demand: Electrochemical Control of SAM-Based Reactions. *Angewandte Chemie International Edition* **2006,** 45, (30), 4894-4897.

234. Wang, X.; Katz, E.; Willner, I., Potential-induced switching of electrical contact by controlling droplet shapes at hydrophilic/hydrophobic interfaces. *Electrochemistry Communications* **2003,** 5, (9), 814-818.

235. Isaksson, J.; Tengstedt, C.; Fahlman, M.; Robinson, N.; Berggren, M., A Solid-State Organic Electronic Wettability Switch. *Advanced Materials* **2004,** 16, (4), 316-320.

236. Katz, E.; Lioubashevsky, O.; Willner, I., Electromechanics of a Redox-Active Rotaxane in a Monolayer Assembly on an Electrode. *Journal of the American Chemical Society* **2004,** 126, (47), 15520-15532.

237. Riskin, M.; Basnar, B.; Chegel, V. I.; Katz, E.; Willner, I.; Shi, F.; Zhang, X., Switchable Surface Properties through the Electrochemical or Biocatalytic Generation of Ag0 Nanoclusters on Monolayer-Functionalized Electrodes. *Journal of the American Chemical Society* **2006,** 128, (4), 1253-1260.

238. Krupenkin, T. N.; Taylor, J. A.; Schneider, T. M.; Yang, S., From Rolling Ball to Complete Wetting: The Dynamic Tuning of Liquids on Nanostructured Surfaces. *Langmuir* **2004,** 20, (10), 3824-3827.

239. Millefiorini, S.; Tkaczyk, A. H.; Sedev, R.; Efthimiadis, J.; Ralston, J., Electrowetting of Ionic Liquids. *Journal of the American Chemical Society* **2006,** 128, (9), 3098-3101.

240. Nanayakkara, Y. S.; Perera, S.; Bindiganavale, S.; Wanigasekara, E.; Moon, H.; Armstrong, D. W., The Effect of AC Frequency on the Electrowetting Behavior of Ionic Liquids. *Analytical Chemistry* **2010,** 82, (8), 3146-3154.

241.   Ricks-Laskoski, H. L.; Snow, A. W., Synthesis and Electric Field Actuation of an Ionic Liquid Polymer. *Journal of the American Chemical Society* **2006,** 128, (38), 12402-12403.

242.   Zhu, L.; Xu, J.; Xiu, Y.; Sun, Y.; Hess, D. W.; Wong, C.-P., Electrowetting of Aligned Carbon Nanotube Films. *The Journal of Physical Chemistry B* **2006,** 110, (32), 15945-15950.

243.   Goldstein, J. I.; Newbury, D. E.; Echlin, P.; Joy, D. C.; Lyman, C. E.; Lifshon, E.; Sawyer, L.; Michael, J. R., *Scanning Electron Microscopy and X-Ray Microanalysis. 3rd edition*. Kluwer Academic/Plenum Publishers: 2003.

244.   Gagnadre, C.; Caron, A.; Guézénoc, H.; Grohens, Y., Electron microscopy pictures, mathematical model and approximate solution of the surface potential. *Kybernetes* **2009,** 38, (5), 780-788.

245.   Zhou, W.; Apkarian, R.; Wang, Z. L.; Joy, D. C., Fundamentals of Scanning Electron Microscopy (SEM). In *Scanning Microscopy for Nanotechnology. Techniques and Applications*, Springer: New York, 2006.

246.   Jaksch, H.; Steigerwald, M.; Drexel, V.; Bihr, H., New Detection Principles and Developments on the GEMINI SUPRA FE-SEM. *Microscopy and Microanalysis* **2003,** 9, (Supplement S03), 106-107.

247.   *SPM Training Notebook*. Veeco Instruments Inc.: 2003.

248.   Horcas, I.; Fernandez, R.; Gomez-Rodriguez, J. M.; Colchero, J.; Gomez-Herrero, J.; Baro, A. M., WSXM: A software for scanning probe microscopy and a tool for nanotechnology. *Review of Scientific Instruments* **2007,** 78, (1), 013705-8.

249.   Appendix C: Contact Angle Goniometry. In *Surface Design: Applications in Bioscience and Nanotechnology*, Wiley-VCH Verlag GmbH & Co. KGaA: 2009; pp 471-473.

250.   Harke, M.; Teppner, R.; Schulz, O.; Motschmann, H.; Orendi, H., Description of a single modular optical setup for ellipsometry, surface plasmons, waveguide modes, and their corresponding imaging techniques including Brewster angle microscopy. *Review of Scientific Instruments* **1997,** 68, (8), 3130-3134.

251.   *Handbook of ellipsometry*. William Andrew publishing, Springer: 2005.

252.   Schuetzner, W.; Kenndler, E., Electrophoresis in synthetic organic polymer capillaries: variation of electroosmotic velocity and .zeta. potential with pH and solvent composition. *Analytical Chemistry* **1992,** 64, (17), 1991-1995.

253.   Brunauer, S.; Emmett, P. H.; Teller, E., Adsorption of Gases in Multimolecular Layers. *Journal of the American Chemical Society* **1938,** 60, (2), 309-319.

254.   Xia, Y.; Whitesides, G. M., Soft Lithography. *Angewandte Chemie International Edition* **1998,** 37, (5), 550-575.

255.   Amigoni, S.; Taffin de Givenchy, E.; Dufay, M.; Guittard, F. d. r., Covalent Layer-by-Layer Assembled Superhydrophobic Organic−Inorganic Hybrid Films. *Langmuir* **2009,** 25, (18), 11073-11077.

256.   Luzinov, I.; Minko, S.; Tsukruk, V. V., Responsive brush layers: from tailored gradients to reversibly assembled nanoparticles. *Soft Matter* **2008,** 4, (4), 714-725.

257.   Ramaratnam, K.; Tsyalkovsky, V.; Klep, V.; Luzinov, I., Ultrahydrophobic textile surface via decorating fibers with monolayer of reactive nanoparticles and non-fluorinated polymer. *Chemical Communications* **2007,** 0, (43), 4510-4512.

258. Motornov, M.; Sheparovych, R.; Lupitskyy, R.; MacWilliams, E.; Minko, S., Superhydrophobic Surfaces Generated from Water-Borne Dispersions of Hierarchically Assembled Nanoparticles Coated with a Reversibly Switchable Shell. *Advanced Materials* **2008,** 20, (1), 200-205.

259. Synytska, A.; Ionov, L.; Dutschk, V.; Minko, S.; Eichhorn, K.-J.; Stamm, M.; Grundke, K., Regular Patterned Surfaces from Core-Shell Particles. Preparation and Characterization. In *Characterization of Polymer Surfaces and Thin Films*, Grundke, K.; Stamm, M.; Adler, H.-J., Eds. Springer Berlin Heidelberg: 2006; Vol. 132, pp 72-81.

260. Garcia, N.; Benito, E.; Tiemblo, P.; Hasan, M. M. B.; Synytska, A.; Stamm, M., Chemically guided topography in alkylsilane- and oligosiloxane-modified silica nanoparticle coatings: from very hydrophobic surfaces to "pearl" bouncing droplets. *Soft Matter* **2010,** 6, (19), 4768-4776.

261. Jiang, S.; Chen, Q.; Tripathy, M.; Luijten, E.; Schweizer, K. S.; Granick, S., Janus Particle Synthesis and Assembly. *Advanced Materials* **2010,** 22, (10), 1060-1071.

262. Berger, S.; Ionov, L.; Synytska, A., Engineering of Ultra-Hydrophobic Functional Coatings Using Controlled Aggregation of Bicomponent Core/Shell Janus Particles. *Advanced Functional Materials* **2011,** 21, (12), 2338-2344.

263. Tsai, P.-S.; Yang, Y.-M.; Lee, Y.-L., Hierarchically structured superhydrophobic coatings fabricated by successive Langmuir–Blodgett deposition of micro-/nano-sized particles and surface silanization. *Nanotechnology* **2007,** 18, (46), 465604.

264. Yao, T.; Wang, C.; Lin, Q.; Li, X.; Chen, X.; Wu, J.; Zhang, J.; Yu, K.; Yang, B., Fabrication of flexible superhydrophobic films by lift-up soft-lithography and decoration with Ag nanoparticles. *Nanotechnology* **2009,** 20, (6), 065304.

265. Du, X.; Liu, X.; Chen, H.; He, J., Facile Fabrication of Raspberry-like Composite Nanoparticles and Their Application as Building Blocks for Constructing Superhydrophilic Coatings. *The Journal of Physical Chemistry C* **2009,** 113, (21), 9063-9070.

266. Tsai, H.-J.; Lee, Y.-L., Facile Method to Fabricate Raspberry-like Particulate Films for Superhydrophobic Surfaces. *Langmuir* **2007,** 23, (25), 12687-12692.

267. Ming, W.; Wu, D.; van Benthem, R.; de With, G., Superhydrophobic Films from Raspberry-like Particles. *Nano Letters* **2005,** 5, (11), 2298-2301.

268. Ionov, L.; Sidorenko, A.; Stamm, M.; Minko, S.; Zdyrko, B.; Klep, V.; Luzinov, I., Gradient Mixed Brushes: "Grafting To" Approach. *Macromolecules* **2004,** 37, (19), 7421-7423.

269. Ionov, L.; Zdyrko, B.; Sidorenko, A.; Minko, S.; Klep, V.; Luzinov, I.; Stamm, M., Gradient Polymer Layers by "Grafting To" Approach. *Macromolecular Rapid Communications* **2004,** 25, (1), 360-365.

270. Iyer, K. S.; Zdyrko, B.; Malz, H.; Pionteck, J.; Luzinov, I., Polystyrene Layers Grafted to Macromolecular Anchoring Layer. *Macromolecules* **2003,** 36, (17), 6519-6526.

271. Liu, Y.; Klep, V.; Zdyrko, B.; Luzinov, I., Synthesis of High-Density Grafted Polymer Layers with Thickness and Grafting Density Gradients. *Langmuir* **2005,** 21, (25), 11806-11813.

272. Zdyrko, B.; Klep, V.; Luzinov, I., Synthesis and Surface Morphology of High-Density Poly(ethylene glycol) Grafted Layers. *Langmuir* **2003,** 19, (24), 10179-10187.

273. Synytska, A.; Svetushkina, E.; Puretskiy, N.; Stoychev, G.; Berger, S.; Ionov, L.; Bellmann, C.; Eichhorn, K.-J.; Stamm, M., Biocompatible polymeric materials with switchable adhesion properties. *Soft Matter* **2010,** 6, (23), 5907-5914.

274. Matyjaszewski, K.; Dong, H.; Jakubowski, W.; Pietrasik, J.; Kusumo, A., Grafting from Surfaces for "Everyone": ARGET ATRP in the Presence of Air. *Langmuir* **2007,** 23, (8), 4528-4531.

275. Dettre Robert, H.; Johnson Rulon, E., Contact Angle Hysteresis. In *Contact Angle, Wettability, and Adhesion*, AMERICAN CHEMICAL SOCIETY: 1964; Vol. 43, pp 136-144.

276. *Dictionary of Geology and Mineralogy.* 2nd Edition ed.; McGraw-Hill: 2003.

277. *Extracting Bioactive Compounds for Food Products: Theory and Applications.* CRC Press: 2009.

278. Jing, Z.; Maeda, H.; Ioku, K.; Ishida, E. H., Hydrothermal synthesis of mesoporous materials from diatomaceous earth. *AIChE Journal* **2007,** 53, (8), 2114-2122.

279. Spellman, F. S., *Handbook of Water and Wastewater Treatment Plant Operations.* Lewis Publishers: 2003.

280. Oliveira, N. M.; Reis, R. L.; Mano, J. F., Superhydrophobic Surfaces Engineered Using Diatomaceous Earth. *ACS Applied Materials & Interfaces* **2013,** 5, (10), 4202-4208.

281. Acres, G. J. K.; Bird, A. J.; Jenkins, J. W.; King, F., The design and preparation of supported catalysts. In *Catalysis: Volume 4*, Kemball, C.; Dowden, D. A., Eds. The Royal Society of Chemistry: 1981; Vol. 4, pp 1-30.

282. Zhao, Y.; Fang, J.; Wang, H.; Wang, X.; Lin, T., Magnetic Liquid Marbles: Manipulation of Liquid Droplets Using Highly Hydrophobic Fe_3O_4 Nanoparticles. *Advanced Materials* **2010,** 22, (6), 707-710.

283. Stimuli-Responsive Materials: Polymers, Colloids, and Multicomponent Systems. *Langmuir* **2006,** 23, (1), 1-2.

284. Cole, M. A.; Voelcker, N. H.; Thissen, H.; Griesser, H. J., Stimuli-responsive interfaces and systems for the control of protein–surface and cell–surface interactions. *Biomaterials* **2009,** 30, (9), 1827-1850.

285. Mendes, P. M., Stimuli-responsive surfaces for bio-applications. *Chemical Society Reviews* **2008,** 37, (11), 2512-2529.

286. Stuart, M. A. C.; Huck, W. T. S.; Genzer, J.; Muller, M.; Ober, C.; Stamm, M.; Sukhorukov, G. B.; Szleifer, I.; Tsukruk, V. V.; Urban, M.; Winnik, F.; Zauscher, S.; Luzinov, I.; Minko, S., Emerging applications of stimuli-responsive polymer materials. *Nat Mater* **2010,** 9, (2), 101-113.

287. Sun, A.; Lahann, J., Dynamically switchable biointerfaces. *Soft Matter* **2009,** 5, (8), 1555-1561.

288. Tokarev, I.; Minko, S., Stimuli-responsive hydrogel thin films. *Soft Matter* **2009,** 5, (3), 511-524.

289. Ionov, L.; Houbenov, N.; Sidorenko, A.; Stamm, M.; Luzinov, I.; Minko, S., Inverse and Reversible Switching Gradient Surfaces from Mixed Polyelectrolyte Brushes. *Langmuir* **2004,** 20, (23), 9916-9919.

290. Ionov, L.; Houbenov, N.; Sidorenko, A.; Stamm, M.; Minko, S., Smart Microfluidic Channels. *Advanced Functional Materials* **2006,** 16, (9), 1153-1160.

291. Synytska, A.; Stamm, M.; Diez, S.; Ionov, L., Simple and Fast Method for the Fabrication of Switchable Bicomponent Micropatterned Polymer Surfaces. *Langmuir* **2007,** 23, (9), 5205-5209.

292.   Ionov, L.; Sapra, S.; Synytska, A.; Rogach, A. L.; Stamm, M.; Diez, S., Fast and Spatially Resolved Environmental Probing Using Stimuli-Responsive Polymer Layers and Fluorescent Nanocrystals. *Advanced Materials* **2006,** 18, (11), 1453-1457.

293.   Tagit, O.; Tomczak, N.; Benetti, E. M.; Cesa, Y.; Blum, C.; Subramaniam, V.; Herek, J. L.; Vancso, G. J., Temperature-modulated quenching of quantum dots covalently coupled to chain ends of poly(N -isopropyl acrylamide) brushes on gold. *Nanotechnology* **2009,** 20, (18), 185501.

294.   Tokareva, I.; Minko, S.; Fendler, J. H.; Hutter, E., Nanosensors Based on Responsive Polymer Brushes and Gold Nanoparticle Enhanced Transmission Surface Plasmon Resonance Spectroscopy. *Journal of the American Chemical Society* **2004,** 126, (49), 15950-15951.

295.   Sidorenko, A.; Krupenkin, T.; Taylor, A.; Fratzl, P.; Aizenberg, J., Reversible Switching of Hydrogel-Actuated Nanostructures into Complex Micropatterns. *Science* **2007,** 315, (5811), 487-490.

296.   Sidorenko, A.; Minko, S.; Schenk-Meuser, K.; Duschner, H.; Stamm, M., Switching of Polymer Brushes. *Langmuir* **1999,** 15, (24), 8349-8355.

297.   Motornov, M.; Zhou, J.; Pita, M.; Gopishetty, V.; Tokarev, I.; Katz, E.; Minko, S., "Chemical Transformers" from Nanoparticle Ensembles Operated with Logic. *Nano Letters* **2008,** 8, (9), 2993-2997.

298.   Alarcon, C. d. l. H.; Pennadam, S.; Alexander, C., Stimuli responsive polymers for biomedical applications. *Chemical Society Reviews* **2005,** 34, (3), 276-285.

299.   Ionov, L.; Stamm, M.; Diez, S., Reversible Switching of Microtubule Motility Using Thermoresponsive Polymer Surfaces. *Nano Letters* **2006,** 6, (9), 1982-1987.

300.   Ionov, L.; Synytska, A.; Diez, S., Temperature-Induced Size-Control of Bioactive Surface Patterns. *Advanced Functional Materials* **2008,** 18, (10), 1501-1508.

301.   Yamada, N.; Okano, T.; Sakai, H.; Karikusa, F.; Sawasaki, Y.; Sakurai, Y., Thermo-responsive polymeric surfaces; control of attachment and detachment of cultured cells. *Die Makromolekulare Chemie, Rapid Communications* **1990,** 11, (11), 571-576.

302.   Marmur, A., Wetting on Hydrophobic Rough Surfaces: To Be Heterogeneous or Not To Be? *Langmuir* **2003,** 19, (20), 8343-8348.

303.   Marmur, A., The Lotus Effect: Superhydrophobicity and Metastability. *Langmuir* **2004,** 20, (9), 3517-3519.

304.   Velikov, K. P.; Velev, O. D., Stabilization of Thin Films, Foams, Emulsions and Bifluid Gels with Surface-Active Solid Particles. In *Colloid Stability and Application in Pharmacy*, Wiley-VCH Verlag GmbH & Co. KGaA: 2007; pp 277-306.

305.   Binks, B. P.; Horozov, T. S., *Colloidal particles at liquid interfaces*. Cambridge University Press: 2006.

306.   Kralchevsky, P. A.; Nagayama, K., *Particles at Fluid Interfaces and Membranes*. Elsevier: Amsterdam, 2001.

307.   Kralchevsky, P. A.; Denkov, N. D.; Danov, K. D., Particles with an Undulated Contact Line at a Fluid Interface: Interaction between Capillary Quadrupoles and Rheology of Particulate Monolayers. *Langmuir* **2001,** 17, (24), 7694-7705.

308.   Stamou, D.; Duschl, C.; Johannsmann, D., Long-range attraction between colloidal spheres at the air-water interface: The consequence of an irregular meniscus. *Physical Review E* **2000,** 62, (4), 5263-5272.

309.   Berger, S.; Synytska, A.; Ionov, L.; Eichhorn, K.-J.; Stamm, M., Stimuli-Responsive Bicomponent Polymer Janus Particles by "Grafting from"/"Grafting to" Approaches. *Macromolecules* **2008,** 41, (24), 9669-9676.

310.   Öner, D.; McCarthy, T. J., Ultrahydrophobic Surfaces. Effects of Topography Length Scales on Wettability. *Langmuir* **2000,** 16, (20), 7777-7782.

311.   Hosono, E.; Fujihara, S.; Honma, I.; Zhou, H., Superhydrophobic Perpendicular Nanopin Film by the Bottom-Up Process. *Journal of the American Chemical Society* **2005,** 127, (39), 13458-13459.

312.   Zheng, Z.; Azzaroni, O.; Zhou, F.; Huck, W. T. S., Topography Printing to Locally Control Wettability. *Journal of the American Chemical Society* **2006,** 128, (24), 7730-7731.

313.   Zhai, L.; Cebeci, F. Ç.; Cohen, R. E.; Rubner, M. F., Stable Superhydrophobic Coatings from Polyelectrolyte Multilayers. *Nano Letters* **2004,** 4, (7), 1349-1353.

314.   Tuberquia, J. C.; Nizamidin, N.; Harl, R. R.; Albert, J.; Hunter, J.; Rogers, B. R.; Jennings, G. K., Surface-Initiated Polymerization of Superhydrophobic Polymethylene. *Journal of the American Chemical Society* **2010,** 132, (16), 5725-5734.

315.   Gao, L.; McCarthy, T. J., A Perfectly Hydrophobic Surface (θA/θR = 180°/180°). *Journal of the American Chemical Society* **2006,** 128, (28), 9052-9053.

316.   Feng, L.; Song, Y.; Zhai, J.; Liu, B.; Xu, J.; Jiang, L.; Zhu, D., Creation of a Superhydrophobic Surface from an Amphiphilic Polymer. *Angewandte Chemie International Edition* **2003,** 42, (7), 800-802.

Acknowledgements

Finally I want to thank my parents and my brother who believe in my success and help me in some difficult moments. Also I appreciate all my friends especially my classmates from Moscow State University Mr. Denis Okhrimenko, Mr. Evgeny Revunov, Mr. Dmitry Chistyakov, Dr. Dmitry Morozov, Dr. Alexei Godina, Dr. Arseny Kovyrshin, Dr. Nikita Kovalenko, Dr. Alexander Ryabchun, Mrs. Tatiana Ryabchun who stayed close to me and organized amazing events during these years.

Curriculum vitæ

Personal

Name   Nikolay

Surname   Puretskiy

Born: July 6th 1987, Tula, Tula region, Russian Federation

Nationality: Russian Federation

Marital Status: Single

Education

Oct 2009-   Technische Universität Dresden
Feb 2014
                Fakultät Mathematik und Naturwissenschaften

                Fachrichtung Chemie und Lebensmittelchemie, PhD student

Sep 2004-   M.V. Lomonosov Moscow State University
Jun 2009
                Specialist (Diploma) in Chemistry (Organic Chemistry), GPA 4.75 of
                5.00

1999-2004   Lyceum №2, Tula, Tula Region

1994-1999   School №71, Tula, Tula Region

Professional Experience

From May 2013	**Leibniz-Institut für Polymerforschung Dresden e. V.**
	Teilinstitut Physikalische Chemie und Physik der Polymere
	Nanostrukturierte Materialien
	Research advisor: Dr. Leonid Ionov
	Position: Scientist
Oct 2009- May 2013	**Leibniz-Institut für Polymerforschung Dresden e. V.**
	Teilinstitut Physikalische Chemie und Physik der Polymere
	Nanostrukturierte Materialien
	Research advisor: Dr. Leonid Ionov
	Position: Guest scientist
	"Design of self-healing materials with switchable and ultrahydrophobic properties using Janus particles"
May 2008- Sep 2008	**Johannesburg Technology Centre, BHP Billiton, South Africa**
	Process and Environmental Chemistry Laboratory
	Summer research fellow
	Research advisors: Senior Principle Scientist Elmar L. Muller, Principle Engineer Petrus Basson
	"Investigation of the Effect of Various Parameters on the Surface Potential of a Pyrite Electrode under Typical Thermophile Bioleach (solution) Conditions"
Jun 2007- Aug 2007	**Johannesburg Technology Centre, BHP Billiton, South Africa**
	Process and Environmental Chemistry Laboratory
	Summer research fellow
	Research advisors: Senior Principle Scientist Elmar L. Muller, Principle Engineer Petrus Basson
	"Investigating the Effect of Chloride Concentration on the Leaching Kinetics of Chalcopyrite"

Methods and instruments:

1. AFM – Dimension V Scanning Probe Microscope (Veeco Instruments, Inc., USA)
   Dimension III Scanning Probe Microscope (Veeco Instruments, Inc., USA)
2. SEM – NEON® 40 (Carl Zeiss NTS GmbH)
3. DSA – Krüss Drop Shape Analysis (Krüss GmbH)
   DataPhysics OCA (DataPhysics Instruments GmbH)
4. ZP and DLS – Zetasizer Nano ZS (Malvern Instruments, UK)
5. GPC – Agilent Technologies 1260 Infinity
6. Null-ellipsometry – Multiskop (Optrel GbR, Sinzing, Germany)
7. AAS – Varian AA140
8. UV-spectroscopy – Shimadzu UVmini-1240CE
9. IR-spectroscopy – ThermoNicolet IR-200
10. Column and thin layer chromatography
11. Optical and fluorescence microscopy – Zeiss Axio
12. NMR data processing and evaluation
13. TGA data processing and evaluation
14. Preparation of thin polymer films by "grafting from" and "grafting to" approaches
15. Free radical polymerization, ATRP and AGET-ATRP

Personal scills

Languages: Russian (native speaker)

English (fluent)

German (intermediate)

Software: MS-Office, Origin, Maple, ChemOffice, ACD Labs

List of publications

Journal articles:

1. Kudina, Olena; Zakharchenko, Andrey; Trotsenko, Oleksandr; Tokarev, Alexander; Ionov, Leonid; Stoychev, Georgi; **Puretskiy, Nikolay**; Pryor, Scott W.; Voronov, Andriy; Minko, Sergiy "Highly Efficient Phase Boundary Biocatalysis with Enzymogel Nanoparticles" Angewandte Chemie International edition, accepted (10.1002/anie.201306831)

2. Zakharchenko, Svetlana; **Puretskiy, Nikolay**; Stoychev, Georgi ; Waurisch, Christian ; Hickey, Stephen G.; Eychmueller, Alexander ; Sommer, Jens-Uwe; Ionov, Leonid „Stimuli-responsive hierarchically self-assembled 3D porous polymer-based structures with aligned pores" Journal of Materials Chemistry B, 2013, 1 (13), 1786-1793

3. **Puretskiy, Nikolay**; Stoychev, Georgi ; Synytska, Alla; Ionov, Leonid "Surfaces with Self-repairable Ultrahydrophobicity Based on Self-organizing Freely Floating Colloidal Particles" Langmuir, 2012, 28 (8), 3679-3682

4. **Puretskiy, Nikolay**; Ionov, Leonid "Synthesis of Robust Raspberry-like Particles Using Polymer Brushes" Langmuir, 2011, 27 (6), 3006-3011

5. Svetushkina, Ekaterina; **Puretskiy, Nikolay**; Ionov, Leonid; Stamm, Manfred; Synytska, Alla "A comparative study on switchable adhesion between thermoresponsive polymer brushes on flat and rough surfaces" Soft Matter, 2011, 7 (12), 5691-5696

6. Stoychev, Georgi; **Puretskiy, Nikolay**; Ionov, Leonid "Self-folding all-polymer thermoresponsive microcapsules" Soft Matter, 2011, 7 (7), 3277-3279

7. **Puretskiy, Nikolay**; Stoychev, Georgi; Stamm, Manfred; Ionov, Leonid "Switchable Surfaces Based on Freely Floating Colloidal Particles" ACS Applied Materials & Interfaces, 2010, 2 (10), 2944-2948

8. Synytska, Alla; Svetushkina, Ekaterina; **Puretskiy, Nikolay**; Stoychev, Georgi; Berger, Sebastian; Ionov, Leonid; Bellmann, Cornelia; Eichhorn, Klaus-Jochen; Stamm, Manfred "Biocompatible polymeric materials with switchable adhesion properties" Soft Matter, 2010, 6 (23), 5907-5914

9. Zakharchenko, Svetlana; **Puretskiy, Nikolay**; Stoychev, Georgi ; Stamm, Manfred; Ionov, Leonid "Temperature controlled encapsulation and release using partially biodegradable thermo-magneto-sensitive self-rolling tubes" Soft Matter, 2010, 6 (12), 2633-2636

Contributed conferences:

1. **Puretskiy, Nikolay**; Stoychev, Georgi ; Synytska, Alla; Ionov, Leonid „Design of self-repairable superhydrophobic materials using colloidal particles" (Poster) Bayreuth Polymer Symposium (BPS 2013); 15 – 17 September 2013, Bayreuth, Germany.

2. **Puretskiy, Nikolay**; Stoychev, Georgi ; Synytska, Alla; Ionov, Leonid „Design of the self-repairable materials using colloidal particles" (Oral presentation) DPG-Frühjahr Tagung (DPG Spring Meeting) Regensburg 2013; 10 – 15 March 2013, Regensburg, Germany.

3. **Puretskiy, Nikolay**; Stoychev, Georgi ; Synytska, Alla; Ionov, Leonid "Design of the self-repairable materials using colloidal particles" (Oral presentation) 26th Conference of the European Colloid and Interface Society (ECIS 2012); 02 – 07 September 2012, Malmö, Sweden

4. **Puretskiy, Nikolay**; Ionov, Leonid "Synthesis and properties of robust raspberry-like particles" (Poster) 26th Conference of the European Colloid and Interface Society (ECIS 2012); 02 – 07 September 2012, Malmö, Sweden

5. **Puretskiy, Nikolay**; Ionov, Leonid "Synthesis and some properties of polymer brushes covered robust raspberry-like particles" (Poster) 25th Conference of the European Colloid and Interface Society (ECIS 2011); 04 – 09 September 2011, Berlin, Germany

6. **Puretskiy, Nikolay**; Stoychev, Georgi; Stamm, Manfred; Ionov, Leonid "Switchable surfaces based on freely floating colloidal particles" (Poster) 24th Conference of the European Colloid and Interface Society (ECIS 2010); 05 – 10 September 2010, Prague, Czech Republic

Patent:

1.   Ionov, Leonid; **Puretskiy**, **Nikolay**; Stoychev, Georgi; Stamm, Manfred "Switchable surfaces based on freely floating colloidal particles". Application number EP10169077.4.

Versicherung

Hiermit versichere ich, dass ich die vorliegende Arbeit ohne unzulässige Hilfe Dritter und ohne Benutzung anderer als der angegebenen Hilfsmittel angefertigt habe; die aus fremden Quellen direkt oder indirekt übernommenen Gedanken sind als solche kenntlich gemacht. Die Arbeit wurde bisher weder im Inland noch im Ausland in gleicher oder ähnlicher Form einer anderen Prüfungsbehörde vorgelegt.

Dresden, den 15. November 2013

Nikolay Puretskiy

Erklärung

Hiermit erkläre ich, dass diese Arbeit unter wissenschaftlicher Betreuung von Herrn Prof. Dr. Manfred Stamm und Herrn Dr. Leonid Ionov in der Zeit von Oktober 2009 bis Oktober 2013 am Leibniz-Institut für Polymerforschung Dresden e.V. angefertigt wurde.

Bislang haben keine weiteren Promotionsverfahren stattgefunden.

Hiermit erkenne ich die Promotionsordnung der Fakultät Mathematik und Naturwissenschaften der Technischen Universität Dresden vom 23.02.2011 an.

Dresden, den 15. November 2013

Nikolay Puretskiy